USE OF CAPILLARY ACTION TO CONTROL SOIL MOISTURE

by

MAHYAR HEIDAR BARGHI

A thesis submitted to the University of Birmingham for the degree of

DOCTOR OF PHILOSOPHY

Department of Civil Engineering

School of Engineering

College of Engineering and Physical Sciences

The University of Birmingham

August 2018

Abstract

Heavy rainfall on sloping ground preceded by prolonged dry period can lead to increased risk of failure of slopes. This can lead to significant impact on infrastructure (both road and rail), which invariably comprises both embankments and cuttings. With global warming, there is an increase in risk of extreme weather and hence likelihood of failure incidents is higher.

Capillarity is one of the major water movement mechanisms in soil and thus, there was the need to study the subject. A laboratory based investigation was conducted with the aim of raising water by capillary action and removal of water from the soil surface by the action of wind. The first series of experiments were conducted to investigate the capillary rise of water in soils and more importantly how to improve the height of capillary rise and the volume of water that could be drawn up using capillary action. It included column tests with the base of the soil columns in water and in soil with a range of moisture contents. Final series of tests were conducted to assess the feasibility of using a soil column to draw up water from a free water surface to a higher level where water was removed from the surface by the action of wind with a view to continuously remove water. This involved placing the top of the column in a wind tunnel while the column was stood in water.

Overall this study shows that both capillarity and suction created by the wind has the potential to be developed for successful lifting of water. Such a system would not require much energy input, however, it may take longer to lift water at a lesser rate compared to conventional pumping systems.

Dedication

This work is dedicated to Mahsa, Moonia, Fariba and Kazem.

Acknowledgements

I will always feel indebted to both my supervisors Dr. Gurmel Ghataora and Dr. Michael Burrow. Their continuous support and enthusiasm during all stages of the project always drove me forward and made me feel passionate about the subject throughout my research. I would like to express my special thanks and appreciation to Dr Ghataora and Dr Burrow for the critical review of my thesis.

I must acknowledge the support of laboratory technicians Mr. Sebastian Ballard, Mr. Luis Portela, Mr. Michael Vanderstam, Mr. James Guest, Mr. David Allsop, Mr. David Cope, Mr. Mark Carter and Mr. James Glover at the University of Birmingham.

I would like to thank Emmanuel Hitimana, Nowsherwan Abbas and Mengqi Lyu, M.Sc. students at the Department of Civil Engineering, for their assistant during the laboratory work. Special thanks goes to Stefanie Gillmeier for kindly demonstrating the use of smoke generator in the laboratory. I would also like to acknowledge the support of my friends, colleagues and all the staff at the University of Birmingham.

Finally, I most gratefully acknowledge my family, Kazem, Fariba, Mahsa and Moonia for their love, encouragement, patience and support in all of my endeavours in my life.

Table of Contents

List of Figures

List of Tables

1 INTRODUCTION

1.1 *Statement of the research problem*

The climate of the UK is set to change considerably over the next century, and is expected to significantly affect the stability of earth slopes (Glendinning et al., 2008). Future climate change scenarios in the UK over the next century predict, in general, an increased and more intense precipitation in winter, a decreased but more intense precipitation in summer as well as consistent and significant increases in annual mean temperatures of around 2 to 5°C (Hulme et al., 2002). Accordingly it is reasonable to suggest that changes in rainfall patterns and increased temperatures have the potential to change the water regimes within infrastructure slopes and the patterns of vegetation growth on slopes. Subsequently, an increased number of successive shrink-swell cycles may increase the rate of degradation of certain types of clay materials and the frequency of failures by progressive means. Increased periods of dry weather conditions due to hotter drier summers leads to shrinkage of clay soils and surface cracking. Surface cracks potentially increase surface permeability and water infiltration to the slopes. An increased and more intense rainfall in the following autumn and winter will change pore water pressure equilibration and may increase pore water pressures within slopes leading to more slope failures.

An efficient and operational transport system is important to a sustainable community and climate change has the potential to negatively affect certain infrastructure (Kilsby et al., 2009) and is already having an impact on the UK road and railway system, including major landslides in Scotland (e.g. A890 near Stromeferry), over 100 slope failures on the national rail network in winter 2000/1 and closure of A46 in Gloucestershire in summer 2007 for several months (Kilsby et al., 2009, Glendinning et al., 2008, O'Brien, 2001 and 2007, Ridley A. et al 2004, Toll D. G. 2001, Brooks S. M. et al 2004, Borga M. et al 2002). The summer of

2007, recorded as one of the wettest summers, caused many slope failures however more importantly, heavy rainfall did not allow the normal suction generation during summer that maintain stability during the winter (Loveridge, 2007; Kilsby et al., 2009).

Earth slopes are significant to the UK transport systems include both road and rail, which invariably comprises both embankments and cuttings. A large proportion of UK transport infrastructure is made up of earth slopes. Approximately £20B of the estimated £60B i.e. one third of asset value of UK major highway infrastructure transport network infrastructure is contributed to earthwork slopes (Glendinning et al., 2006; Hughes et al., 2008). Major failures of earth slopes will result in disruption to network operation and frustration to the travelling public due to delays to services or temporary route closures. Minor failures of earth slopes will result in speed restrictions and daily commuter misery due to delays (Ridley et al., 2004; Hughes et al., 2008; Kilsby et al., 2009).

In order to avoid major and minor failures, continuous maintenance of earth slopes is thus essential. In 1998/99, the maintenance of UK embankments alone cost £50 million (Perry J. 2001). Taking into consideration that the cost of emergency maintenance works is ten times greater than planned repair works (O'Brien, 2001), the ability to predict and reduce the possibility of occurrence of potential failures would be of considerable financial benefits (Glendinning et al., 2006; Hughes et al., 2008).

1.2 *Potential impacts of climate change on earth slopes*

There are two major factors that control the stability of slopes including 1) the status of the water retained within the pore spaces of soil materials and 2) the strength of the materials that slopes are created from or formed within (Hughes et al., 2009; Kilsby et al., 2009; Leroueil, 2001; Vaughan, Soda and Walbancke, 1978). Increases and decreases in the water content of clay materials may result in an increased and decreased volume changes by swelling and

shrinkage respectively (i.e. clay materials may undergo volume changes by shrink-swell actions). Changes to the water content of clay materials and the associated volume changes will results in an increased number of successive shrink-swell cycles leading to strength-reduced areas and eventually ultimate limit state failures. In the UK, embankments are generally created from, and cuttings are, in general, formed within over-consolidated clay materials. These embankments and cuttings may (are designed to) experience high negative pore water pressures (i.e. suctions), providing apparent stability to the slopes, which may last for an average of approximately 10–15 years after construction (Hughes et al., 2009). Over a period of time, precipitation will result in an increase in pore water pressures, which may lead to potential slope instability. The successive cycles of shrink-swell action may create surface cracks; consequently, water can infiltrate the embankment and accelerate the failure process. The most crucial time would be when a very heavy and intense rainfall follows a long period of drought (i.e. very dry weather). The scenario of hotter drier summers, followed by periods of more intense and heavy rainfall has the potential to change pore water pressure equilibration conditions. Consequently the climate change has considerable impacts on the degradation rates of the engineering conditions of infrastructure embankments.

Additionally, vegetation is considered as another major factor that has significant impacts on the status of the water retained within the pore spaces of materials within slopes.

The presence of vegetation on a slope brings both hydrological and mechanical benefits to the stability of slopes. Vegetation modifies the moisture content of the soil, so influencing soil strength, and the presence of roots in the soil also increases soil strength and, thus, its stability. The effect of vegetation can be viewed as an indirect drainage measure as its presence can reduce the soil moisture content and the pore water pressure near the slope surface and prevent ingress of water into and possible erosion of weathered soil at the

surface. Vegetation cover can reduce soil moisture content through (1) foliar interception and direct absorption and evaporation of rainwater, which reduces the amount infiltrating into the soil; and (2) extracting soil moisture via the transpiration processes, which will reduce pore water pressure and counteract the reduction in soil strength caused by wetting (Kilsby et al., 2009).

Transpiration is greater when plants are growing rapidly in the summer, under non-limiting moisture conditions. Many plants that live in damp habitats are characterised by high transpiration rates, and so have a high capacity to remove water from the soil. Such plants are potentially useful for reducing high pore water pressures, but their tolerance of drier soils may be limited (MacNeil et al., 2001). In view of the fact that the metabolic activity of plants and the rates of transpiration are generally lower over the winter, the impact vegetation has on soil/water relationships (i.e. soil moisture depletion) is reduced during the period when rainfall is at a maximum, i.e. when earthwork slopes are most vulnerable to failure and slope stability problems generally arise. Consequently, Coppin and Richards (1990) argued that the ability of trees to reduce soil water and affect soil strength would be less than the effect their roots had on soil reinforcement, especially at the times critical for slope stability, i.e. in the spring when soil moisture is high and before transpiration rates begin to increase. However with the increasing impact of climate change and the increased possibility and frequency of intense summer storms, the use of vegetation may become more important and valuable (Coppin et al., 1990).

1.3 *Failure modes of slopes due to climate change*

Hughes et al. (2009) proposed a number of potential inter-related failure mechanisms for infrastructure slopes due to climate change, which are as follows (Hughes P. N. et al 2009):

1.3.1 Shrink–swell

In general, the slopes in the UK may either be formed in clay soils or contain clay materials and they can experience volume changes due to changes to the water content of existing clay materials. Decreases in water content will result in a decrease in soil volume; on the other hand, increases in water content will result in a volume increase. Variations in water content are consequences of seasonal fluctuations in rainfall combined with both seasonal and spatial changes in water demands from vegetation (Hughes et al., 2009; Kilsby et al., 2009).

Variations in water contents and the associated volume changes, especially for railway tracks built on embankments, may cause serviceability problems because tracks must be kept inside a precise route and tolerances have to be balanced. Volume changes may disturb the layout of track settings. If high-plasticity materials and deciduous trees exist in slopes, volume change and the associated problems may even get worse. Increase in temperature and seasonal variations of temperature will result in a change in rainfall patterns and consequently shrink-swell cycles, with the potential to increase in magnitude. Change in rainfall patterns may also change patterns of vegetation growth, with the potential to increase in magnitude i.e. to greater depths due to the reason that during periods of drought, plants root to greater depths (Hughes et al., 2009; Kilsby et al., 2009).

1.3.2 Progressive failure

Successive shrink-swell cycles (consecutive cycles of swelling and shrinkage) will result in strength-reduced areas within the clay slopes. The strain-softened areas may form shear planes and lead to progressive slope failures. The failure begins to happen at the toe of the

slope and gradually increase until eventually results in an ultimate limit state failure. Climate change will result in more slope failures by increasing the number of shrink-swell cycles. In conclusion, changes to the water content results in an increased number of successive shrink-swell cycles leading to strength-reduced areas and formation of shear planes within the clay slopes. This will result in progressive and eventually an ultimate limit state failure. Consequently, climate change has the potential to increase progressive slope failure by reducing times required to reach ultimate limit state failure (Hughes et al., 2009).

1.3.3 Pore water pressure equilibration (re-wetting)

Generally in the UK, embankments are created from, and cuttings are formed within over-consolidated clay materials. These embankments and cuttings may experience high negative pore water pressures (i.e. suctions), providing apparent stability to the slopes, which may last for an average of approximately 10–15 years after construction. Over period of time, precipitation will result in an increase in pore water pressures, which may lead to potential slope instability. Increase in rainfall during winter, (due to climate change) has the potential to increase pore water pressures, beyond the design value, which may result in instability of structures (e.g. slopes); on the other hand, increased temperatures during summer may improve slope stability by building up negative pore water pressures i.e. increasing suctions (Hughes et al., 2009; Kilsby et al., 2009).

1.3.4 Surface creep

During dry periods, the action of shrinkage and drying of clay soils due to an increased period of summer drought may lead to surface cracking. Subsequently, water can infiltrate the embankment through open cracks appeared at the surface, potentially increasing surface permeability. This water infiltration will accelerate the re-wetting process and decrease the number of cycles required to reach failure by progressive mechanisms. In addition, during

winter rainfall and wetting, surface cracks will be closed again. Due to gravitational forces, this closure will have the tendency towards downslope direction. Increased number of consecutive cycles will result in a mass surface movement downslope that has the potential to lead to shallow, surface failure. Increase in summer temperatures and the associated shrinkage and drying lead to deeper cracks, consequently, the downslope mass movement may penetrate deeper into the soil leading to substantial slope failures and eventually ultimate limit state failures (Hughes et al., 2009; Kilsby et al., 2009).

1.4 *Methods of slope drainage*

The stability of highway cuttings and embankments is critically dependent on the magnitude and distribution of pore water pressures within the materials (soils, rock and earthworks fill) forming the slopes. Pore pressures arise from the presence of water within the slopes, and may be introduced via natural infiltration from runoff and/or groundwater flow and possibly through artificial recharge. In the case of infiltration, rainfall will enter earthwork slopes and the underlying soil through the surface in quantities, which depend on the duration and intensity of the rainfall, the soil type, the topography, and the vegetative cover. Groundwater flow into a slope will depend on the local hydrogeological regime. Artificial recharge can arise from deliberate sources such as soakaways or accidental sources such as leakage from blocked drainage systems.

The increasing frequency of extreme rainfall events caused by climate change requires greater emphasis to be placed on a consideration of storm water and surface run-off at the design stage. This is to avoid in-service problems with mud and debris slides and to minimise the infiltration of water into clay slopes after the development of shrinkage cracks during prolonged hot spells. Clay slopes are particularly susceptible to drying during prolonged dry summers and this leads to the formation of shrinkage cracks that rapidly fill with water

during intense rainstorms. This ingress of water can lead to softening of clay slopes and adversely affect slope stability in critical cases. More severe winter conditions with heavier extreme rainfalls will lead to a rise in the water table with increased pore water pressures in the slope leaving soils, especially those that are clayey, vulnerable to reductions in soil strength which adversely affect slope stability. Slope instability affects the infrastructure foundation and can damage other assets located on the embankment or in the cutting. Large slope movements or settlements lead to traffic speed restrictions or route closure, and can damage the carriageway and any footpath. Hence the understanding and management of drainage provisions to improve the longevity and stability of slopes is of prime importance to all infrastructure owners.

Slope drainage can control the movement of surface water and the subsurface pore water pressure in the slope. Major slope drainage techniques are summarised in Table 1.1.

Table 1.1 Major slope drainage techniques (after Halcrow group limited and TRL limited, 2008)

Slope drainage techniques	Specifications/Comments	Advantages	Drawbacks
1. Trench (or slope) drains Drains that run down the slope, perpendicular to the crest, draining the upper 2m of soil.	• **Counterfort drains** Deep trench drains, which sometimes penetrate to the full depth of the embankment below any potential slip surface.	• Reducing pore water pressures in a slope • Intercepting run-off	In general this type of drain requires a positive fall to a collection point to prevent ponding and to avoid introducing water into the slope.
	• **Rock ribs** Where the counterfort drains are filled with coarse materials (stone-fill).	• Providing a resistance to soil shear and thus have a stabilising effect	
2. Shallow slope drains Also known as chevron or herringbone drains because of the pattern in which they are laid, are typically about 300mm wide and 300mm deep and stone-filled.	A herringbone or chevron pattern on the face of the slope can be effective in catching run-off, although other patterns can be employed.	• Intercepting run-off and controlling infiltration into the slope	• Very prone to clogging • Very limited service life • Not cost effective • Trenching for the installation of drains may increase the risk of water infiltration into the slope
3. Drainage blankets Comprise a granular layer, installed at the base of an embankment.	Drainage blankets are often employed in conjunction with vertical sand drains particularly when constructing embankments on alluvial deposits.	• Dissipating excess pore pressures during construction and providing a drainage path	• Prone to form a softened zone in the clay fill adjacent to the filter material • Not permanent
4. Filter and fin drains	• **Filter (or French) drains** Comprise a carrier pipe bedded in a granular material close to the bottom of a trench.	• Filter drains can function very effectively as a combined surface and sub-surface drain. • Filter drains can accommodate high volumes of flow, all of which should be within the carrier pipe. • Filter drains are well suited for slope drainage applications and are often sited at the toe and/or the crest of a slope.	• Filter drains often have a working life of only about 15 to 20 years.
	• **Narrow filter drains** Constructed similar to a filter drain with a maximum diameter of the carrier pipe equal to 100mm. • **Fin (or geo-composite) drains** Comprise a 3D planar geosynthetic composite with a very high in-plane permeability, and a carrier pipe.		

Slope drainage techniques	Specifications/Comments	Advantages	Drawbacks
5. Surface water channels	• Concrete channels Usually have a triangular cross-section but trapezoidal sections are used where greater flows are expected. Their usage is often combined with a fin or filter drain to intercept groundwater flow.	• Collect and reduce surface flows and transport water off a slope • Reduce the potential for erosion on the slope • Accommodate high flow capacities • Simple to inspect and maintain • Robust and highly durable	• Not as effective as the grassed channels to reduce the flow peaks • Mean flow velocities in the grassed channels (with grass of 40mm height) are likely to be around 25% of those estimated for concrete channels
	• Grassed channels The surface geometry is similar to concrete channels. Grassed channels are constructed by placing topsoil to provide the desired profile; turfs are then laid on top. Hydro-seeding of the topsoil may also be used.	• Attractive natural appearance • Sustainable drainage performance due to the ability to absorb spillages and provide vegetative treatment • Reduced peak flow downstream due to the greater resistance and storage volume of grassed channels	• Heavy vehicles, braking on the channel, may suffer a decrease in control and in some circumstances cause substantial damage to the channel.
6. Vertical and horizontal drains • Vertical drains are long, thin elements installed through soft clay soils to accelerate the rate of consolidation by reducing drainage path lengths. • Horizontal drains have been used as a means of stabilising wet unstable ground in slopes, or as a drainage measure to improve the stability of cutting and embankment slopes, and slopes in natural ground that have been displaying movement.	• **Band or wick drains** Prefabricated drains using corrugated polymeric materials for the core, and fabrics, fibre or paper, for the filter. Typically about 100mm wide and 4mm thick and installed using displacement methods and washing (or jetting) techniques. • **Sandwicks** Prefabricated sand drains made of polypropylene and melt-bonded fabric stockings filled with clean sand.	• Accelerate the rate of consolidation by reducing drainage path lengths • Controlling consolidation during construction of an embankment • Can be effective for in-service slopes where there is a perched water table and a convenient underlying permeable stratum to carry the water away • Displacement sand drains are low-cost and simple to install.	• Displacement sand drains cause the most disturbance and are prone to borehole smear. • Non-displacement installation methods are more effective in limiting disturbance, but there will be a smear zone around the borehole walls.
	• **Horizontal bored drains** Comprise small-diameter wells, typically less than 150mm diameter, drilled into the slope to remove groundwater and seepages. • **Horizontal wick drains** Comprise flat, geotextile-coated plastic channels that are driven into the ground rather than drilled.	• Advanced plastic drains are resistant to corrosion, more rigid and thus more suitable for longer drains than conventional bored drains. • Horizontal wick drains are resistant to clogging, they are low cost, they are flexible (can be stretched by up to 100% before rupturing) and simple to install.	• Horizontal wick drains are NOT suitable for ground conditions where SPT values greater than 30 have been measured, where drain lengths in excess of 30m in harder soils and 45 to 60m in softer soils are required, and where obstructions such as bedrock, large rocks, dense sand or gravel are expected.

Slope drainage techniques	Specifications/Comments	Advantages	Drawbacks
7. Electro-osmosis Under electro-potential gradient water will migrate from the anode towards the cathode, whence it may be removed.	**Electro-Kinetic Geosynthetics (EKGs)** Advanced electro-conductive geosynthetics that also provide the more traditional functions of geosynthetics, such as drainage and soil reinforcement thus providing additional stabilisation. EKGs are available in many different forms, e.g. sheets, strips or 3D products.	• Increase the effective stress, by generating a reduction in pore water pressure, and thus an increase in the shear strength of the soil mass. • Control of seepage forces and pore water pressures during construction. • Installation of EKGs into existing slopes may be achieved without causing disruptions to traffic operations, and will result in rapid drainage and consolidation of the soil.	• High costs • Metallic electrodes are prone to corrosion • EKGs degrade under extreme conditions • The process is considered to be irreversible; however as the electrodes are unlikely to be removed after use, they may be reused as required simply by reconnecting the electrical supply.
8. Vegetation The effect of vegetation can be viewed as an indirect method of providing slope drainage. Vegetation limits ingress of surface water into slopes and encourages runoff at a controlled rate. Transpiration acts to reduce pore water pressures and the root growth binds the surface layers together minimising both erosion and the formation of shrinkage cracks.	• **Grasses** tend to be relatively shallow rooting and more suited to surface protection, binding the surficial layers together, and may either attenuate or promote surface water run-off depending on the species selected. • **Herbs and legumes** are commonly used in conjunction with grasses. Some species are deeper rooting than grasses, and therefore more suitable for deeper stability, but many die back in winter. • **Shrubs and trees** take longer to fully establish than grasses and herbs. However, higher suctions would be generated under trees and shrubs. Those of deeper rooting habit will have a potential role in stabilising shallow slope failures in the longer term.	• Soil moisture reduction and extraction, through (1) foliar interception and direct absorption and evaporation of rainwater, which reduces the amount infiltrating into the soil; and (2) the transpiration processes, thus reducing pore water pressure and counteracting the reduction in soil strength caused by wetting. • Surface cover shading, of the soil provides some protection against intensive drying in full sun and the formation of shrinkage cracking, which allows deep infiltration of rainwater.	• Prolonged extraction of moisture by plant roots can lead to desiccation and thus to the formation of shrinkage cracks. • Planting of trees on slopes may possibly give rise to other problems such as leaf fall, disruption to the network if blown over by strong winds, and the need for coppicing. • Seeds of herbaceous species can be expensive and certain species may prove difficult to establish.

1.5 *Background Theory of the research*

If a soil gets saturated and allowed to drain, then only free, “gravitational water” can be removed. The remaining water will comprise of water held in soil mineral structure, adsorbed water (hygroscopic water) and capillary water. The two former types of water are not easily removed, as they are essentially part of soil minerals. Capillary water is held in the soil by surface tension, at the points of contact and/or in the pore space between the particles. The amount of capillary water retained by the soil is primarily dependant on the soil texture, soil structure (i.e. its condition with regard to granulation into compound particles and arrangement or packing or compaction), and water content (Buckingham, 1907).

If the surface of the soil is now exposed to evaporation, drying takes place; most at the surface, but to some extent also at depths below the surface. However, this loss of water at depths below the surface is greater than can be accounted for by the assumption that the water evaporates directly into the pores of the soil and then escapes as vapour by diffusion. Buckingham (1907) stated that the loss of water by direct evaporation from depths below the surface of a moist soil is, in general, negligible. The simple mechanism is that as the surface soil dries out, a moisture gradient is established; the dry surface soils attraction for water increases so that it (i.e. the dry surface soil) sucks up water (by capillary action) from the moister soil below, with which it was previously in equilibrium.

The phenomenon of the capillary motion of water is, of course, not limited to the vertical but may occur in any direction from places of high water content to areas of lower water content of the soil.

If a column of dry soil, in a tube covered at the bottom with cotton cloth or fine wire gauze, is placed vertically with its lower end in a container of water, water begins to rise into the soil, the dry soil sucking water away from the moister soil below. If the tube is not too

long, and if its upper end is exposed to evaporation into the air, a steady state of flow is eventually established in which the percentage of moisture at any level in the soil does not change with the time. When this state of affairs has been set up the amount of water that reaches any level from below must be the same as the amount that moves that level to the soil above, and the same as evaporates from the surface at the top of the column. Before this steady state is set up, the capillary flow is not constant and the water content at any given point in the tube varies with the time.

Thus, in an unsaturated soil, water is attracted towards the soil surface by capillary action and the drier the soil, the larger the attraction would be (Narasimhan, 2005). From the statements above, it can be understood that the evaporation from the soil surface is related to capillary rise. Terzaghi et al., (1996) stated that if a specimen of soft clay is exposed to the air, water is drawn up from the interior of the specimen toward the surface where it evaporates. During this process, commonly referred to as “drainage by desiccation”, the clay becomes stiffer and finally very hard. Lu and Likos (2004) also realized the importance of capillary rise for subsurface irrigation and drainage design.

From the background theory, it can be seen that there is a potential to develop a system of water removal comprising a column of soil with certain particle size to draw up water from a free water surface to a higher level where water is removed from the surface by evaporation either through the action of wind, radiation, vegetation or by other means. In this study, the effect of evaporation on capillary rise (the effect of removal of water from the surface of the column on capillary rise) through the action of wind is only investigated.

1.6 *Current commercialised capillary drainage technology*

There is only one commercialized capillary and siphonage drainage technology within the industry, which is known as Capiphon™ in the Australia or Smart Drain™ in the USA. It is made of polyvinyl chloride and comes in forms of a belt and a round pipe that can be used with or without the belt as shown in Figure 2 in Appendix A.3. The belt is approximately 2 mm thick, 10 or 20 cm wide, and 100 m long, having a series of omega-shaped grooves also known as micro siphons or micro channels running down its length. The omega-shaped grooves have an opening of approximately 0.3 mm and an internal diameter of one millimetre as shown in Figure 3 in Appendix A.3.

When the belt is placed in a saturated soil, water moves into the belt. The micro channels start lifting the water into the cavities, while solids are held back in the soil by gravity. Water moves into the micro channels by capillary action, and is held within them by surface tension acting as a capillary straw. When the belt is inclined (1-2% slope) or below water table, the water in the soil reaches a critical head in the soil and the critical capillary head is exceeded causing the capillary straws within the channels to move down the belt and the water in the channels begins to flow. The movement of the water within the micro channels creates a negative pressure that draws water up from the soil. The belts are slotted into the collection pipes at a downward angle generating the siphoning action along the micro channels as shown in Figure 4 in Appendix A.3. The movement of the capillary straw within the channels and the weight of the water create negative pressure that speeds the water into the collection pipe and, additionally, helps to suck up more water into the system. The siphoning action will continue draining the soil provided that there is an effective capillary straw within the soil i.e. when the belt is on a slight slope, or where there is a “tail” of the belt to create a head. This

siphoning action becomes greater, as the angle of descent increases. An illustration showing how the Capiphon works is presented in Figure 5 in Appendix A.3.

Sileshi et al. (2010a) and (2010b) have established that Capiphon is less likely to block over time, as gravity would allow particulates to fall out. However, plant roots may enter and clog micro siphon channels if the Capiphon is used in a rainwater garden.

Fenn (2012) compared the performance of Capiphon with Drain Coil in water and soil. In saturated soil, Capiphon consistently started flowing earlier, flowed longer and delivered a greater volume of water than Drain Coil. It also had a higher flow-rate in free water at low hydraulic head. Therefore, in certain circumstances, there may be a potential advantage of using capillary removal of water over gravity drainage based methods, which are susceptible to blockage and stop flowing at low hydraulic heads. Although the performance of Capiphon in water and in saturated soil is examined and it showed promising results, the current capillary drainage technology is not really capable of lifting water to a great height and is prominently dependent on syphonic action to drain water. While the proposed method by this study works based on capillary action and evaporation to remove water and is capable of lifting water to a greater height.

1.7 *The Aim and Objectives of the research*

The aim of this study was to experimentally assess the use of capillary action to control soil moisture content. This was achieved through the following objectives:

1) Review literature to ascertain state of knowledge moisture transport mechanism of a liquid in capillaries.
2) Develop and apply a laboratory testing apparatus and methodology to evaluate capillary rise of water in soils and the effect of removal of water by the action of wind from the soil surface on the extent of capillary rise.
3) Further develop and apply capillary test set up to improve the height of capillary rise and the volume of water that could be drawn up by capillary action.
4) Develop and apply a laboratory testing apparatus and methodology to assess the feasibility of using a capillary column to draw up water from a free water surface to a higher level where water is removed by wind action with a view to continuously remove water.
5) Develop and apply a laboratory testing apparatus and methodology to evaluate the effect of wind, soil type, and moisture content on loss of water from soils.

1.8 *Scopes and limitations of the study*

In this study, the vertical movement of water is only investigated. The horizontal movement of water is also important and requires further investigation. Furthermore, distilled water is used as the groundwater of the soils.

The economic aspects of implementation of this technique for field application are not assessed in this study.

2 LITERATURE REVIEW

This chapter presents theoretical considerations of capillary rise and mechanisms of water movement in soils, primarily through capillary action. It also provides a summary of previous experimental studies on capillary rise related to the research.

2.1 *Physical properties of soils*

2.1.1 Soil type based on particle size

The type of a soil is referred to the relative percentage by mass of sand, silt and clay size particles in a sample of soil. A soil can be classified based upon the size fraction ratios. Clays have particle sizes less than 0.002 mm. Silts have particles with diameter ranges between 0.002 and 0.063 mm. Sands have particles with diameter ranges between 0.063 and 2.0 mm. Table 2.1 shows the soil type classification based on their particle size diameters according to BS 5930:1999.

Table 2.1 Soil type classification based on their particle diameters (mm) according to BS 5930:1999

Soil group	Soil type	Particle diameters (mm)
Very Coarse Soils	BOULDERS	> 200.0
	Larger boulder	> 630.0
	Boulder	200.0 – 630.0
	COBBLES	63.0 – 200.0
Coarse Soils (over about 65% sand and gravel sizes)	GRAVEL	2.0 – 63.0
	Coarse	20.0 – 63.0
	Medium	6.3 – 20.0
	Fine	2.0 – 6.3
	SAND	0.063 – 2.0
	Coarse	0.63 – 2.0
	Medium	0.2 – 0.63
	Fine	0.063 – 0.2
Finer Soils (over about 35% silt and clay sizes)	SILT	0.002 – 0.063
	Coarse	0.02 – 0.063
	Medium	0.0063 – 0.02
	Fine	0.002 – 0.0063
	CLAY	< 0.002

2.1.1 Soil particle density

One of the important physical properties of soil is particle density, also called specific gravity. This is generally represented by the symbol ρ_p and is also known as density of soil solids or true density. The definition of particle density states that it is the ratio of the mass of the soil solids to its volume as expressed in Equation 2.1 (Fredlund and Rahardjo, 1993).

$$\text{Particle density} = \frac{\text{Mass of soil solids}}{\text{Volume of soil solids}} = \frac{M_s}{V_s} = \frac{M}{L^3} = \frac{g}{cm^3} = \frac{Mg}{m^3} \quad \text{(Eq. 2.1)}$$

For mineral soils, particle density does not vary much because the dominant minerals are silicate minerals (quartz, feldspar, mica). If the particle density of mineral soil is unknown, it is usually taken as 2.65 g/cm^3. It is stated to vary between 2.6 and 2.7 g/cm^3. It is also stated to follow the order sand $<$ silt $<$ clay (Shukla, 2014). The presence of iron oxides and heavy metals, such as magnetite, limonite, or hematite, can increase the value of particle density. Conversely, the presence of solid organic materials can decrease particle density.

2.1.2 Soil bulk density

Soil bulk density is defined as the ratio of the mass of soil to its total volume. The total volume consists of the volume of soil solids (organic and inorganic) and the volume of pores (water filled and air filled). Soil bulk density could be classified as wet soil bulk density and dry soil bulk density. The numerator in wet soil bulk density determination consists of the total in situ mass of soil, including the mass of soil solids as well as the mass of the water in the soil, as shown in Equation 2.2 (Fredlund and Rahardjo, 1993; Shukla, 2014).

$$\text{Wet bulk density} = \frac{\text{Wet mass of soil}}{\text{Total volume of soil}} = \frac{g}{cm^3} = \frac{Mg}{m^3} \quad \text{(Eq. 2.2)}$$

Thus, wet bulk density is not a constant but variable, depending on the water content of soil. In contrast, the numerator in dry soil bulk density determination consists of only the dry

mass of soil solids (organic and inorganic), and thus it is not a function of soil water content, as shown in Equation 2.3 (Fredlund and Rahardjo, 2012; Shukla, 2014).

$$\text{Dry bulk density} = \frac{\text{Dry mass of soil solids}}{\text{Total volume of soil}} = \frac{\text{g}}{\text{cm}^3} = \frac{\text{Mg}}{\text{m}^3} \quad \text{(Eq. 2.3)}$$

In general, the numerator or the mass of soil for bulk density determination is the mass after oven-drying the soil at $105^{\circ}C$ for 24 hours. The dry soil bulk density is also expressed as ρ_b and is more commonly used for most agricultural applications, and unless otherwise stated, bulk density usually refers to dry soil bulk density. The volume of soil usually consists of particles smaller than 2 mm. If coarser fragments (>2 mm) are found in the soil volume, it is essential to subtract the mass and volume of those coarser particles. The volume of coarser particles can be obtained by dividing the known mass of coarser particles by their densities. In engineering applications, coarser fragments are included in bulk density calculations.
The bulk density for most mineral soils is between 1.0 and 2.0 Mg m^{-3}. Several factors that affect soil bulk density include soil type, organic matter content, compaction and porosity (Fredlund and Rahardjo, 2012; Osman, 2013).

2.1.3 Soil porosity

The porosity of soil is defined as the ratio of the volume of the pores filled with water or air to the total volume of soil. It can also be calculated from the known soil bulk density and particle density (i.e. specific gravity), as expressed in Equation 2.4:

$$\text{Soil porosity (P)} = \frac{\text{Total volume of pores}}{\text{Total volume of soil}} = 1 - \frac{\text{Bulk density}}{\text{Particle density}} \quad \text{(Eq. 2.4)}$$

The percentage solid space is calculated as 100-percentage pore space (or porosity). The porosity of soil is inversely related to the particle size and decreases with increasing particle size. Thus, clay soils generally have higher porosities compared to silt or sand soils. However, this tendency is not absolute because, particle packing also has an effect on

porosity (Osman, 2013). Large pores are usually associated with rapid movement of water through the soil, and smaller pores are associated with the retention of water inside the pore. Thus, sandy soils can transmit water through them rapidly, and clay soils can store large amounts of water in them.

In the engineering field, instead of total porosity, void ratio is commonly used. Void ratio is defined as the ratio of the total volume of the pores and the volume of soil solids (inorganic and organic), as expressed in Equation 2.5. Void ratio is more appropriate for soils where the volume of the soil does not stay constant, for example, swelling and shrinking types of soils (Shukla, 2014).

$$\text{Void ratio(e)} = \frac{\text{Total volume of pores}}{\text{Total volume of soil solids}} \quad \text{(Eq. 2.5)}$$

The porosity and void ratio are related to each other as follows:

$$P = \frac{e}{1+e} \text{ or } e = \frac{P}{1-P}$$

2.1.4 Soil water content

Soil water content is the quantity of water contained in a given soil mass or volume and denotes the percentage wetness of soil. It can range from extremely dry (or ~ 0) to the value of the porosity at full saturation. Soil water content is also known as soil moisture content. The water content of soil can be expressed on a mass basis and is known as gravimetric soil water content, as shown in Equation 2.6. It can also be expressed on a volume basis and is known as volumetric water content, as shown in Equation 2.7 (Shukla, 2014).

$$\text{Gravimetric water content} = \frac{\text{Mass of water}}{\text{Mass of dry soil}} = \frac{g}{g} \quad \text{(Eq. 2.6)}$$

$$\text{Volumetric water content} = \frac{\text{Volume of water}}{\text{Total volume of soil}} = \frac{cm^3}{cm^3} \quad \text{(Eq. 2.7)}$$

The volumetric water content can be estimated from the known gravimetric water content and soil bulk density, as shown in Equation 2.8 (Fredlund and Rahardjo, 2012).

$$\text{Volumetric water content} = \text{Gravimetric water content} \times \frac{\text{Soil bulk density}}{\text{Density of water}} \qquad \text{(Eq. 2.8)}$$

2.2 *Mechanisms of water movement in soils*

The mechanism that drives the movement of water, in either the liquid or vapor phase, or as mixture of the two, in soils is the gradient of water potential. For unsaturated soil materials, water potential can be cast in either liquid or vapour form. Several distinct physical mechanisms can contribute to water potential in pore water, namely, gravity, pressure, kinetics, and osmosis (Lu and Godt, 2013).

From the second law of thermodynamics (matter moves from high energy places to low energy places), a change in phase from liquid water to vapour in soil pores will occur if a gradient in potential exists. If the total water potential of pore water is greater than the vapour potential, evaporation will occur. By the same thermodynamic equilibrium concept, within each of the phases, if a gradient exists in the total potential, liquid or vapour flow will occur (Lu and Godt, 2013).

The total potential (in terms of head) is the energy stored in liquid pore water that is available to drive fluid motion in the absence of any chemical reaction. The total potential is often simplified using the superposition principle, so that it can be expressed as the sum of the head(s), h_t, as shown in Equation 2.9:

$$h_t = h_m + h_g + h_o + h_\upsilon \qquad \text{(Eq. 2.9)}$$

Where h_m, h_g, h_o and h_υ are the heads due to pore-water pressure, gravity, osmosis and kinetic energy respectively.

Among the four possible mechanisms for energy or potential to be stored in pore water,

kinetic energy h_υ is typically negligible, as the velocity of most subsurface flow is less than 10^{-3} m/s and thus the corresponding kinetic energy ($\upsilon^2/2g$) is generally small, less than 10^{-7} m in terms of head. Thus, the three other mechanisms are important. The importance of gravitational and pressure mechanisms in a hillslope is illustrated in Figure 2.1 (Lu and Godt, 2013).

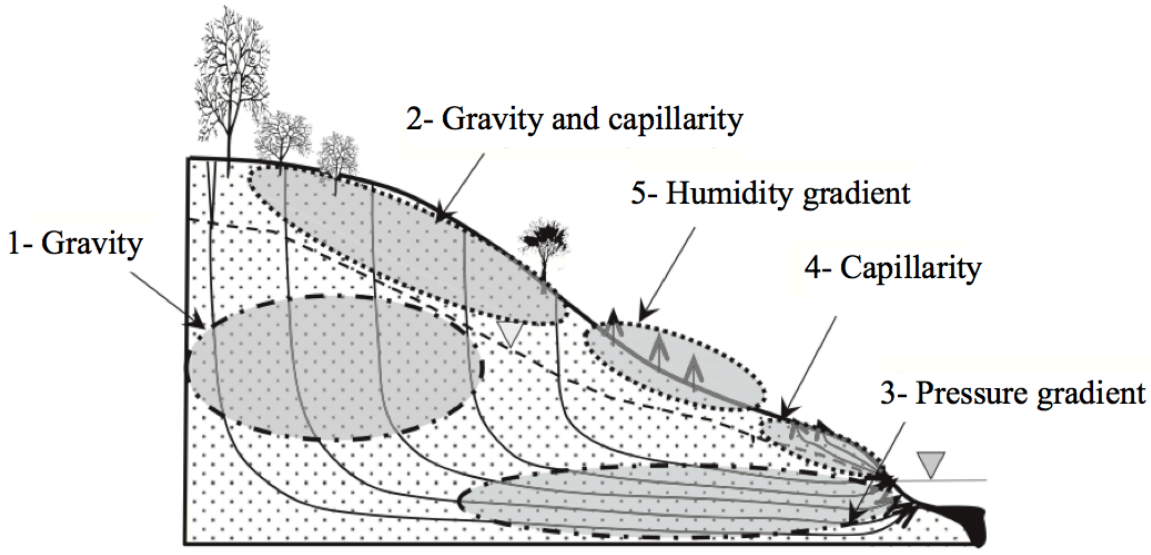

Figure 2.1 Diagram of the major water potential processes (gravitational and pressure) in a humid hillslope with a perennial channel (after Lu and Godt, 2013).

In a soil profile such as that illustrated in Figure 2.1, (1) gravity drives the flow of liquid water in the unsaturated zone predominantly in the downward direction (infiltration) invariant of time and location. (2) At the proximity of the ground surface, both gravity and the gradient of pore-water pressure (also known as capillarity in unsaturated soil) can cause significant water movement in both horizontal and vertical directions. (3) In the saturated zone, the geometry of the soil profile such as that illustrated in Figure 2.1 often results in the horizontal movement of water due to the existence of a pressure gradient between a stream located at the toe of the slope and the hillslope above. (4) Capillary rise can cause upward seepage in the unsaturated zone near a stream. (5) Evaporation and transpiration can induce significant

upward water vapour movement near the ground surface if the gradient of relative humidity between the atmosphere and subsurface is high (Lu and Godt, 2013).

The total potential is commonly described in three inter-changeable units: length (m), pressure (Pa), and chemical potential (J/mol), as shown in Equations 2.10, 2.11 and 2.12, respectively. They are inter-changeable in that they are defined by the same physical concept; i.e. the ability of a unit of water to store energy. They differ in the way a unit of water is defined. In the case of head potential, it is defined as energy per unit weight of pore water, as shown in Equation 2.10:

$$h_t = \frac{\text{force} \times \text{distance}}{\text{force}} = \text{distance} = [\text{m}] \qquad \text{(Eq. 2.10)}$$

In the case of pressure potential, it is defined as energy per unit volume of pore water, as shown in Equation 2.11:

$$\psi_t = \frac{\text{force} \times \text{distance}}{\text{volume}} = \frac{\text{force}}{\text{distance}^2} = \frac{[\text{newton}]}{[\text{m}^2]} = [\text{Pa}] \qquad \text{(Eq. 2.11)}$$

In the case of chemical potential, it is defined as energy per unit mass either in moles or kilograms, as shown in Equation 2.12:

$$\mu_t = \frac{\text{force} \times \text{distance}}{\text{mole}} = \frac{[\text{J}]}{[\text{mol}]} \quad \text{or} \quad \mu_t = \frac{\text{force} \times \text{distance}}{\text{mass}} = \frac{[\text{J}]}{[\text{kg}]} \qquad \text{(Eq. 2.12)}$$

2.2.1 Pressure potential

Pressure potential explicitly accounts for energy stored in pore water under pressure. For soil water below the water table, pore pressure is compressive, thus it stores more pressure energy than water at ambient atmospheric pressure conditions (usually about 100kPa at sea level). On the other hand, pore-water pressure above the water table is tensile, thus water in the unsaturated zone stores less pressure energy than water at ambient atmospheric pressure.

Because compressive and tensile pore-water pressures are mutually exclusive, only one term in the total potential, (Eq. 2.9) is necessary. When soil is under unsaturated conditions, pore-water pressure is often called capillary pressure, as the word “capillary” or “capillarity” indicates that the gas, liquid, or/and solid phase(s) of water co-exist in the soil (Lu and Godt, 2013).

Determination of the magnitude of compressive or tensile pore-water pressure (stored energy) under saturated conditions does not require soil properties as it is independent of the type of soil involved. However, determination of the magnitude of tensile pore-water pressure under unsaturated conditions does involve soil properties, as it depends on the type of soil and water content (Lu and Godt, 2013).

Soil suction also called matric suction, is defined as the pressure difference between the ambient air and pore water. It is a combination of two quite different physical mechanisms; meniscus curvature or capillarity, which occurs across an air-water interface, and adsorption due to surface hydration, van der Waals attraction, and electrical double-layer interaction, which occurs at and near the solid-water interface. Since clay particles are much smaller than sand and their surface area per unit volume, or specific surface, is much larger, clay has a much higher matric suction or lower water potential than sand under the same volumetric water content. Most soil materials have many oxygen and hydroxide ions near the particle surface. This provides very strong adsorptive forces along the solid surface that attract the hydrogen cations of water. Thus, when the water content of the soil is low, matric suction predominantly results from surface hydration forces. Hydration forces will quickly diminish as the water content increases beyond three water molecular levels and the soil water forms menisci. This yields a matric suction of several thousands of kPa. At higher water contents, capillarity starts to take over. As the soil becomes wetter and wetter towards full saturation,

the area of the air-liquid interface diminishes and matric suction reduces to nearly zero. The relationship between water content and matric suction in soil is controlled by the particle surface area and pore structure. Because particle surface area and pore structure vary from soil to soil, each soil has a unique constitutive relationship between matric suction and soil water content. This constitutive relationship is known as the Soil Water Characteristic Curve (SWCC) or Soil Water Retention Curve (SWRC) as shown in Figure 2.2. When the water content is low, surface hydration (the ability of the solid surface to attract water molecules) dominates, leading to a much lower potential (negative) relative to free water. This state of water retention is also called the pendular regime. As the water content increases (middle panel), menisci or capillary water increases and both capillary and hydration effects are present. Eventually, as more water is drawn into the complex, the capillary effect is the dominant mechanism of water storage and water movement in soil (Lu and Godt, 2013).

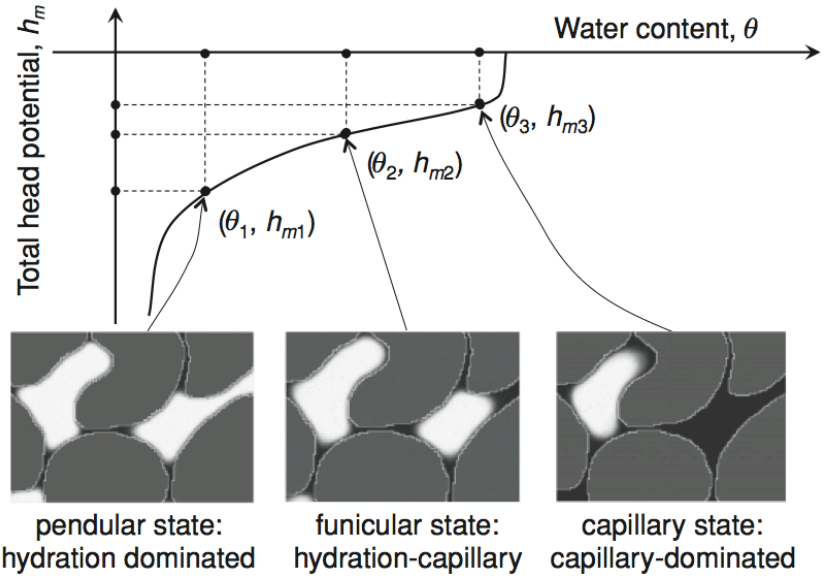

Figure 2.2 Diagram of the general relationship between water content and total head potential (after Lu and Godt, 2013).

2.3 *Development of surface tension at the gas-liquid interface*

The molecules inside bulk liquid experience equal forces in all directions because of the surrounding molecules, as shown in Figure 2.3. These forces are attractive and repulsive forces. In general, the attractive forces are the dominant ones since the repulsive forces have much shorter ranges and are only important at very high external pressures (Hunter 2001). The resultant force averaged over a macroscopic time will be zero (Isenberg 1992). Therefore the molecules inside bulk liquid experience no unbalanced net force. On the other hand, the molecules near the surface of the liquid (i.e. at the air-water interface) have a reduced number of neighbours thus experience unbalanced attractive forces with a downward resultant force pulling them back into the bulk of liquid (Figure 2.3). For a molecule to move from interior to surface and to stay at the surface, it must do work against this force to gain excess energy over the molecules inside the bulk liquid. Accordingly the energy of the molecules at the air-water interface is greater than those inside the bulk liquid (Brown 1947). This excess energy (surface free energy) is known as the surface tension, which is measured as the tensile force per unit length of the air-water interface (N/m) (Fredlund and Rahardjo, 2012). Surface tension can be defined as the energy stored per unit area of the interface.

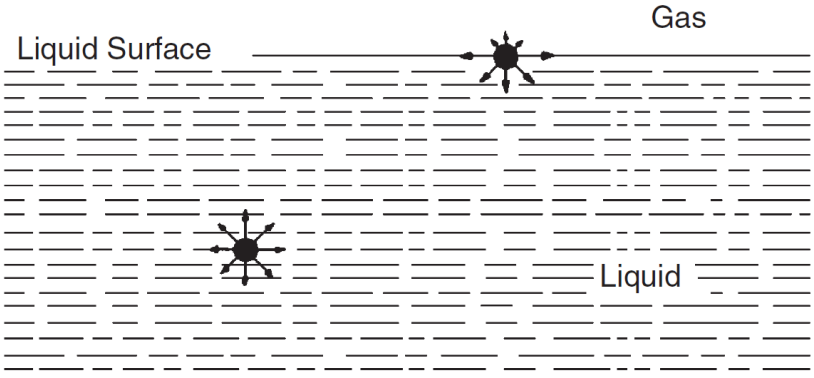

Figure 2.3 Development of surface tension at the gas-liquid interface (after Hillel, 2004).

The interaction of a molecule with its surrounding molecules results in a decrease in its potential energy. The molecules at the liquid surface have a smaller number of nearest neighbours and therefore they possess higher potential energy than the molecules inside the bulk liquid (Brown 1947). According to the principle that every system moves to a state of minimum potential energy, if free to do so, the surface molecules will continue to move inside the liquid until the decreased number of molecules at the surface build up a pressure gradient in opposition to the inward attraction of molecules (Brown 1947). This is the reason that the surface area tends to decrease. Eventually, the repulsive forces between the molecules act opposite to this surface contraction to prevent a complete inward "collapse" of the liquid (Temperley and Travena 1978). In other words, intermolecular forces act to stabilize the system (Pellicer et al. 1995). The smallest surface area and thus the lowest energy content for a given mass of water is that of a sphere. Consequently, the meniscus of water in a capillary is, in general, assumed to be the spherical shape (Sophocleous, 2010).

2.4 *The importance of wetting on capillary rise*

2.4.1 Pressure difference across an interface and contact angle

The Liquid (L) – Vapour (V) interface can be (a) horizontal, (b) concave to liquid phase, and (c) convex to liquid phase (Fig. 2.4). In case of a curved liquid-vapour interface, the resultant surface tension force normal to the L–V interface generates a pressure difference across the interface, which is given by the Young-Laplace equation (Eq. 2.13). The pressure at the concave side of the interface is greater by an amount, which is dependent on the surface tension of the liquid and the radius of curvature of the meniscus (Or and Wraith 2002; Or and Tuller 2005).

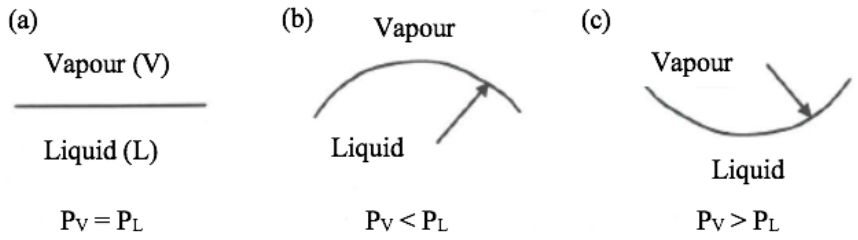

Figure 2.4 Pressure difference across three liquid-vapour interfaces: (a) horizontal, (b) concave to liquid, (c) convex to liquid (after Shukla, 2014).

$$\Delta P = \gamma_{LV}\left(\frac{1}{R_1} + \frac{1}{R_2}\right) \quad \text{(Eq. 2.13)}$$

Where γ_{LV} represents as the liquid-vapour surface tension, R_1 and R_2 are the two principal radii of curvature of the interface, and $\Delta P = P_V - P_L$ for an interface concave to vapour phase (e.g. water in a capillary) or $\Delta P = P_L - P_V$ for an interface concave to liquid phase (water droplet in air); P_V and P_L are the vapour and liquid pressures, respectively. For a hemispherical liquid–vapor interface with a radius of curvature equal to R, where $R_1 = R_2 = R$, Eq. (2.13) reduces to

$$\Delta P = \frac{2\gamma_{LV}}{R} \quad \text{(Eq. 2.14)}$$

When an air-liquid surface meets a solid surface, adhesion of the liquid with the solid and the surroundings air interact with cohesion of the liquid. The contact angle, θ (i.e. the angle between the air-liquid surface and the solid surface) is formed as a result of mechanical equilibrium between these interacting forces. The contact angle is usually measured through the liquid, on the line of triple contact i.e. at a point where all three interfaces meet as illustrated in Fig. 2.5 (Sophocleous, 2010).

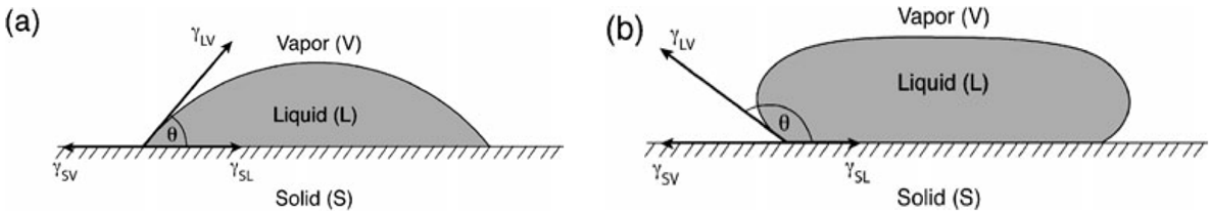

Figure 2.5 Solid-liquid-vapour interfaces and contact angle: (a) hydrophilic surface with contact angle $\theta < 90°$, where liquid wets the solid surface, and (b) hydrophobic surface with $\theta > 90°$, where liquid repels the solid surface (from Sophocleous, 2010).

Thomas Young (1805) argued that the contact angle is derived from a mechanical equilibrium of the forces acting on a unit length of the line of contact (Roura 2007). As illustrated in Fig. 2.5, one force is the surface tension of liquid-vapour interface, γ_{LV}, with its normal and tangential components being as $\gamma_{LV} \sin\theta$ and $\gamma_{LV} \cos\theta$ respectively. The normal component to the surface, $\gamma_{LV} \sin\theta$, would be equilibrated by the adhesion of the liquid molecules to the solid surface. To equilibrate the tangential component, $\gamma_{LV} \cos\theta$, an interfacial surface tension for the solid–vapor, γ_{SV}, and solid–liquid, γ_{SL}, must be introduced. The equilibrium of these forces parallel to the solid surface (Fig. 2.5) results in the Young's equation (1805) or Young-Dupré equation, for a perfectly smooth surface as shown in Equation 2.15:

$$\gamma_{LV} \cos\theta = \gamma_{SV} - \gamma_{SL} \qquad \text{(Eq. 2.15)}$$

Where γ_{SV}, γ_{SL} and γ_{LV} represent as the solid-vapour, solid-liquid and liquid-vapour surface tensions respectively.

This equation indicates that whenever $\gamma_{SV} > \gamma_{SL}$, $\cos\theta$ is positive, indicating that the value of the contact angle for the liquid is $< 90°$ so that the liquid will wet the solid. In other words, when adhesive forces between water molecules and a surface (a solid or a soil pore) are stronger than cohesive forces between water molecules, capillary attraction allows

entry of water in the pore space. Such types of surfaces (or soils) are known as hydrophilic soils. On the other hand, whenever $\gamma_{SV} < \gamma_{SL}$, $\cos\theta$ is negative indicating that the value of the contact angle is $> 90°$ (between $90°$ and $180°$), so that liquid will not wet the solid. In other words, when cohesive forces are stronger than the adhesive forces, the surface repels water (capillary repulsion preventing water from entering soil pores) and is known as the hydrophobic surface. Hydrophobic soils restrict the entry of water into the soil, and water can sit on the surface as droplets for a long time (Shukla, 2014).

In Eq. 2.15, it is assumed that (1) the solid phase is an ideal one; (2) the liquid phase is pure; and (3) the adsorption of vapour to the solid is negligible (Gilboa et al. 2006; Kwok and Neumann 1999). Consequently, Eq. 2.15 has a limited use for the study of soil-water behaviour since soils are heterogeneous, deformable, irregularly shaped, rough, elastic, anisotropic and may react with a wetting liquid (Bachmann et al. 2003), thus γ_{SV} and γ_{SL} are very difficult to measure in soil; in spite of this, Young's Equation (Eq. 2.15) is considered to be the start point for the study of soil surface properties.

Orowan (1970) indicated that $\gamma_{SV} - \gamma_{SL}$ in Eq. (2.15) must be interpreted as a difference in surface energies (more correctly "free" surface energies to represent as the "mechanical" energies stored per unit area of surface, free to do mechanical work), corresponding to the tangential stresses exerted by the solid on the segment of adjacent liquid (Sophocleous, 2010).

2.5 *Capillarity*

2.5.1 Theoretical considerations of capillary rise

According to Ehlers and Goss (2003), adhesion and cohesion forces cause water to rise in a glass tube and in the pores of a soil. The adhesion forces attach water molecules to the solid surface, cause the rise in a capillary, and the cohesion forces makes all the water molecules to stick together and follow the upward pull. The concave to air curvature in a capillary tube shows that the pressure below the surface of the water (below the air-water interface) is smaller than the surrounding normal, atmospheric pressure; In other words, indicates a sub-atmospheric or "negative" pressure in the water.

McCaughan (1987), Tabor (1991) and a number of researchers suggested that water is driven up the capillary due to the pressure difference at the meniscus across the air-water interface. Followed by McCaughan (1987) and ignore air (and vapour) pressure, $P_A = P_C = 0$, and by Pascal's principle, $P_C = P_D = 0$ (Fig. 2.6a), where P_A represents as the pressure at point A, just below the meniscus in the capillary, and P_D and P_C represent as the pressures at the liquid reservoir level inside and outside the capillary, respectively (Fig. 2.6a). Subsequently, $P_B < P_A$, where P_B is the pressure at point B just below the central surface of the meniscus in the capillary, thus $P_D > P_B$ and an existing pressure gradient produce an upward force acting on the entire bulk of liquid column opposite to a downward resisting force exerted by the weight of the liquid column (Fig. 2.6a). This can be expressed quantitatively based on the Newton's second law as Equation 2.16:

$$(P_D - P_B - \rho gh)\pi r^2 = 0, \qquad \text{(Eq. 2.16)}$$

Where ρ is the density of liquid, g is the acceleration due to gravity, r is the radius of capillary, and h is the height of the raised liquid in the capillary.

From Eq. (2.14), $P_A - P_B = \frac{2\gamma_{LV}}{R} = P_D - P_B$. By substituting $\left(\frac{2\gamma_{LV}}{R} - \rho g h\right)\pi r^2 = 0$ is obtained. As illustrated in Fig. 2.6 $\cos\theta = r/R$. By substituting and rearranging, the height of rise of liquid in a capillary can be given by the following formula:

$$h = \frac{2\gamma_{LV}\cos\theta}{\rho g r} \qquad \text{(Eq. 2.17)}$$

In the stated approach by McCaughan (1987), the liquid in the curved part of the meniscus that stands higher than point B is not taken into consideration (Fig. 2.6a) (Sophocleous, 2010).

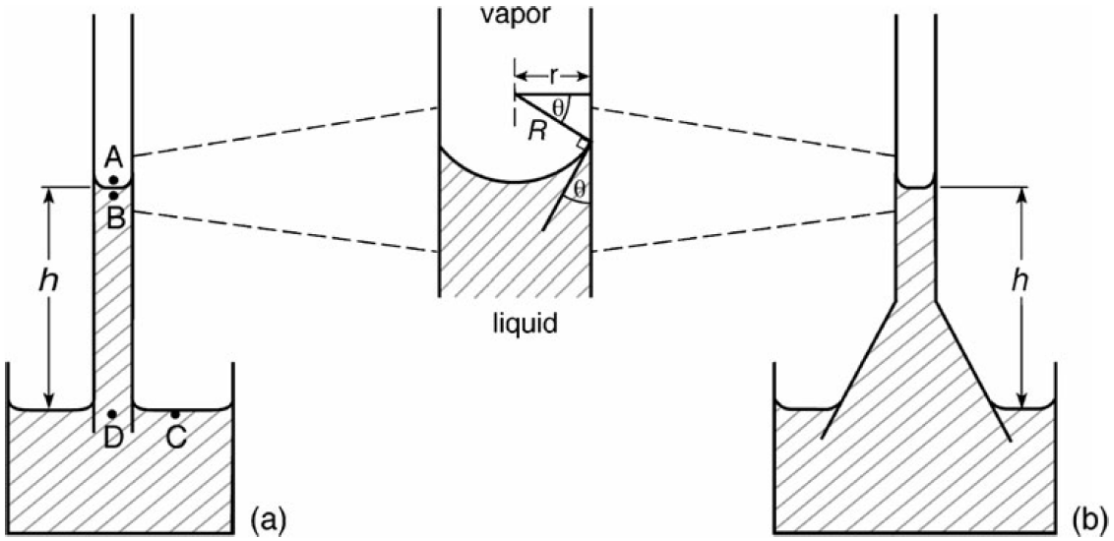

Figure 2.6 The rise of liquid (a) in a straight and (b) in a conical capillary of radius r at the meniscus (after Sophocleous, 2010).

Tabor (1991), experimentally observed that in a capillary with a conical shaped base, the same result could be obtained (Fig. 2.6b). However, the situation in the conical or other shaped capillary is stable only if the liquid is at first sucked up to height h and afterwards the means of suction is removed because the liquid would not be able to pass through the wider parts of the conical or other shaped capillary on its own. According to Hunter (2001), from this point of view, only the radius across the meniscus is taken into account to determine the

height of raised liquid that can be supported in a capillary (Sophocleous, 2010).

McCaughan (1992) provided further explanatory comments on capillary rise as follows. In a capillary, the pressure below the curved surface is lower than the pressure above the curved surface. When a capillary is immersed in a large reservoir of a liquid, the liquid just below the curved surface in the capillary is, at first, at the same level but a lower pressure relative to the liquid at the flat surface of the reservoir, which has a pressure equal to that just above the curved surface in the capillary. As a result of this external pressure gradient, the liquid is drawn up the capillary and the column of liquid is pushed upward (Sophocleous, 2010).

Following the prior explanation of the capillary rise, the question is raised that why the higher pressure above the liquid in the capillary has no tendency to push the liquid down? This definitely would have occurred if the liquid-vapour interface were acting similar to a piston. Bikerman (1970) suggested two satisfactory answers to this question using the similar relationships between the molecular and gravitational forces, as well as the surface tension and the tension of an inflated rubber balloon which are explained as follows:

(1) Due to the gravitational forces, the deeper layers of the Earth are subjected to a higher pressure, however this excess pressure does not tend to push the Earth–atmosphere interface toward the atmosphere. (2) The pressure inside an inflated balloon is greater than the outside pressure by $2\gamma/R$, however a decrease in radius, R, has no tendency to swell and push the walls out as it is exactly compensated by the stresses in the rubber envelope. In other words, an increase in volume would require an increase in the area, which is not favourable in terms of energy (Bikerman 1970).

According to Tabor (1991), in some textbooks, capillary rise is explained by the mechanical equilibrium of the surface forces (i.e. surface tension of the liquid) around the periphery of the meniscus and the weight of the raised liquid in a capillary (Fig. 2.7c). For

straight-wall capillaries at the meniscus, there is an upward force, $2\pi r\,\gamma_{LV}\,cos\,\theta$ (where $2\pi r$ is the peripheral length of the meniscus and θ is the contact angle) that is balanced by the downward force exerted by the weight of the raised liquid, $mg = \rho Vg = h\pi r^2\rho g$. Therefore, $h = \frac{2\gamma_{LV}\cos\theta}{\rho g r}$, a result already obtained in Eq. (2.17). The mechanical interpretation of capillary rise given in the above approach and in a number of textbooks (Bear 1979; Sears et al. 1982; Kane and Sterheim 1984; Snow and Shull 1986; Miller and Schroeer 1987; Giancoli 1988; Marshall and Holmes 1988; Tipler 1991; Fredlund and Rahardjo 1993; Hillel 1998; Jury and Horton 2004; Lu and Likos 2004a; Kirkham 2005; Fredlund 2012; Shukla 2013 and others), only consider the liquid-vapour surface tension and the capillary rise is explained by the mechanical equilibrium of the surface tension of the liquid, γ_{LV}, and the weight of the raised liquid in a capillary (Pellicer et al. 1995). The force exerted by the solid walls on the liquid column is then considered as the reaction force exerted by the γ_{LV} on the contact line as illustrated in (Fig. 2.7c). The equation of capillary rise is then written as follows (Pellicer et al. 1995),

$$2\pi r\gamma_{LV}\cos\theta = \rho g\,\pi r^2 h, \qquad \text{(Eq. 2.18)}$$

By rearranging, Eq. (2.17) is obtained. Although Eq. (2.17) is correct, it must exist at the meniscus across any curved interface (Tabor, 1991). For instance, Eq. (2.17) is still valid for a conical shaped capillary (Fig. 2.6b). However it should be clear that the upward force (i.e. $2\pi r\gamma_{LV}\cos\theta$) could be significantly less than the downward force (i.e. weight of the conical column of liquid) Fig. 2.6b.

Pellicer et al. (1995) suggested a different mechanical equilibrium approach to arrive at the equations of capillary rise. In the following approach not only the surface tension of liquid at the liquid-vapour interface but also the surface tension forces of the solid-liquid and

solid-vapour interfaces, which act on the line of triple contact, and the weight of the column of liquid, are taken into account (Figures 2.7a, and 2.7b).

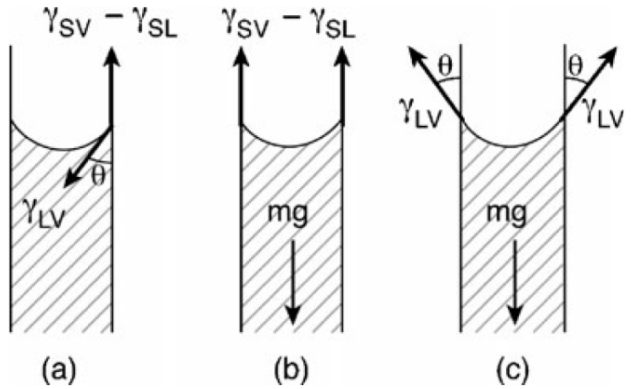

Figure 2.7 Balance of forces in capillary rise: (a) equilibrium of the line of triple contact (Eq.2.15); (b) equilibrium of the column of liquid (Eq.2.19); and (c) equilibrium conditions frequently represented in the textbooks of physics (Eq.2.17) (after Pellicer et al., 1995).

Two conditions of mechanical equilibrium are therefore required to obtain the equations for capillary rise, which are as follows. (1) The equilibrium of the column of liquid and (2) the equilibrium of the line of contact (Pellicer et al. 1995). Considering the column of liquid in (Fig. 2.7b), the force exerted by the solid walls on the column of liquid, $(\gamma_{SV}-\gamma_{SL})\,2\pi r$, must be balanced by the weight of the column of liquid, mg. This is given in Eq. (2.19):

$$(\gamma_{SV}-\gamma_{SL})2\pi r = mg \qquad \text{(Eq. 2.19)}$$

When $\gamma_{SL} < \gamma_{SV}$, the liquid will rise in the capillary; when $\gamma_{SL} > \gamma_{SV}$ the liquid will drop in the capillary. By substituting $m = \rho V = \rho\pi r^2 h$ into Eq. (2.19) and rearranging, the capillary rise can be expressed in terms of difference in surface free energy as shown in Equation (2.20):

$$(\gamma_{SV}-\gamma_{SL})2\pi r = \rho\pi r^2 hg \rightarrow h = \frac{2(\gamma_{SV}-\gamma_{SL})}{\rho g r} \qquad \text{(Eq. 2.20)}$$

Consequently, it is clear that the difference in the surface tensions of the solid-vapour and solid-liquid interfaces is the driving force for capillary rise. In other words, the difference in surface free energies, $\Delta\gamma^s = (\gamma_{SV} - \gamma_{SL})$, cause the liquid to rise in the capillary if $\Delta_\gamma^s > 0$ i.e. if the liquid has a tendency to wet the solid surfaces of the capillary (Henriksson and Eriksson 2004).

It is worth noting that the surface tension of the liquid, γ_{LV}, or the curvature of the meniscus is not involved in Eq. 2.20. Consequently, according to the mechanical equilibrium approach developed by Pellicer et al. (1995), it is clear that the pressure difference at the curved interface is not the driving force for capillary rise (Sophocleous, 2010).

Following Pellicer's et al. (1995) analysis of capillary rise, the second stage is the equilibrium of the line of triple contact as illustrated in Fig. 2.7a that includes changes in the contact angle but not in the mass/volume of the liquid in the column. Subsequently, the surface tension of the liquid, γ_{LV}, and the contact angle, θ, are introduced in terms of the Young's equation (Eq. 2.15). Substituting Eq. (2.15) into Eq. (2.20) will result in the following equation(s):

$$2\pi r\, \gamma_{LV} \cos\theta = \rho g \pi r^2 h \qquad \text{(Eq. 2.21)}$$

Or

$$\frac{2\gamma_{LV}\cos\theta}{\rho g r} = \frac{2(\gamma_{SV}-\gamma_{SL})}{\rho g r} = h \qquad \text{(Eq. 2.22)}$$

Assume that the volume of the curved interface is negligible. Accordingly, the left-hand side of Eq. (2.22) points out that the effects of the solid-vapour and solid-liquid interfacial surface energies are hidden in the contact angle θ (Sophocleous, 2010).

Pellicer et al. (1995), noted a number of weak points in the derivation of Equation (2.17) or (2.21). (1) The physical magnitudes determining the value of the contact angle are not made clear. (2) Equation (2.17) gives the idea that the rise of liquid in the capillary is directly associated with the surface tension of liquid, γ_{LV}, despite the fact that the true force exerted by the solid walls of the capillary on the column of liquid is directly related to the difference in the surface tension forces of the solid-vapour and solid-liquid interfaces, $(\gamma_{SV} - \gamma_{SL})$, as illustrated in Fig. 2.7b, Equations 2.19 and 2.20. (3) According to Pellicer et al. (1995), the direction of the surface tension of liquid-vapour interface, γ_{LV}, in Fig. 2.7c is misleading because the true force exerted by the solid walls on the column of liquid is in the direction of the solid-liquid interface and as a result it is not possible for the solid walls to form an angle θ with the solid-liquid interface (Pellicer et al. 1995). (4) The important role of wetting on the capillary rise is not shown in the derivation of Eq. (2.17), while the action of wetting of the solid surface of the capillary wall is the key factor for the capillary rise due to the fact that the liquid will rise in the capillary when the capillary wall is wetted by the liquid (McCaughan, 1992), otherwise the liquid will drop in the capillary (Sophocleous, 2010).

2.5.2 Source of the energy for capillary rise

Brown (1941) stated that the energy required to set up capillary rise and accompany the movement of the liquid in the capillary is caused by a decrease in free surface energy. Subsequently, the equation of capillary rise given in (Eq. 2.17) may have been established from a mechanical equilibrium of the work done during the motion of the liquid to the loss of free surface energy (Sophocleous, 2010). The potential energy of a raised liquid in a capillary, ΔE_g is given by:

$$\Delta E_g = mgh_{cm} = 1/2\pi r^2 h^2 \rho g \qquad \text{(Eq. 2.23)}$$

Where m represents as the mass of the liquid, ($m = \pi r^2 h\rho$) and h_{cm} is the center of mass of the column of liquid with respect to the free surface in the reservoir of liquid, ($h_{cm} = 1/2h$).

Tabor (1991) suggested that this potential energy is originated from the wetting of the walls of capillary by the liquid. This again indicates the important role of wetting on the capillary rise.

From Young's equation (Eq. 2.15), the equilibrium condition can be written as:

$$\gamma_{SV} = \gamma_{LV} \cos\theta + \gamma_{SL} \qquad \text{(Eq. 2.24)}$$

According to Tabor (1991), in an attempt of the liquid to advance along the tube in order to cover a unit area of the surface (i.e. 1 m^2 of the surface), the area of γ_{SV} would be decreased by one unit area (i.e. γ_{SV} would be decreased by 1 m^2), on the other hand, the area of γ_{SL} would be increased by one unit area (i.e. γ_{SL} would be increased by 1 m^2). The area of the meniscus at the liquid-vapour interface, γ_{LV}, would not change for a constant cross section of capillary. When an area of the wall of the capillary equal to $2\pi rh$ is wetted, the reduction in free surface energy or the energy given up by the system would be given by $2\pi rh\,(\gamma_{SV} - \gamma_{SL})$ or, by Young's equation, $2\pi rh\gamma_{LV}\cos\theta$. Therefore, each unit area (i.e. each 1 m^2) of wetted surface by capillary may release an energy equal to $\gamma_{LV}\cos\theta$. Consequently, the energy, ΔE_γ, released for a liquid to rise to a height h in a capillary tube of radius r is as follows:

$$\Delta E_\gamma = \gamma_{LV} \cos\theta\, 2\pi rh \qquad \text{(Eq. 2.25)}$$

The liquid would rise in a capillary as a result of a decrease in the area of liquid-vapour interface or the reduction in the interfacial energy of liquid-vapour interface can be considered as the force that pulls the liquid up in a capillary against gravity (Sophocleous,

2010).

Outside the tube, the weight of the elevated liquid acts as the resisting force to prevent further rise of the liquid on the outside wall surface, thus essentially, it is not physically possible to reduce the area of the liquid-vapour interface and the capillary rise is ceased. On the other hand, inside the capillary, it is possible to reduce the liquid-vapour interfacial area by filling the capillary with water (Koorevaar et al. 1983) because the resisting force against capillary rise exerted by the weight of the raised liquid is reduced due to the small diameter capillary bore. Koorevaar et al. (1983) suggested that the walls of the capillary are covered with an extremely thin film of water, also known as the capillary layer just above and below the water level in the capillary. Therefore, once the walls of capillary are initially wetted, the interfacial energy of solid-liquid interface would remain unchanged independent of the height of capillary rise. Consequently, according to Koorevaar et al. (1983), water will carry on flowing into the capillary until the interfacial energy of the air-water interface is reduced. This take place once the increased volume of raised water being equivalent to the increased gravitational energy of that raised water in the capillary (Koorevaar et al. 1983).

By Substituting Eq. (2.17) into Eq. 2.25, the loss of free surface energy of the system, ΔE_γ, can be expressed as:

$$\Delta E_\gamma = \pi r^2 h^2 \rho g \qquad \text{(Eq. 2.26)}$$

The resultant loss of free surface energy of the system, ΔE_γ, Eq. (2.26), is exactly twice the gained potential energy by the liquid in the raised column, ΔE_g, Eq. (2.23). This suggests that a non-viscous liquid would rise to a height 2h and fluctuate between 0 and 2h with its mean position at h (Tabor 1991). In fact viscosity can practically consume the excess energy very quickly. According to Tabor (1991), the behaviour is very similar to a vertical spring,

which a weight is suddenly being attached to its end. Instantaneously the weight falls to make double its equilibrium double the initial value and fluctuates between this value and zero until the kinetic energy is gradually decreased and used up by friction and finally the static equilibrium is achieved (Sophocleous, 2010).

2.5.3 Concluding considerations on capillary rise

From the literature it can be understood that equating the force of surface tension γ_{LV} around the circumference of the meniscus to the weight of the liquid column in a capillary tube is a misleading approach. Sophocleous (2010) suggested the following explanatory statements to qualitatively explain the capillary rise based on phenomenon of surface energy.

When a capillary is immersed in a container of a liquid that has a tendency to wet a solid surface and adhere to the solid walls of the capillary, vapour molecules, escaping from the liquid, will adsorb to the solid wall surfaces, developing an extremely thin film of that liquid known as capillary film, on the solid surface just above the liquid-vapour interface. The bulk liquid tends to cohere to this capillary film. Cohesion forces between the molecules of bulk liquid and the molecules of thin capillary layer develop a raised meniscus, in the both sides (i.e. inside and outside) of the tube walls. The raised meniscus creates a larger liquid-vapour interfacial area representing relatively high energy (i.e. high potential). The system attempts to move to a state of lower potential energy if there is a possibility to reduce the area of liquid-vapour interface. Outside the tube, the weight of the elevated liquid acts as the resisting force to prevent further rise of the liquid on the outside wall surface, so it is not physically possible to reduce the area of liquid-vapour interface. On the other hand, inside the capillary, the resisting force exerted by the weight of the elevated liquid against the rise of the liquid is smaller due to the small diameter of the capillary so that the liquid will rise to a

higher level. Accordingly, the liquid may rise to a considerable height depending on the diameter of the capillary tube and the rise will cease once the weight of the elevated column of liquid is equivalent to the driving force of capillary rise.

Just above the liquid level in the reservoir, the volume of raised liquid outside the capillary is equal to the volume of raised liquid inside the capillary, however that volume of liquid is elevated to a higher level inside the tube due to the confined bore space of the capillary.

Furthermore, inside the capillary, there is possibility to reduce the area of liquid-vapour interface by filling the capillary with liquid as the liquid has the tendency to wet the solid surface of the capillary. Consequently, an increase in the solid-liquid interface (i.e. capillary rise effect) will result in a decrease in the energy of the system (i.e. liquid-vapour interfacial area). In summary, the rise of the liquid in the capillary against gravity is not caused by the mechanical equilibrium of surface tension of liquid around the circumference of the meniscus and the weight of the liquid in a capillary that must exist across any curved interface. Alternatively, the rise of liquid in a capillary against gravity is caused by the difference in interfacial energy of the solid-liquid and the solid-vapour interfaces ($\gamma_{SL} < \gamma_{SV}$) leading to a decrease in free surface energy. The energy required to set up capillary rise and accompany the movement of the liquid in the capillary is resulted from a decrease in free surface energy, which is balanced by the potential energy of the raised liquid in the capillary.

Despite the fact that using Young's equation in soil has some limitations, in the idea of author, the above statements by Sophocleous (2010) is a respectable attempt to better understand the fundamentals with regards to explaining the mechanism of capillary rise in soils.

2.5.4 Conceptual capillary finger model

The "capillary finger model" or the uniform capillary tube model is a conceptual model, which is often used to explain capillary rise above the water table and the related pore water retention characteristics. Despite the fact that the concept of perfectly uniform tubes in soil is idealistic rather than realistic, the continuous water "fingers" or fringes that develop above the water table can be conceptualized as bundles of capillary tubes with a range of diameters (Lu and Likos, 2004a).

Capillary suction causes water to rise above the water table through the pores of a soil. Immediately above the water table, the pores of a soil are predominantly filled with water and the soil remains essentially saturated, until the air-entry head, h_a, at which air starts to displace water from the pores of a soil. The zone extending from the water table up to the air-entry head is called the capillary fringe zone, as shown in Figure 2.8. The water content within the capillary fringe zone is generally known as the saturated water content, θ_s. With increasing height above the air-entry head, the water content decreases, as a result of a decrease in the number and the diameter of capillary fingers available at a given cross section of the soil column with an increased elevation. Consequently, at relatively large values of suction head (i.e. at relatively high elevations above the water table), very little amount of water, principally in the form of thin films surrounding the particle surfaces is retained by the soil, described by the residual water content, θ_r (Lu and Likos, 2004a).

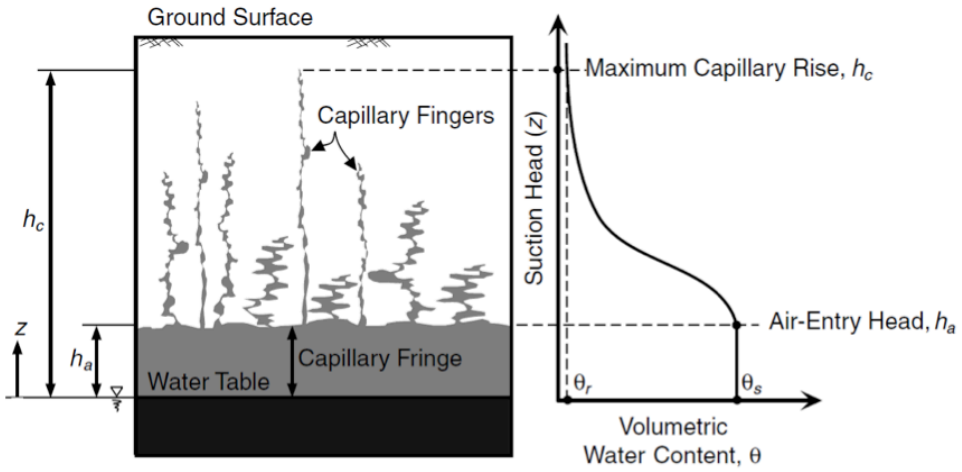

Figure 2.8 Schematic diagram of capillary rise in an unsaturated soil profile along with the related SWCC of moisture profile at hydrostatic conditions (after Lu and Likos, 2004a).

2.5.5 Height of capillary rise in soils

As shown in Fig. 2.8, for a certain type of soil, capillary rise will cease at a certain height h_c, known as the maximum capillary rise, above which the pore water is in discontinuous form. When the action of capillary rise ceases, the total potential head everywhere reaches a constant equal to the potential head at the water table (Lu and Godt, 2013).

Theoretically, the maximum capillary rise, h_c, is directly related to the suction head (i.e., the height above the water table) at which a soil reaches the residual water content, θ_r.

The height of capillary rise is a function of the size of pore space, which is varied for different soils. Generally, among clayey, silty and sandy soils, as particle size increases from clay to sand, the height of capillary rise decreases (Shukla, 2014).

According to Lu and Likos (2004a), analytical evaluation of the height of capillary rise is very difficult due to a non-uniform particle size distribution and complex packing geometry of real soil (Lu and Likos, 2004a). Thus, a number of empirical expressions have been developed in order to better quantify the height of capillary rise in soils and overcome this difficulty by relating the height of capillary rise to more easily measured soil properties

including particle or pore size distribution parameters, void ratio, and air-entry head. Furthermore, the empirical expressions generally assume that an initially dry soil undergoing a wetting process from a stationary water table.

Peck *et al*. (1974) developed an empirical solution in which the height of capillary rise (in mm) is inversely proportional to the product of void ratio, e, and the particle size at the 10% and finer fraction, D_{10}, which can be expressed as:

$$h_c = \frac{C}{eD_{10}} \quad \text{(Eq. 2.27)}$$

Where C is an empirical parameter varying between 10 and 50 mm^2 based on particle shape and impurities of soil surface, e is the void ratio and D_{10} (in mm) is the particle size at the 10% and finer fraction. Eq. 2.27 illustrates that an increase in the average particle/pore size, results in a decrease in the height of capillary rise (Lu and Likos, 2004a).

According to Kumar and Malik (1990), the height of capillary rise (in cm) can be defined as a function of the air-entry head, h_a (cm), and the average pore size, r (μm):

$$h_c = h_a + 134.84 - 5.16\sqrt{r} \quad \text{(Eq. 2.28)}$$

Where h_a (cm) represents as the air-entry head and r (μm) is the average pore size.

Based on the analysis of capillary rise experiments carried out by Lane and Washburn (1946) for eight different types of soil, Lu and Likos (2004a) arrived at an empirical equation in which the height of capillary rise (in mm) can be defined as a function of the particle size (mm) at the 10% and finer fraction D_{10}:

$$h_c = -990\ln(D_{10}) - 1540 \quad \text{(Eq. 2.29)}$$

Equations 2.27 and 2.29 suggest that D_{10} may be sufficient to represent as the effective diameter of the smallest continuous capillary fingers in soil.

According to Lu and Likos (2004a), the most consistent technique to determine the height of capillary rise in soil is by direct measurement using soil column or open-tube tests carried out in the laboratory. Table 2.2 shows a summary of the experimental capillary rise results described in the literature (e.g., Lane and Washburn, 1946; Malik et al., 1989; Kumar and Malik, 1990) on different soils representing an extensive range of soil types. Lane and Washburn (1946), used transparent plastic tubes of 5- and 10-cm diameter and various lengths of up to 400 cm. Malik et al., (1989) and Kumar and Malik (1990), used 200-cm long glass columns of 2-cm inside diameter.

Following the parameters presented in Table 2.2, Maximum capillary rise h_c was determined by manual observation of the wetting front for each type of soil.

Air-entry head, h_a, or the height of capillary fringe was determined from the soil-water characteristic curve, which in turn provided by measuring either the equilibrium water content of the entire soil column or representative specimens as a function of height from the water table.

h_c/h_a is defined as the dimensionless ratio of ultimate height of capillary rise to air-entry head, and its value was found to vary between 2 and 5 with only a few exceptions for a wide range of soil tested.

The theories on the rate of capillary rise in soils are discussed in Appendix B.2.

Table 2.2 Experimental capillary rise parameters in different soil types (after Lu and Likos, 2004a)

Test No.	Soil	Gravel (%)	Sand (%)	Silt/Clay (%)	Clay (%)	Void ratio	h_a (cm)	h_c (cm)	$\frac{h_c}{h_a}$
1	Class 5	25.0	68.0	7.0	–	0.27	41.0	82.0	2.0
2	Class 6	0.0	47.0	53.0	–	0.66	175.0	239.6	1.4
3	Class 7	20.0	60.0	20.0	–	0.36	39.0	165.5	4.1
4	Class 8	0.0	5.0	95.0	–	0.93	140.0	359.2	2.6
5	Ludas sand	–	–	–	–	–	29.1	72.1	2.5
6	Rawalwas sand	–	–	–	–	–	29.6	77.5	2.6
7	Rewari sand	–	–	–	–	–	29.4	60.9	2.1
8	Bhiwani sand	–	–	–	–	–	27.6	65.6	2.4
9	Tohana loamy sand 1	–	–	–	–	–	37.4	117.0	3.1
10	Hisar loamy sand 1	–	–	–	–	–	37.5	149.4	4.0
11	Barwala sandy loam 1	–	–	–	–	–	41.2	158.4	3.8
12	Rohtak sandy loam 1	–	–	–	–	–	48.7	155.7	3.2
13	Hisar sandy loam 1	–	–	–	–	–	47.7	174.5	3.7
14	Pehwa sandy clay loam	–	–	–	–	–	44.5	154.6	3.5
15	Hansi clayey loam 1	–	–	–	–	–	29.6	127.5	4.3
16	Ambala silty clay loam 1	–	–	–	–	–	15.0	141.5	9.4
17	Tohana loamy sand 2	–	89.0	6.0	5.0	0.92	66.7	117.0	1.8
18	Hissar loamy sand 2	–	82.5	11.5	6.0	0.90	72.9	149.4	2.0
19	Barwala sandy loam 2	–	75.0	13.5	11.5	0.94	47.3	158.4	3.3
20	Rohtak sandy loam 2	–	63.0	23.0	14.0	1.01	44.0	155.7	3.5
21	Hissar sandy loam 2	–	63.0	24.0	13.0	0.99	66.0	174.5	2.6
22	Pehowa sandy clay loam	–	55.0	27.0	18.0	1.06	59.6	154.6	2.6
23	Hansi clayey loam 2	–	30.2	26.5	43.3	1.27	16.3	127.5	7.8
24	Ambala silty clay loam 2	–	15.0	49.0	36.0	1.49	16.9	141.5	8.4

Note the following from the above table:

Test No. 1-4: Lane and Washburn (1946): Apparatus consisted of 5- and 10-cm diameter soil-filled tubes of transparent plastic.

Test No. 5-16: Malik et al. (1989); and Test No. 17-24: Kumar and Malik (1990): Test set-up used was 200-cm long glass columns of 2-cm inside diameter.

Parameters used in this table are described in Figure 2.8.

2.6 *Summary of previous experimental studies related to the research*

Buckingham (1907) carried out experiments to demonstrate the links between evaporation and the strength of capillary moisture conduction. He designed a set of experiments to assess the evaporation rate from a soil column in which, the soil columns were supplied with water from the below through capillary conduction for a period of time to simulate a stationary water table at the bottom. Two types of evaporation conditions were simulated. These comprised arid and humid. A current of air was blown over the top surface of the soils by means of an electric fan. To imitate arid conditions, heated air with constant absolute humidity was blown over the columns. To simulate the high surface temperatures of soils under the strong sunshine of arid climates, the electrical coils were used to heat the uppermost section of the soil columns to the same temperature as the heated air. The air stream at about 1.3 m/s was kept throughout the test. The heated current was turned on for six hours a day. The principal outcome from these experiments was that the evaporation or the loss of water from a soil under arid conditions was much more rapid at first, but declined noticeably with time. On the other hand, the evaporation or the loss of water from a soil under humid conditions was less variable over long periods of time so that the total loss or the total cumulative evaporation under humid conditions overtakes that under arid conditions and is thereafter increasingly greater. It thus appears that, under this imitation of arid and humid conditions, the arid conditions have actually established a dry surface layer, which has to a considerable degree protected the soil below it from further loss. These laboratory experiments, therefore, cleared up the field observations in a very satisfactory manner and concluded that during dry seasons, the soils of arid regions, at depths a little below the surface, are generally wetter and hold their moisture for much longer periods than do the soils of humid areas (Narasimhan, 2005).

Lane and Washburn (1946), Malik et al., (1989) and Kumar and Malik, (1990) conducted an extensive experimental investigation on the height and rate of capillary rise using soil column or open-tube tests in the laboratory on different types of soil represented a wide range of textural classes of soils which were summarised in Table 2.2. Lane and Washburn (1946), used transparent plastic tubes of 5- and 10-cm diameter and various lengths of up to 400 cm. Malik et al., (1989) and Kumar and Malik (1990), used 200-cm long glass columns of 2-cm inside diameter. The height of capillary rise in the soil columns was recoded as a function of time until the height of the capillary rise appeared to be constant with time and the capillary rise practically ceased, requiring less than 10 days for the relatively coarse-grained soils and up to 400 days for some of the more fine-grained materials however, the maximum capillary rise in the fine-grained materials was considerably higher than in coarse-grained soils (Lu and Likos, 2004).

Maskong (2010) conducted an experimental study on capillary rise in saline and non-saline soil using 95-cm long soil columns in order to examine capillary rise control of saline groundwater flow. Two soil types of sand and sandy loam were tested. Two types of groundwater including (1) deionized (non-saline) groundwater (DG) and (2) saline groundwater (SG) were used for these experiments. The experimental studies were divided into several different cases as follows: (1) Sand with deionized groundwater (DG) and saline groundwater (SG) (2) Sandy loam with DG and SG (3) Sandy loam with SG and adding artificial sunlight to increase evaporation and (4) Sandy loam with SG and adding water to the surface to stop the capillary process. The results of capillary rise experiments for saline and non-saline sand and sandy loam samples are shown in Figure 1 and Figure 2 in Appendix B.1, respectively. The capillary rise results between DG and SG for sand were similar. For both DG and SG sand samples, the maximum capillary rise was 30 cm, as shown in Figure 1

in Appendix B.1. For sandy loam however, the results between DG and SG were explicitly different, as shown in Figure 2 in Appendix B.1. The maximum capillary rise for DG and SG sandy loam samples were 70 cm and 90 cm, respectively. SG provided high capillary rise, high capillary rate and high soil moisture content (water storage capacity) compared to DG at equal level of soil depth. This is because the sodium ion (Na+) brought by saline water and remaining in the voids between soil particles can absorb more water giving higher moisture content. For sandy loam, soil moisture is accumulated at the soil surface in high water content, compare to the other level of soil depth. If this saline moisture is evaporated by artificial radiation, salt's crystallization will be found on the soil surface. If high soil moisture content on the surface is maintained by adding water to the soil surface of sandy loam, SG movement will be ceased keeping constant high moisture on the soil surface is a potential measure to solve the problem of soil salinity dispersion (Maskong, 2010).

Although the importance of capillary rise for drainage purposes has been recognised, there are limited studies on the applicability of capillary rise to remove water from soil. Experimental setup similar to this study has been used to measure capillary rise or evaporation for other purposes but none studied the applicability of capillary rise to remove water from soil the way this study (Use of Capillary Action to Control Soil Moisture) did. Since the height, and the rate of capillary rise are not considerably high, from practical point of view, the use of capillary rise for removal of water has been pretty much left untried. This study was undertaken to address this. Furthermore there is not a single study, which has been evaluated capillary rise in multi-layered soil systems (based on particle/pore size). This study has been focused on a new insight of capillary rise and aims to generate a natural pump that can continuously lift water against gravity.

2.7 *Evaporation and Evapotranspiration*

2.7.1 General

Evaporation is defined as the process of change of the state of water from liquid to vapour. In the presence of vegetation, evaporation and transpiration are together known as evapotranspiration. Evaporation and evapotranspiration are important components of the water cycle in the hydrosphere. The present study only considers evaporation from non-vegetated surfaces, thus the term "evaporation" will be used exclusively.

2.7.2 Physical Conditions of Evaporation from Soils

Evaporation occurs from open water surfaces, soil surfaces, and plant canopies. Water is also lost due to the root water uptake and transpiration by plants. Evaporation from open bodies of water are dependent on the surface area. The larger the surface area, the higher the evaporation will be. Surface soil conditions also influence evaporation, for example, presence of mulch on the soil surface could decrease evaporation. Other factors that can influence evaporation from soil are soil depth, soil structure, and degree of homogeneity of soil. Soil type also influences the rate of evaporation. More water can be evaporated from saturated clayey soil than saturated sandy soils because more water is stored in a saturated clayey soil than in a saturated sandy soil (Shukla, 2014).

Evaporation from soil can be continued, provided there is enough continuous supply of water from a deeper layer. The available water can be transported upward toward the soil surface so that enough water is always available at the soil surface for evaporation. The amount of water and the supply to the surface depend on the soil water content, soil water potential, unsaturated hydraulic conductivity of soil, soil type, bulk density, soil homogeneity or heterogeneity, and the depth to the water table. If a high water table (near the surface) is present in an area, evaporation can be sustained at a steady state for a long time. If the rate of

evaporation is equal to the rate of replenishment of soil water content from the water table, soil water content does not change, and soil profile is considered in equilibrium with the water table. However, when evaporation rate is higher than the rate of replenishment of water from underlying soil layers, the soil moisture content changes, and soil at the surface gets drier than at greater depths. The water table is usually low in this situation, and there is no hydraulic continuity of water from the water table to the soil surface. Under this condition, the soil profile is not in equilibrium with the water table (Hillel, 2004; Shukla, 2014).

Evaporation can also be continued, provided there is continuous supply of energy, for example, solar energy. The direct or radiated solar energy is required in the form of latent heat (approximately 2.453×10^6 J/kg at 20°C) for evaporation to take place. Once evaporation starts, for it to sustain, there has to be a vapour pressure gradient between soil and the atmosphere so that water vapour from soil can be transported to the atmosphere. The transport of water vapour could take place through the process of diffusion or convection. Usually, vapour transport is external to the soil and depends primarily on meteorological factors such as air temperature, wind velocity, relative humidity, and solar radiation. Environmental conditions have an important influence on evaporation. These external meteorological conditions could be regular, for example, diurnal or annual cycles of temperature and radiation; or irregular, for example, spells of warm and cold weather, drying and rewetting of soil (Hillel, 2004; Shukla, 2014).

In general, the rate of evaporation from wet soil is dependent upon external meteorological conditions, whereas the evaporation rate for drier soils depends on the unsaturated hydraulic conductivity of soil that determines the rate of upward movement of water (Philip, 1957). Water evaporation can be at the maximum rate or potential rate from the wet soil, whereas it is less than potential from the dry soil. The evaporation rate can be initially controlled by the

meteorological factors; however, the control can be shifted to soil factors such as unsaturated hydraulic conductivity. This is particularly true for transient-state evaporation or drying (Hillel, 1980).

2.7.3 Evaporation processes

The evaporation process starts with the transport of water toward the soil surface. The transport takes place due to the hydraulic gradient between the soil surface and a deeper layer that causes upward flow of water through capillary rise. This process continues as long as there is enough water in the soil. Usually, the upward movement is longer after the end of an irrigation or good precipitation event. At or near the surface, water changes its state from liquid to vapour due to the solar energy and the latent heat of vaporisation. The energy balance of the soil depends on the physical and thermal properties of soil. Liquid water can also change its state due to exothermic reactions and microbial activities that can release enough heat to vaporise water. The water vapour diffuses (by the process of convection) to the atmosphere if the vapour pressure inside the soil is greater than the vapour pressure above the evaporating surface (Bruch, 1993; Hillel, 2004; Shukla, 2014).

2.7.4 Stages of evaporation

The evaporation process is divided into three stages: (1) an initial constant rate stage, (2) an intermediate falling rate stage (transition stage), and (3) a residual slow rate stage (Rose, 1968; Idso et al., 1974; Gardner, 1974; Hillel, 1980; Wilson, 1990; Bruch, 1993; Hillel, 2004; Shukla, 2014).

For evaporation to take place at Stage (1), the soil must be wet and there must be enough water available for evaporation at the maximum rate. The rate of evaporation during Stage (1) is controlled by atmospheric conditions (such as incoming solar radiation, wind, humidity, etc.), but not by the hydraulic properties of soil. During this stage, the Actual Evaporation

(E_a) and the Potential Evaporation (E_p) are nearly the same. Hence, Stage (1) is also known as climate-controlled or potential evaporation stage. The evaporation rate can remain nearly constant provided that sufficient water is available (either from the water table or soil storage) and the increase in gradient near the surface compensates for the decrease in the hydraulic conductivity. This stage is sustained because as the soil water content decreases, the hydraulic conductivity decreases, but the gradient across the evaporating surface and soil below it increases and compensates for the reductions in the hydraulic conductivity. A well-structured soil can sustain evaporation at Stage (1) for a much longer duration than a structure-less (less-structured) soil.

The intermediate falling rate stage starts when the soil can no longer supply sufficient water to the evaporative front to satisfy the evaporative demand. At this stage, evaporation is no longer at the potential rate but starts to decrease with time. The process is no longer controlled by atmospheric condition but by the soil profile properties. Hence, Stage (2) is also known as the soil profile-controlled stage. The soil water content is low, and the increase in gradient could not compensate for the decrease in hydraulic conductivity of soil. Soil water pressure at this stage is nearly equal to the partial water vapour pressure; thus the hydraulic gradient may not increase appreciably. As soon as hydraulic conductivity decreases to a level that an increase in gradient can no longer compensate, the second stage of drying starts. The depth of the dry soil profile continuously increases, and the ability of soil to conduct water upward decreases further.

The residual slow rate stage gradually develops as the soil surface becomes desiccated and the primary mode of water movement near the surface is due to vapour diffusion. The third stage of evaporation is usually steady, and evaporation takes place at a low rate and can continue for several days. Liquid water conductance is very low, and the stage is also known

as vapour diffusion stage because water transport is primarily by water vapour diffusion (Hillel, 1980; Bruch, 1993; Hillel, 2004; Shukla, 2014).

2.7.5 Controlling parameters of evaporation from soil surfaces

2.7.5.1 Radiation

The main controlling variable on evaporation is the incoming solar radiation as it provides the latent heat of evaporation required to change the state of water from liquid to gas and thus controls the rate at which evaporation takes place (Matsoukas et al., 2011; Fernández-Prieto et al., 2012). According to Shaw (1994), both solar and terrestrial radiations (also known as shortwave and long-wave radiations respectively) contribute to the evaporation processes (Shaw, 1994). Furthermore, plants also use radiation for photosynthesis and transpiration. That being said, there are a number of additional factors including seasonal changes, day length, latitude, air pollution and cloud cover that can affect the net amount of solar radiation available for evapotranspiration (Briggs and Smithson, 1985).

2.7.5.2 Temperature

The temperature of water surface and the air above it, which are also controlled by incoming solar radiation, may significantly affect the evaporation rate (Petropoulos, 2014). This is because the vapour-holding capacity of the air is actually controlled by them (Meinzer, 1942). In other words, an air parcel at a high temperature will have a higher saturation vapour pressure and will be able to hold more water than an air parcel at a lower temperature (Petropoulos, 2014). Therefore the rate of evaporation will, in general, be higher at higher temperature (Shaw, 1994; Lui et al., 2011). The temperature of water surface also principally controls the rate at which water molecules leave the surface of water and enter the air above it. Consequently, variations in the temperature of

water surface may result in an abrupt change in evaporation rate in the short-term (Ward and Robinson, 2000). In spite of this, Roderick et al. (2009) stated that variations in solar radiation, wind speed and humidity can counterbalance and offset the effect of increasing temperature, based on the data observations of the recent decrease in pan evaporation rates across the globe (Roderick et al., 2009).

2.7.5.3 Wind

Wind is one of the key controlling variables on the rate of evaporation rate as it allows molecules of water to be removed from the soil surface by eddy diffusion (Zheng et al., 2009; McVicar et al., 2012). The removal of water molecules from the surface can maintain the vapour pressure gradient above the surface area by moving the saturated air away from the evaporative surface and bringing air at a different temperature and with a different relative humidity in its place. The efficiency of this process can be controlled by a number of variables including the wind speed; also the rate of mixing which is dependent on the turbulence of the air and the rate of change of wind speed with height and wind movement (i.e. laminar or turbulent) (Briggs and Smithson, 1985). The effect of laminar wind movement on evaporation may not be as significant as turbulent wind movement, particularly over large bodies of water where the temperature of the air (T_a) and the relative humidity is uniform with height. On the other hand, turbulent flow in the canopy layer may have considerable effect on evaporation and can increase evaporation rate by removing water vapour from contact with the water surface (Meinzer, 1942).

2.7.5.4 Humidity

Jones (1997) stated that the evaporation rate at any given temperature is proportional to the difference between the absolute humidity and the saturated humidity. However,

there will only be a slight change in absolute or actual humidity (i.e. the moisture in the air, regardless of temperature) during the course of a day in comparison with relative humidity (the water vapour present in the air expressed as a percentage of the amount that would be present in saturated air at the same temperature) that is a function of temperature and thus is much more variable (Penman, 1968). As the relative humidity of air over an evaporative surface increases, a smaller or limited number of the water molecules leaving the evaporative surface can be retained in the air and therefore the evaporation over that surface decreases (Petropoulos, 2014). Barometric pressure may also have an effect on evaporation rate and can be used to measure changes in evaporation with altitude (Meinzer, 1942; Ji and Zhou, 2011).

2.7.5.5 Soil moisture content

Soil moisture content can have significant effect on evaporation rate to an extent that actual evaporation (i.e. soil water evaporation) may theoretically reach potential evaporation (i.e. free water evaporation) (Bougeault, 1991; Lockart et al., 2012). In general, a decrease in soil moisture content leading to a decrease in soil water evaporation. As soil moisture content decreases to zero, evaporation falls rapidly (Green, 1959). Evaporation from the surface is most significantly controlled by the topsoil moisture, i.e. the soil moisture content of the first top few centimetres of the soil surface. On the other hand, sub-soil moisture is generally slow moving as sub-soil has lower hydraulic conductivity than topsoil due to higher compaction etc. and by itself may have a negligible influence on evaporation rates from the soil surface (Ward, 1975). The texture of a soil may also have a considerable effect on evaporation, with soils with smoother surfaces and finer textures, having thinner boundary layer and enhanced capillary connectivity, allowing higher evaporation rates from the soil surface (Ward, 1975;

Wesseling et al., 2009). Furthermore, soil colour may also have an effect on evaporation rates, with soils with darker colours, having lower albedo (less reflective), absorbing more heat than soils with lighter colours. Soil colour is an indication of chemical compositions in a soil and therefore the ability of soil for water absorption (Petropoulos, 2014).

2.7.5.6 Vegetation

Vegetated surfaces generally comprise a mixture of species (e.g. croplands surrounded by hedgerows), except under rare or specific conditions (e.g. uniformly distributed forests or agricultural crops) (Petropoulos, 2014). On a land surface where there is not continuous vegetation cover, evapotranspiration is equal to the sum of evaporation from the soil and evaporation from the vegetation (transpiration). In general, vegetation will make a reduction in soil water evaporation by shading and covering the soil surface from direct solar radiation and therefore reducing temperatures of the soil surface by decreasing wind speed, and by increasing the relative humidity of the lower layers of the air in the atmosphere (Ward and Robinson, 2000; Breshears and Ludwig, 2010). The density of the vegetation cover is another important plant factor in evaporation from vegetated surfaces, which may also affect evaporation rates significantly (Shaw, 1994; Villegas et al., 2010).

2.8 *Effects of layering of soils on water movements in a soil profile with a water table*

2.8.1 Water movement in homogeneous soils

In the capillary zone of a homogenous soil profile, the soil at proximity of the water table is nearly saturated when hydrostatic equilibrium is achieved during the evaporation process; as the height from the water table increases, the soil water content gradually decreases until it becomes negligible at the upper limit of the capillary rise. As a result, wet and dry zones are introduced to the soil profile from the water table to the soil surface. The interface between the wet and dry zones is known as the evaporation front and the distance from the water table to the evaporation front is termed the capillary fringe or the maximum height of capillary rise (h_{max}) (Fig. 2.9; Shokri and Salvucci, 2011). There is a situation under which the evaporation front is at the soil surface; when the water table rises, a critical depth is introduced where the maximum height of capillary rise equals the water table depth. This depth is known as Evaporation Characteristic Length (ECL), which is the maximum depth at which the water table is hydraulically connected to the soil surface (Fig. 2.9; Lehmann et al., 2008).

Hydraulically, Shokri and Salvucci (2011) suggested that the ECL associates with the pressure head (in terms of length) on the soil water retention curve close to residual water content under hydrostatic conditions. When the water table is lower than the ECL, the soil above the ECL becomes too dry to allow considerable amount of water in liquid form to be transported; thus, the dominant form of water movement through the overlying dry layer would be through vapor diffusion. The matric potential above the evaporation front significantly drops at proximity of the residual water content with no noticeable change in the water content, and the rate of evaporation considerably reduces because there is no hydraulic connectivity within soil above the evaporation front (Steenhuis et al., 2005; Lehmann et al.,

2008; Shokri and Salvucci, 2011).

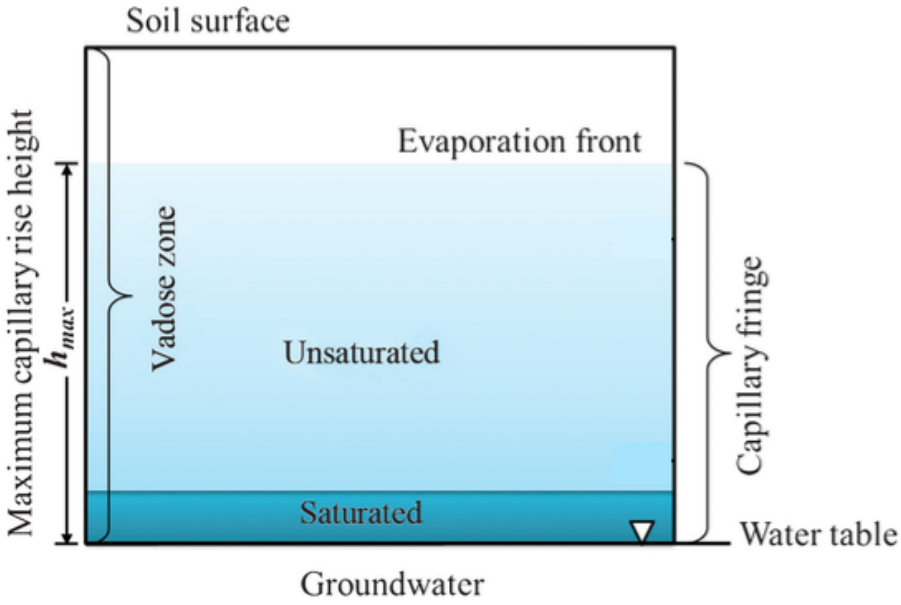

Figure 2.9 Schematic illustration of a soil profile in the presence of a water table (after Li et al., 2013).

2.8.2 Water movements in layered soils

There is a wide distribution of layered soils in the field. According to Phillips (2001), layered soils can be found in the field quite widely and their formation can be through several mechanisms including deposition or inheritance, erosion, bioturbation and surface removal, eluviation–illuviation, or a combination of several of the above mechanisms (Phillips, 2001). Several factors that can affect water dynamics in a layered soil include the inner-layer properties, the thickness of the layers, and their spatial configuration. Layered soils have quite different water dynamics compared to the homogeneous soils due to the discontinuity of their hydraulic properties (Li et al., 2013).

The water movement in layered soils can be affected in two directions: these are (1) the downward infiltration and water redistribution processes, and (2) the upward capillary rise during the evaporation (or evapotranspiration) process. Layering in soil can impede vertical water movement and increase water storage during both infiltration and evaporation

processes (Bruch, 1993; Zornberg et al., 2010; Huang et al., 2011).

2.8.2.1 Downward water movement in layered soils

Soil layering can impede the downward water movement during infiltration and soil water redistribution process. The two phenomena causing water stagnation and increased water storage in layered soils are the capillary barrier and the hydraulic barrier that are jointly known as flow barriers (Alfnes et al., 2004; Si et al., 2011).

The capillary barrier also known as a wick cover is a layer of soil that has the capillary break effect (Bruch, 1993). It is often observed under unsaturated conditions. The capillary break effect generally happens during infiltration, when a fine-grained layer overlies a coarse-grained layer in the soil profile. It is understood from the literature that capillary movement of water and hydraulic conductivity are closely associated with soil particle size (Campbell, 1985). The capillary break effect usually caused by the layer that has a lower hydraulic conductivity than the neighbouring layer under dry conditions (i.e. when the soil is nearly dry), but has a higher hydraulic conductivity under saturated or high moisture conditions (i.e. when there is ample amount of water available in soil or when the soil profile is close to saturation) (McCartney and Zornberg, 2010). If such a soil layering exists in the vertical soil profile, it probably would be the coarse-grained soil layer where there is loss of effective hydraulic connection in this layer when the soil profile is dry and it has much lower hydraulic conductivity than that of the neighboring fine-grained soil layer (it should be noted that when they are close to saturation, the condition is completely opposite). Thus, when during infiltration, water flows from the overlying fine-grained soil layer into the unsaturated coarse-grained soil layer, the infiltrated water is unable to directly cross the interface between the two (i.e. the fine-grained and coarse-grained) layers, because of the weaker water suction and the inefficient unsaturated hydraulic conductivity in the capillary barrier layer (i.e. the

coarse-grained layer). Once the capillary break effect take place, more water will be retained and stored in the upper layer that is expected to normally drain to the deep under the action of gravity if there was no capillary barrier layer; This increases the water storage capacity and the water retention of the overlying fine-grained layer (Li et al., 2013). As the water content in the upper layer increases, the difference between the unsaturated hydraulic conductivities of the fine-grained and coarse-grained layers at the interface decreases. The infiltrating water will percolate the lower (coarse-grained) layer provided that the suction at the interface falls to some degree at which an effective hydraulic conductivity can be established within the lower layer; in this circumstance the capillary break effect disappears (Bruch, 1993; Si et al., 2011).

If the configuration of soil layers is reverse, with a coarse-grained soil layer overlying a fine-grained soil layer, another type of flow barrier will be introduced termed as a hydraulic barrier, which is caused by the weak hydraulic conductivity of the underlying fine-grained soil layer and can also impede water infiltration (Hillel and Talpaz, 1977). Both types of flow barriers (i.e. capillary and hydraulic barriers) can increase lateral soil water movement due to the decreased rate of water infiltrating into the deeper layer particularly if the interfaces are inclined (Si et al., 2011).

2.8.2.2 Upward water movement in layered soils

During the evaporation process, a soil interlayer can either increase or decrease upward water flow depending on its thickness, its hydraulic properties and depth to the water table. The capillary break effect, which decreases the rate of upward water flow, can also happen during the evaporation process, when a coarse-grained soil layer overlies a fine-grained soil layer (Bruch, 1993; McCartney and Zornberg, 2010; Shokri et al., 2010). Once the capillary break effect happens, the rate of upward water flow is reduced and the top layer becomes

drier than if there is no capillary break effect.

On the other hand, a coarse-grained layer located at the proximity of the water table may also enhance upward water flow and evaporation depending on its thickness, because the coarse-grained soil layer generally has higher hydraulic conductivity than a fine-grained layer when it is saturated or close to saturation and the soil generally has high moisture content at the proximity of the water table (Unger, 1971). Additionally, the thickness of the coarse-grained layer is a significant factor that can have an effect on upward water flow as if the coarse-grained layer is too thick and the capillary rise in this layer is less than the thickness of the layer, water will not even reach the interface between the coarse-grained layer and the overlying fine-grained layer. In this circumstance, the coarse-grained layer either reduces or even impedes the upward water flow and evaporation, irrespective of its location. In general, a coarse-grained interlayer near the soil surface is expected to act as a barrier layer during evaporation and upward water flow, on the other hand one close to the groundwater may enhance evaporation and upward water flow if it is not too thick. The theoretical considerations of water movement in layered soils regarding the upward water flow scenarios based on the factors above are discussed in more details in Appendix B.3.

Willis (1960) found that the spatial configuration of soil layers could have significant effects on evaporation rates: Accordingly, a soil profile of a fine-grained soil layer overlying a coarse-grained soil layer experienced smaller evaporation rate compared to a homogeneous profile of a fine-grained soil; but the soil profile with the reversed layer configuration experienced an increased evaporation rate (Willis, 1960). Unger (1971) studied the effect of the gravel layer on soil water distribution and evaporation by introducing a 2.5 cm thick gravel layer at depths of 0, 5, 15, 25 cm in sandy loam and clay loam soils. He found that soils with a gravel layer at the soil surface or at 5 cm depth experienced smaller evaporation

rates than the control (these treatments created the capillary barrier effect), on the other hand soils with gravel layer at 15 or 25 cm depth generally experienced greater evaporation rates than the control (these treatments had increased upward flow rates). Shokri et al. (2008) established that hydrophobic layers in a soil profile could interrupt water flow and reduce evaporative water loss in comparison with a uniform hydrophilic column. Bruch (1993) stated that constructing multilayered soils might cause water ponding or water shortage in the upper soil layer by creating a capillary barrier depending on how the layers are formed.

3 MATERIALS USED AND TESTING METHODOLOGY

3.1 *Introduction*

The main focus of this study was to accelerate raising water by capillary action and to remove water from the soil surface by the action of wind using experimental techniques. This study is thus based on laboratory investigations of various types using a range of materials. A general over view of the experimental investigation is followed by description of materials used and their classification. This is then followed by description of capillary rise tests and removal of water by the action of wind.

3.2 *Overview of Laboratory Experiments*

Two sets of laboratory experiments were designed and conducted to assess capillary rise and evaporation in soils by the action of wind.

The first set of experiments was carried out in three parts. The first part involved carrying out soil column tests in order to understand and evaluate the capillary rise of water in soils where the free surface of water was at the bottom of the column. The second part involved carrying out soil column tests where water for the column was supplied by saturated soil at the bottom of the column. The third part involved carrying out soil column tests where the top of the column was subjected to wind action and the free water surface was at the bottom of the column.

The second set of experiments involved carrying out tests on compacted soil specimen where the soil moulds were placed inside a wind tunnel.

The main laboratory tests conducted in this study are shown in Table 3.1.

Table 3.1 The main laboratory tests conducted in this study

Laboratory Tests Sets	Part	Description	Apparatus
1	1	Capillary rise tests for soil column in free surface of water	75-cm transparent Perspex tube with inside diameter of 5.4 cm
	2	Capillary rise tests for soil column in moist soil	75-cm transparent Perspex tube with inside diameter of 5.4 cm
	3	Capillary rise tests for soil column in a free surface of water with top of column subjected to wind action	30-cm transparent Perspex tube with inside diameter of 5.4 cm
2	-	Evaporation experiments on block samples where the soil moulds were placed inside a wind tunnel	8.3 x 23.4 x 9cm (width x length x height) galvanized steel mould

3.3 *Selection of soils*

Based on the literature review, capillary action is the dominant mechanism of upward water flow and pore water retention in sand. Silt may also adsorb water by capillary action but considerably less than sandy soils. This is due to (1) the significantly larger specific surface area and (2) the larger air-entry pressure controlled by the relatively small pores of silt in comparison with sand. In clay however, due to the relatively large surface area and charged surfaces of clay particles, a much greater amount of pore water is adsorbed by surface hydration mechanisms and extremely small amount of water is adsorbed by capillary action (Lu and Likos, 2004a). The surface adsorption effects are, in general, very limited in sand, because the surface charge properties and the specific surface area of sandy soils are relatively small compared to finer grained materials such as silt and clay. In sand, the water is drawn up prominently by capillary action via the pore spaces between soil particles as capillary tubes. In fact any other material that allow capillary rise and can be packed together to create capillary tubes as the means of water transport mechanism can be used instead of

sand if no other properties (such as surface charge) of that material take part in movement of water. Since, this study was aimed to assess the use of capillary action to remove water from soils, sands that allow capillary rise were of main interest and thus based on extensive literature review the soil types appropriate to carry out this research were selected as shown in Table 3.2. Several pilot tests were carried on a number of soils potentially suitable sands to assess their capillary conductivity and water storage capacity before selecting particular sand for detailed investigation.

Three soil types of medium grained SAND, clayey sandy SILT and the mixture of the two, clayey very silty SAND were selected for the experiments as shown in Table 3.2.

3.4 *Properties of the soils*

Classification tests were conducted on soils in accordance with British Standard (BS 1377) given in Table 3.2. It includes determination of particle size distribution and specific gravity. Each test was repeated at least two times. The average of the two results is given in Table 3.2, if they were in the error margin stated by the Standard.

Table 3.2 Properties of the experimental soils

	Soil types		
	Medium grained SAND	Clayey sandy SILT	Clayey very silty SAND
% Sand	92.8	15.2	65.0
% Silt	7.2 % silt and clay	72.5	26.9
% Clay		12.3	8.1
D_{50} (mm)	0.27	0.010	0.15
C_u	1.71	9.71	70.0
C_c	1.17	0.77	2.39
Specific Gravity	2.638	2.615	2.650
Void Ratio	0.598	0.469	0.456
Porosity	0.374	0.319	0.313
Avg. Pore Size (mm)	0.16	0.005	0.07
Dry Density (Mg/m^3)	1.65	1.78	1.81
MDD (Mg/m^3)	1.76	1.82	1.87
OMC (%)	13.67	14.5	13.06
K_{SAT} (m/s)	8.85×10^{-5}	3.35×10^{-5}	1.03×10^{-5}

3.4.1 Specific gravity

The specific gravity of all soil samples used in this study were determined by using small Pyknometer method in accordance with BS 1377: part 2 (1990). The specific gravity was needed for determination of some other soil properties, for example for hydrometer analysis, porosity and void ratio calculations. This test was repeated for each soil sample until the error margin of 0.03 Mg/m^3 stated by the British Standard was met. The mean values of specific gravity were found to be 2.638, 2.615, and 2.650 for medium grained SAND, clayey sandy SILT and clayey very silty SAND respectively, as presented in Table 3.2.

3.4.2 Particle size distribution

The grading characteristics of the soil samples used in this study were determined by sieving analysis and sedimentation technique (hydrometer method) in accordance with BS 1377: part 2 (1990). Soils were classified according to BS 5930: (1999) as medium grained SAND, clayey sandy SILT and clayey very silty SAND. The particle size distributions are shown in Figure 3.1.

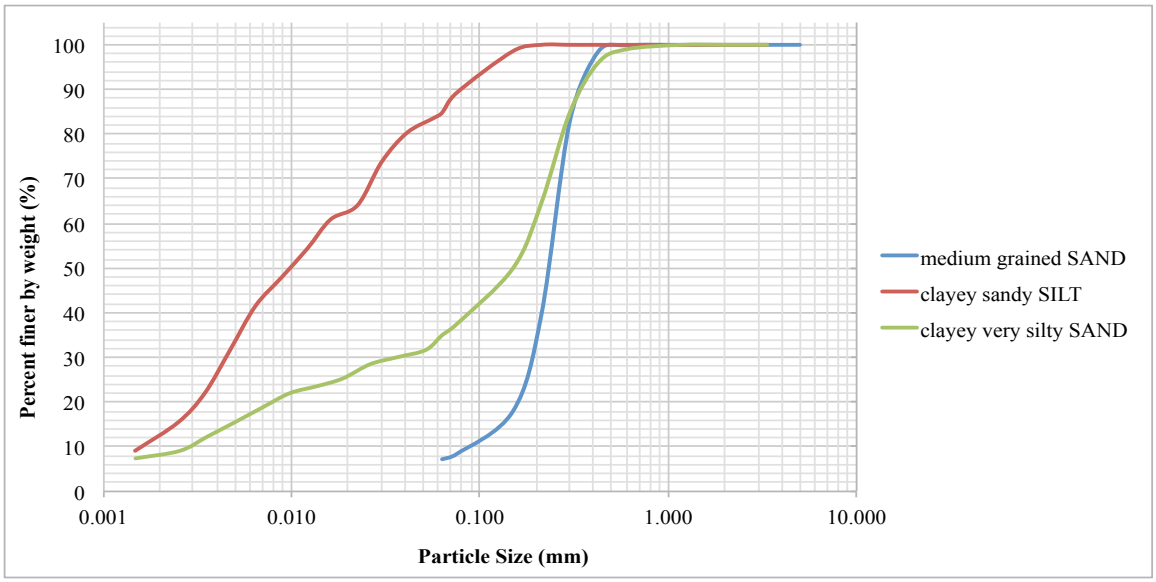

Figure 3.1 Particle size distributions of the soils used in the study.

3.4.2.1 Medium grained SAND

The particle size distribution for the medium grained SAND was obtained using sieve analysis. The particle size analysis indicated that about 93% of the material was appeared to be within the range of sand size particles (i.e., 0.063 to 2.0 mm). The grading characteristics coefficients namely, C_u and C_c were determined as 1.71 and 1.17 respectively. The uniformity coefficient, (C_u) was near unity and less than 6. Thus, the medium grained SAND was considered to be a uniformly graded soil. The medium grained SAND used was commercially available as building sand.

3.4.2.2 Clayey sandy SILT

The particle size distribution for the clayey sandy SILT was obtained using sedimentation analysis (hydrometer method). The particle size analysis indicated that the material was comprised of about 72.5% silt, 15.2% sand and 12.3% clay. The grading characteristics coefficients namely, C_u and C_c were determined as 9.71 and 0.77 respectively. Thus, the clayey sandy SILT was considered to be a well-graded soil. The clayey sandy SILT used was commercially available as Limestone, Superlon, Longcal and Longcliffe.

3.4.2.3 Clayey very silty SAND

The clayey very silty SAND (soil 3) was obtained from a mixture of 65% medium grained SAND (soil 1) and 35% clayey sandy SILT (soil 2) by dry mass. The particle size distribution for the clayey very silty SAND was obtained using sedimentation analysis (hydrometer method). The particle size analysis indicated that the material was comprised of about 65% silt, 26.9% sand and 8.1% clay. The grading characteristics coefficients namely, C_u and C_c were determined as 70 and 2.4 respectively. The uniformity coefficient, (C_u) was greater than

6 and the coefficient of curvature, (C_c) was less than 3 and greater than 1 (between 1 and 3). Thus, the clayey very silty SAND was described as a well-graded soil.

3.5 *Capillary rise experiments*

3.5.1 Setting up the soil columns

The experimental set up was designed based on the literature review and previous experimental studies on capillary rise namely the soil column method proposed by Jitrapinate et al. (2006), Sriboonlue et al. (2006) and Jitrapinate et al. (2011). Jitrapinate et al., (2006) used 100-cm long PVC tubes of 5-cm inside diameter. Sriboonlue et al., (2006) used 5-cm inside diameter and 100-, 150- and 200-cm long PVC tubes. Jitrapinate et al., (2011) used 100-cm long stainless steel tubes of 4.8-cm inside diameter.

All the capillary rise experiments were carried out at temperature of 21±3℃. Three types of capillary rise tests (Set 1/Part 1, Set 1/Part 2 and Set 1/Part 3) were conducted as shown in Tables 3.1 and 3.3: For all test types, transparent Perspex tubes with inside diameter of 5.4 cm were used. The tubes were pre-split along the length so that they could be opened up after the tests for taking samples for moisture content measurements. The two halves of the split tube were held together and joined using a waterproof tape. They were then secured using jubilee clips. For the first two test types (Set 1/Part 1 and Set 1/Part 2), 75-cm long Perspex tubes were used. One of the potential applications of this technique is to use it in railway track and the aim therefore is to lower the water table down to about 0.75 m, at which level it will not have significant effect on the performance of the track (Heath et al., 1972). Thus, 75-cm tube was selected as the length of the soil column. For the third test type (Set 1/Part 3), 30-cm long tube was used. Shorter, 30-cm long soil column was selected based on the results of capillary rise ascertained in the earlier tests described in Section 3.5.2 and Section 4.2.1.

Three different soil types of medium grained SAND, clayey sandy SILT and clayey very silty SAND were tested. Furthermore, in order to accelerate raising water by capillary action (improve the height of capillary rise and the volume of water that could be drawn up using

capillary action), two layered soil systems, namely layered SAND and layered SAND/SILT, were tested. The soil columns tested for different capillary rise experiments (Set 1/Part 1, Set 1/Part 2 and Set 1/Part 3) are presented in Table 3.3.

Table 3.3 Soil columns tested for different capillary rise experiments in this study

Laboratory Tests Sets	Part	Description	Apparatus	Soil columns		
1	1	Capillary rise tests for soil column in free surface of water	75-cm tube with inside diameter of 5.4 cm	1	Loosely compacted SAND	Medium grained SAND
				2	Densely compacted SAND	
				3	Layered SAND system	
				4	Clayey sandy SILT	
				5	Clayey very silty SAND	
				6	Layered SAND/SILT system	
	2	Capillary rise tests for soil column in moist soil	75-cm tube with inside diameter of 5.4 cm	1	Medium grained SAND (dense)	
				2	Layered SAND/SILT system	
	3	Capillary rise tests for soil column in a free surface of water with top of column subjected to wind action	30-cm tube with inside diameter of 5.4 cm	1	Medium grained SAND (dense)	

The first layered system (layered SAND) was a soil column in which the medium grained SAND was packed into several layers as described in detail as follows. This layered system comprised medium grained SAND only. The layered SAND system was made up of several layers having particle size ranges of 0.300 - 2.00 mm, 0.212 - 0.300 mm, 0.150 - 0.212 mm, and 0.063 - 0.150 mm. These ranges were selected based on the particle size data of medium grained SAND and the standard sieve sizes. The first layer, at the base of the column was stood in a container such that the free water surface was 2.5 cm above the base of the column. This layer comprised medium grained SAND with particle size of 0.300 - 2.00 mm. The

fourth layer, at the top of the column comprised medium grained SAND with particle size of 0.063 - 0.150 mm. The thickness of layers was determined based on the estimated maximum capillary height of each particle size range by using Jurin's equation (Eq. 2.17). The average pore size diameter was estimated by using void ratio/porosity and average particle size data for each layer. The average pore size was then used in Equation 2.17 ($h = \frac{2\gamma_{LV}\cos\theta}{\rho g r}$) to give us an approximate value for thickness of each layer. The specimen calculation of layer thickness is shown in Table 1 in Appendix C.1. After carrying out a few pilot tests, the thickness of layers was selected to be 10 cm, 10 cm, 10 cm and 45 cm. The layered SAND system was comprised of a soil column of medium grained SAND in which larger particle size layers underlying smaller (finer) particle size layers. Thus, as the height of layers in soil column increases, the particle size of layers decreases to achieve higher capillary rise. A schematic illustration of layered SAND system along with the position, thickness and particle size ranges of each layer is shown in Figure 3.2.

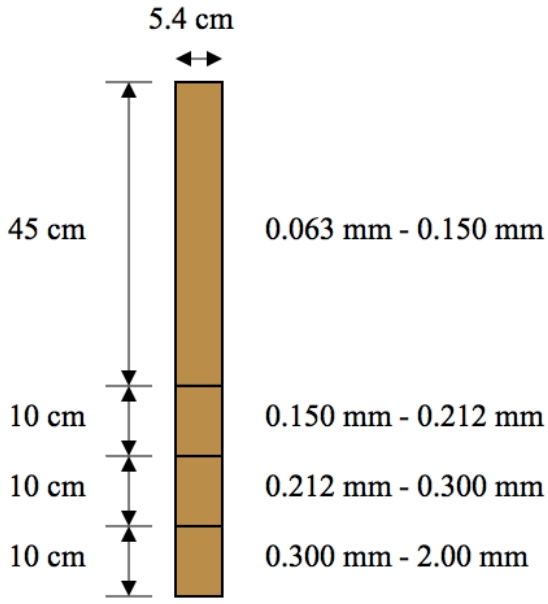

Figure 3.2 Schematic illustration of layered SAND system along with the position, thickness and particle size ranges of each layer.

The second layered system (layered SAND/SILT) was a soil column in which the medium grained SAND and the clayey sandy SILT were packed at the bottom and the top of the soil column respectively. This set up had two layers of soils. The first layer, at the base of the column comprised medium grained SAND, overlain by the second layer, at the top of the column comprised of clayey sandy SILT. The thickness of the first and second layers was 30 cm and 45 cm respectively. A schematic illustration of layered SAND/SILT system along with the position and thickness of each layer is shown in Figure 3.3.

All the soil samples were dried in the oven at 105°C for 24 hours, prior to the experiments.

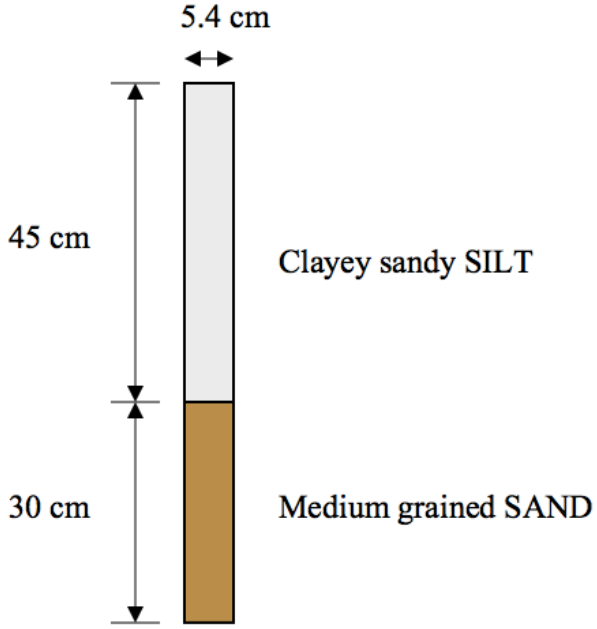

Figure 3.3 Schematic illustration of layered SAND/SILT system along with the position and thickness of each layer.

Soils were compacted into the tube in a standardised manner to achieve uniform packing at the desired dry bulk densities that could be achieved in repeat tests. The test soil column was constructed in 1.67-cm thick layers using a PVC rod with an end plug of 5.2 cm diameter, length of 80 cm, and mass of 667 g. To study the effect of compaction or particle packing on capillary rise, the medium grained SAND sample was packed into the soil column

loosely and tightly to dry densities of 1.50 Mg/m^3 (85% MDD) and 1.65 Mg/m^3 (94% MDD) respectively. The bottom end of the tube was covered with a cloth to prevent soil from falling out. Three types of capillary rise tests (Set 1/Part 1, Set 1/Part 2 and Set 1/Part 3) were conducted: for the first type (Set 1/Part 1), each soil column was placed vertically in a free surface of water (Section 3.5.2). For the second type (Set 1/Part 2), each soil column was placed vertically in a container of moist soil (Section 3.5.3). For the third type (Set 1/Part 3), each soil column was placed vertically in a free surface of water with top of column subjected to wind action (Section 3.5.4).

3.5.2 Capillary rise tests in free surface of water (Set 1/Part 1)

In the first part of first set of tests, capillary flow experiments were carried out by placing each soil column vertically in a container filled with distilled water, with its bottom end immersed to a depth of 2.5 cm below the water surface. A schematic sketch of a representative soil column in a container of free water is shown in Figure 3.4.

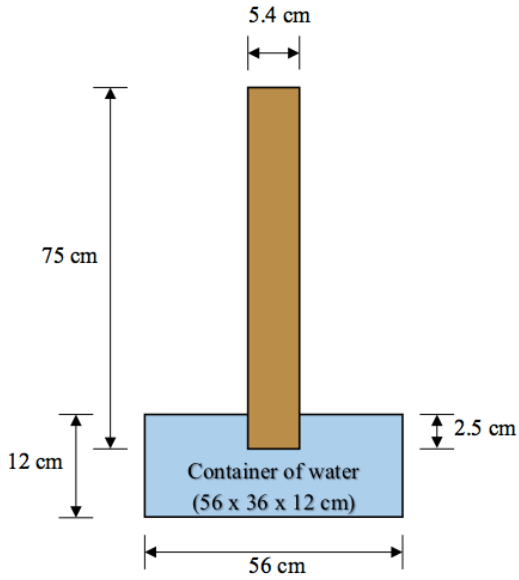

Figure 3.4 Schematic sketch of a representative soil column in a container of free water.

The experimental set up is shown in Figure 3.5.

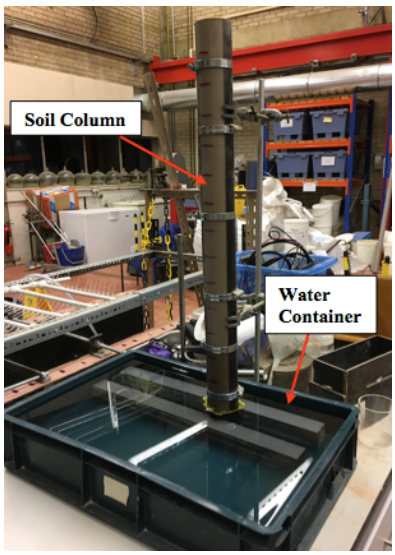

Figure 3.5 Soil column stood vertically in the container of free water.

In this part, six different types of soil column samples were tested comprised of loosely compacted SAND, densely compacted SAND, layered SAND system, clayey sandy SILT, clayey very silty SAND and layered SAND/SILT system. The soil columns were left in the container of water for capillary rise to take place for different time steps of 0.0625, 0.125, 0.25, 1, and 2 days for the loosely compacted SAND; 0.125, 0.25, 1, and 2 days for the densely compacted SAND; 2 days for the layered SAND system; 1, 2, and 4 days for the clayey sandy SILT; 1 and 2 days for the clayey very silty SAND; and 1 and 2 days for the layered SAND/SILT system. The duration of capillary rise tests for soil columns in free surface of water is shown in Table 3.4.

Table 3.4 Duration of capillary rise tests for soil columns in free surface of water

Soil columns		Test duration (Days)
1	Loosely compacted SAND	0.0625, 0.125, 0.25, 1, and 2
2	Densely compacted SAND	0.125, 0.25, 1, and 2
3	Layered SAND system	2
4	Clayey sandy SILT	1, 2, and 4
5	Clayey very silty SAND	1 and 2
6	Layered SAND/SILT system	1 and 2

Thinking of engineering application of this method, shorter duration of time, i.e. a few hours up to a few days was preferred. Thus, shorter test period of up to two days was selected and the capillary rise for each soil column for this period was measured. This work may be extended for longer period as deemed suitable for the target application.

After the pre-defined period of time for each soil column, the PVC tube was split open along the length, and the 75-cm column of soil was divided into 15, 5-cm long sections for determination of gravimetric water content. This is shown in Figure 3.6.

Figure 3.6 Soil sample preparation for the measurement of gravimetric moisture content.

3.5.3 Capillary rise tests in a moist soil (Set 1/Part 2)

The second part of first set of tests was carried out by placing soil column vertically in a container of moist soil prepared to a range of moisture contents. In this part, the soil sample used as the base soil (soil in the container) for all tests was medium grained SAND. The base soil samples were prepared at three moisture contents of 35 % (sample 1), 28 % (sample 2) and 20 % (sample 3). When the base soil was saturated it had gravimetric moisture content of 33 %. The three moisture contents used in the capillary tests reflected degree of saturation, as shown in Table 3.5.

Table 3.5 Moisture contents of base soils used in tests for the second part of the first set (Set 1/Part 2)

Base soil	Moisture content (%)	Percentage of saturation moisture content
Sample 1	34 - 35	105
Sample 2	28 - 29	86
Sample 3	20 - 21	62

In this part, two different types of soil column samples were tested. They comprised the medium grained SAND and the layered SAND/SILT system. The medium grained SAND soil column was stood in the container of moist soil i.e. sample 1, sample 2 and sample 3 and capillary rise was measured for 2, 4, 5, and 10 days; 4, 10, and 14 days; and 4, and 5 days respectively. The layered SAND/SILT soil column was stood in the container of moist soil with moisture content of 35 % (i.e. sample 1), and capillary rise was measured for 4 days. The duration of capillary rise tests for soil columns in moist soil is shown in Table 3.6.

Table 3.6 Duration of capillary rise tests for soil columns in moist soil

Soil columns		Base soil	Test duration (Days)
1	Medium grained SAND (dense)	Sample 1	2, 4, 5 and 10
		Sample 2	4, 10 and 14
		Sample 3	4 and 5
2	Layered SAND/SILT system	Sample 1	4

The soil samples for the base soil were oven dried at a temperature of 105°C for 24 hours and sieved to remove material larger than 2 mm. The soils were then placed in a mixer and distilled water was added to achieve the required moisture content. The base soil samples were compacted in three layers into square Perspex (Plexiglas) containers measuring 6 cm height, 20 cm length and 20 cm width. This size of specimens was selected to be adequate for measuring capillary rise effectively.

The filling soil column of medium grained SAND and layered SAND/SILT system was prepared and packed as described in section 3.5.1. The experimental set up is shown in Figure 3.8.

A schematic sketch of a representative soil column in a container of moist soil is shown in Figure 3.7.

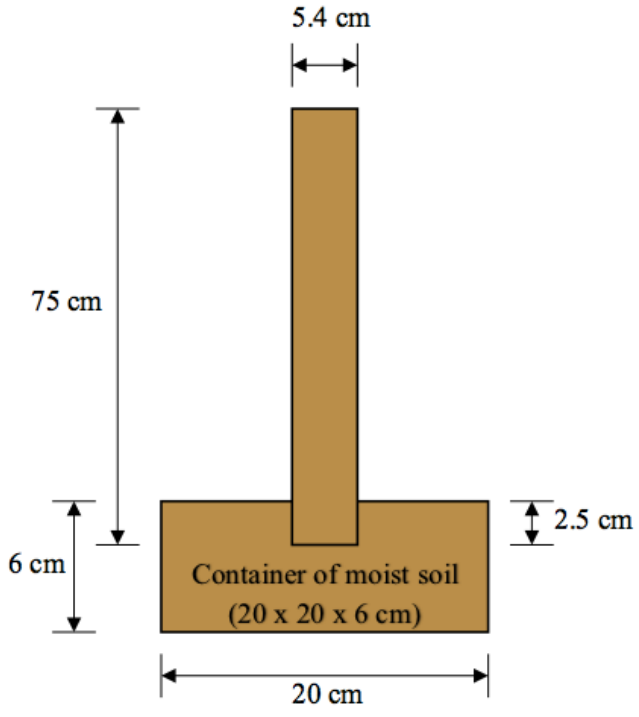

Figure 3.7 Schematic sketch of a representative soil column in a container of moist soil.

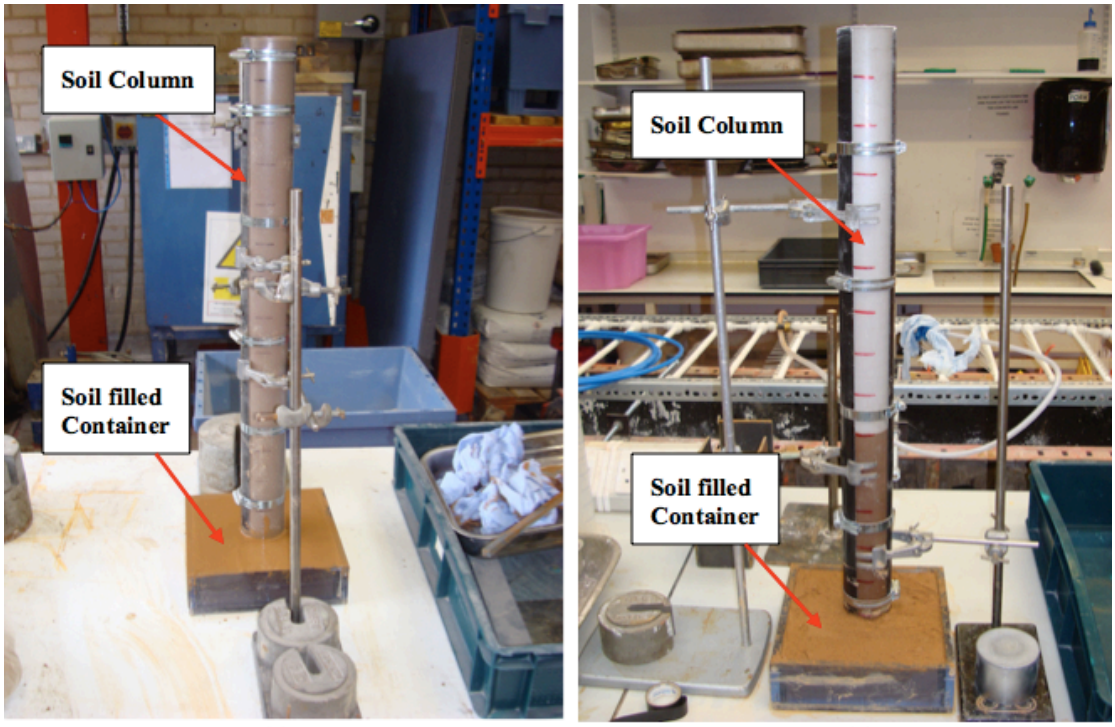

Figure 3.8 Soil columns of (a) medium grained SAND and (b) layered SAND/SILT system stood vertically in the container of moist soil.

After the pre-defined period of time for each soil column, the PVC tube was split open along the vertical joint, and the 75-cm column of soil was divided into 15, 5-cm long sections for determination of gravimetric water content.

3.5.4 Capillary rise tests for soil column in a free surface of water with top of column subjected to wind action (Set 1/Part 3)

The aim of these experiments was to investigate the effect of gradual removal of water from the surface of the column on capillary rise.

The third part of first set of tests was carried out by placing soil column vertically in a container filled with distilled water, with its bottom end immersed to a depth of approximately 2.5 cm below the water surface. The top of the column was subjected to wind as shown in Figure 3.9 and Table 3.7. The wind tunnel setup is described in Section 3.6.3. The arrangement of tests in the wind tunnel (soil column evaporation test setup) is shown in Figures 3.10. These set of experiments were carried out at room temperature using transparent PVC tube pre-split lengthwise with 30 cm height and 5.4 cm inside diameter. Only one soil type, medium grained SAND, was tested in columns in the wind tunnel. The height of the soil column was 30 cm, which was used based on the height and rate of capillary rise as ascertained in the earlier tests described in Section 3.5.2.

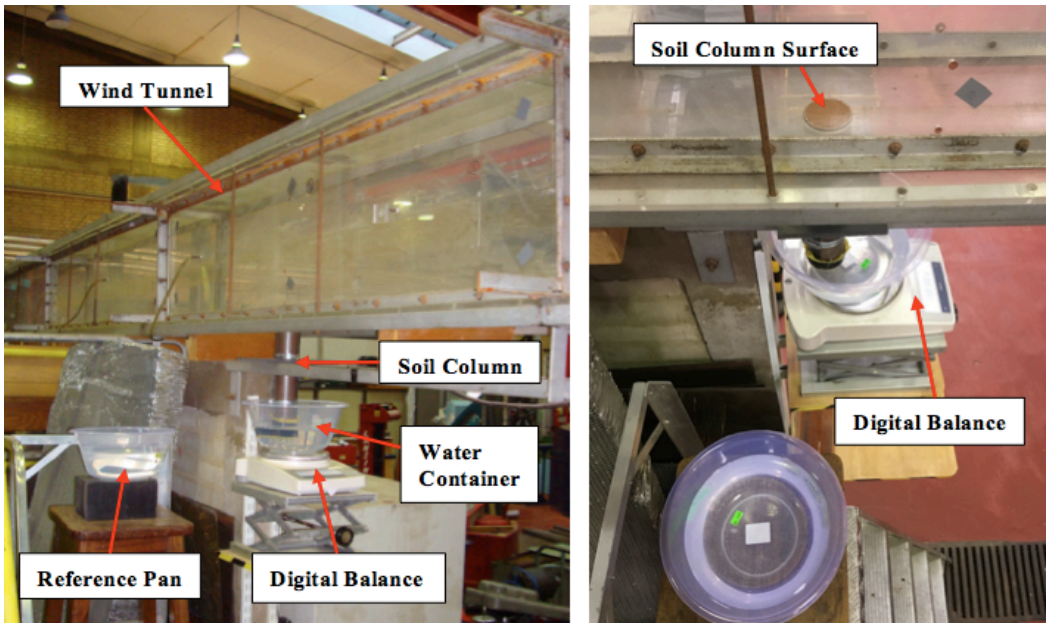

Figure 3.9 Soil column stood vertically in the container of free water with top of the column subjected to wind action.

Table 3.7 The details of capillary rise tests for soil column in a free surface of water with top of column subjected to wind action

	Soil column
Soil type	Medium grained SAND (dense)
Wind velocity (m/s)	0.0, 1.3, 3.0 and 4.9
Test duration (days)	4

The soil column sample of the medium grained SAND was tested at wind velocities of 1.3 m/s, 3.0 m/s and 4.9 m/s. The soil sample was additionally tested in the same setup under windless conditions for baseline comparison purposes. The wind speeds were selected based on the literature review, the wind speed data in the UK (Davarzani et al., 2014, Clark 2013, Natural Energy UK 2016, Department of Energy and Climate Change 2016 and Pascoe 2011) and limitations of the available wind tunnel. The wind velocity before the start of each set of tests was measured using an analog anemometer. The temperature and humidity were 21±2°C and 31±3% respectively; both were monitored continuously during the experiments by Thermo-Hygrometer.

In order to provide a reference for soil evaporation tests, evaporation from a free water surface was measured in a container of distilled water subjected to the same conditions as those for the capillary tests. This was done by placing a pan filled with distilled water next to the test container as shown in Figure 3.9.

Each test was run for four consecutive days and the change in the mass of water in test container, reference pan and soil column were recorded after every 24 hours. The moisture distribution within the soil column and the change in the mass/volume of water in the soil column was also measured by running additional tests for intermediate durations of 1, 2, and 3 days.

As for earlier tests, at the end of each experiment, the soil was removed from the 30-cm column and divided into 6, 5-cm long sections for determination of soil water content.

3.5.5 Moisture content measurement

Having measured the moisture content of each 5 cm section of soil columns by gravimetric method, the volumetric water content was estimated from the known gravimetric water content and soil bulk density as follows: (Eq. 3.1):

$$\theta_v = \frac{\rho_b}{\rho_w}\theta_m \qquad \text{(Eq. 3.1)}$$

Where ρ_b represents as the bulk density of soil and ρ_w is the density of water. The volumetric water content is needed to be ascertained because, it includes dry bulk density of soil in its equation and thus makes the water content measurement more realistic and more comparable by taking the particle packing effect on gravimetric water content into account. Also it is needed to estimate the volume of water within each 5 cm section.

The volume of water accumulated at each 5 cm section of soil column was ascertained from the volumetric moisture content, θ_v, using the following equation:

$$V_w = \frac{\theta_v \times V_C}{100} \qquad \text{(Eq. 3.2)}$$

Where V_w represents as the volume of water at each 5 cm section of soil column and V_C is the volume of each 5 cm section of soil column (volume of cylinder).

3.6 *Evaporation experiments on block samples*

3.6.1 Selection of test soils and sample preparation

This section includes the second set of the laboratory program of this study.

The evaporation tests are related to capillary rise experiments thus; the same soil samples were selected to carry out the following tests as previously used in capillary rise tests. Furthermore, because one of the objectives of this part is to study the effect of soil texture on evaporation, three different soil types including medium grained SAND, clayey sandy SILT and clayey very silty SAND were chosen to carry out the evaporation tests, as only 9 researchers have investigated the effect of wind on evaporation from different soil types (Abbas, 2015).

3.6.2 Sample preparation

One of the objectives of this research was to study the effect of moisture content of soil on loss of water due to evaporation. Hence, the soil samples were prepared to three moisture contents of 13 %, 19 % and 27 %. The moisture content of 13 % was selected in order to study the different stages of evaporation, particularly the second (i.e. falling rate) stage within the specific duration of the tests when the water content of the soil becomes limiting. The moisture contents of 19 % and 27 % were selected in order to study the relationship between potential evaporation, actual evaporation and cumulative evaporation when an ample amount of water is available within the soil. These were based on values of previous studies by Wilson, (1990) and Bruch, (1993).

The soil samples were dried in the oven at a temperature of 105°C for 24 hours and subsequently sieved to remove material larger than 2 mm. The soils were then placed in a mixer and distilled water was added to achieve the required moisture content. Soil samples

were then compacted in three layers into rectangular galvanized steel moulds measuring 8.3 cm width, 9 cm height and 23.4 cm length.

3.6.3 Wind tunnel setup

The experiments were carried out in a wind tunnel located in the Department of Civil Engineering Laboratory at the University of Birmingham. The wind tunnel set up is shown in Figure 3.10. It was a suction-type wind tunnel with test section measuring 18.0 cm wide, 40 cm high, and 925 cm long, as illustrated in Figures 3.10a, and 3.10b. One side of the tunnel consisted of 5 sections, one of 2.25 m length whereas the other four of 1.75 m each. The other side of the tunnel, which was used throughout the evaporation tests, also consisted of five sections bolted together with nuts and bolts, each of 1.75 m and consisting of an entrance inlet of 0.50 m, which was used to place the samples inside the tunnel. The temperature and humidity were 23±2°C and 52±3% respectively which were continuously monitored by Thermo-Hygrometer during the experiments.

Laminar and turbulent flows were used for this part of the study (block evaporation tests). The laminar and turbulent wind flow setups are shown in Figures 3.11 and 3.12, respectively. In both wind movement setups, two ramps made up of high-density foam were used, one placed on the inlet side of the test samples and the other placed on the outlet side as shown in Figures 3.11 and 3.12. Both of these ramps were covered with Eurocel cloth tape in order to create a uniformly smooth surface. The ramp on the inlet side was 87 cm long and the one on the outlet side was 48 cm long. An aluminium honeycomb baffle was installed across the whole section on top of the ramp at the inlet end to smooth the flow lines. The honeycomb was a regular hexagon with an interior angle of 120 degrees and each side of 0.5 cm, as shown in Figure 3.11b.

Turbulence flow was generated by adding four 0.88 mm thick steel strips, bent at an angle of 30^{o} and mounted on the top of foam at the inlet end. The turbulence generating stripes are shown in Figure 3.12b.

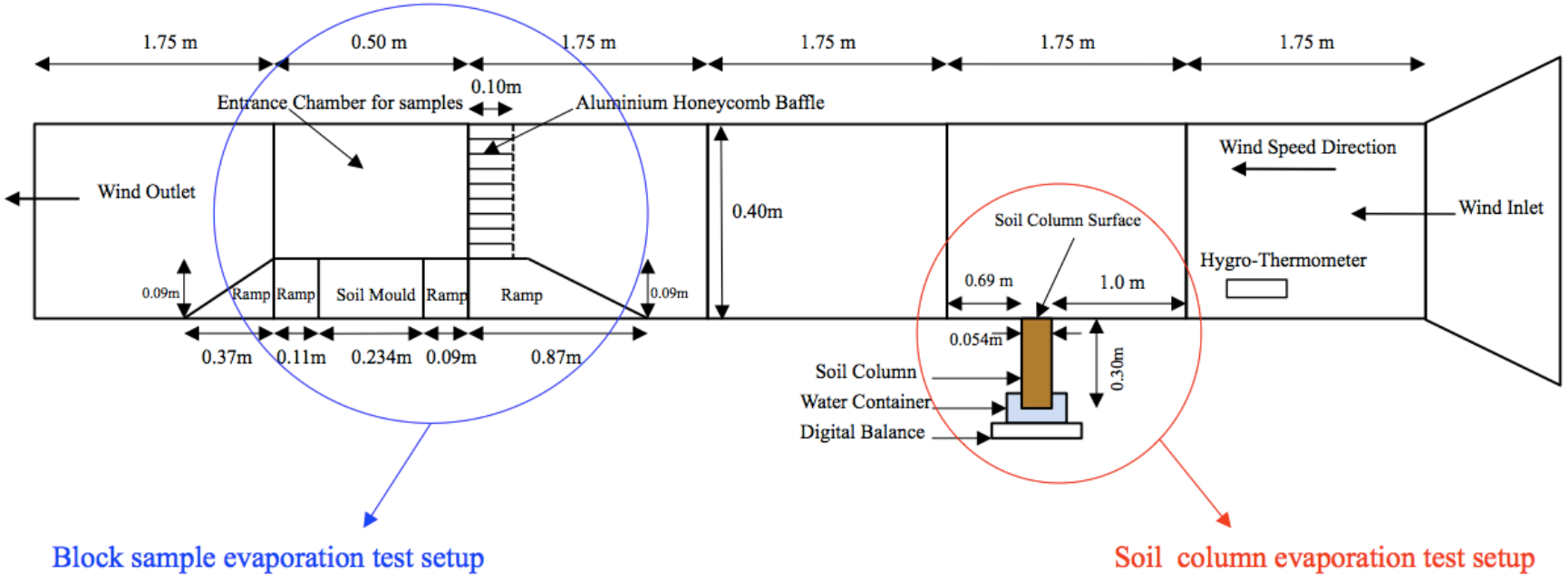

a) Cross-section of wind tunnel

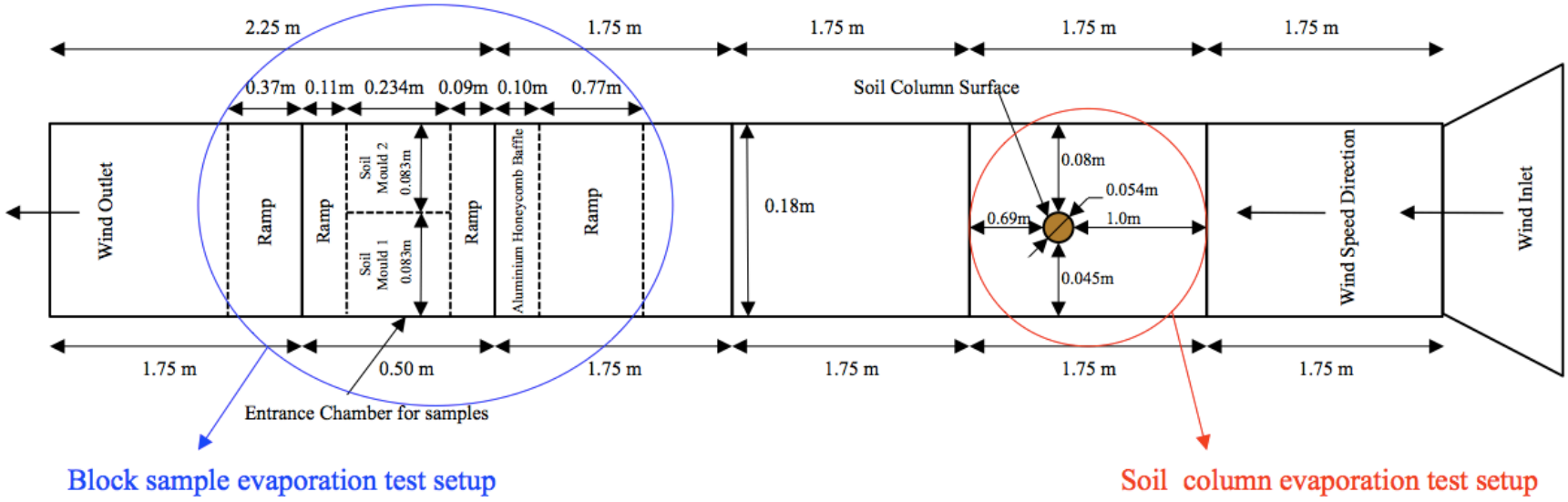

b) Plan view of wind tunnel

Figure 3.10 Wind tunnel setup: a) Cross-section view of wind tunnel b) Plan view of wind tunnel.

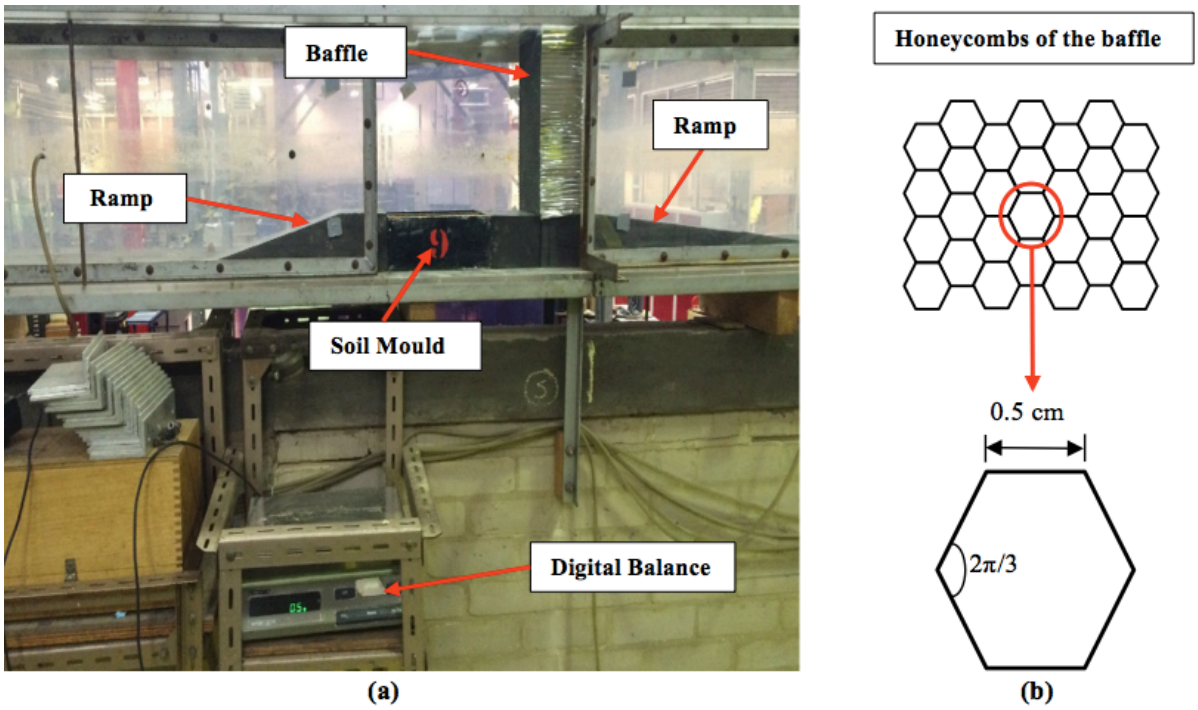

Figure 3.11 Wind tunnel setup: (a) Laminar wind flow setup (b) Dimensions of honeycombs of the aluminium baffle.

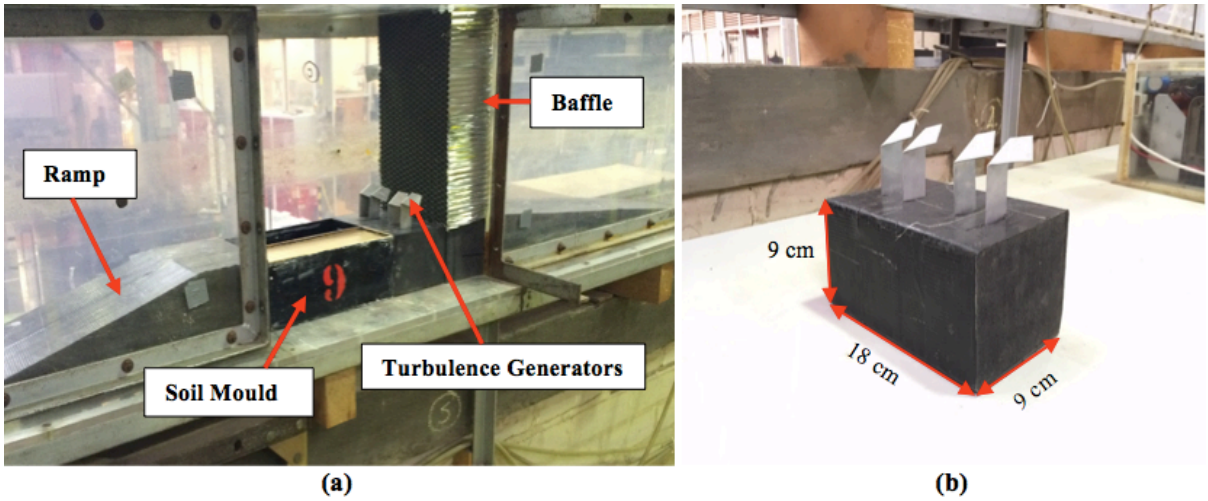

Figure 3.12 Wind tunnel setup: (a) Turbulent wind flow setup (b) Close-up photo of the turbulence generators along with dimensions of the foam base.

3.6.4 Evaporation tests

A series of evaporation tests for three different soil types under varying wind conditions were carried out to study and better understand the effect of wind on evaporation, the change in moisture content with depths, the different stages of evaporation and the transitions between stage 1 and stage 2. The soil samples of the medium grained SAND, the clayey sandy SILT, and the clayey very silty SAND were tested at laminar and turbulent flows at wind velocities of 1 m/s, 3 m/s and 6 m/s as shown in Table 3.8. The wind velocity before the start of each set of tests was measured using an analog anemometer. The wind velocities were selected based on the literature review, the wind velocity data in the UK and the wind tunnel output (Davarzani et al., 2014, Clark, 2013, Natural Energy UK, 2016, Department of Energy and Climate Change, 2016, and Pascoe 2011). These soil samples were additionally tested in the same setup under windless conditions to study the effect of change of wind velocity on cumulative evaporation of water from soil for comparison purposes. At a time, a maximum of two test samples, i.e. soil sample and distilled water sample were placed in the wind tunnel. Each test was run for two consecutive days and the change in the mass of test samples was recorded after every 24 hours. The two days specific duration of tests was selected based on the previous studies in literature review under similar test conditions (Cardon et al. 1992, Hanks et al. 1991, and Jackson et al. 1973). Cardon et al. (1992), Hanks et al. (1991), and Jackson et al. (1973) stated that evaporation would cause the water content near the soil surface to decrease rapidly so the climate-controlled stage would last for only a day or two. This period was selected as Fisher (1923) and Pearson et al., (1949) noted that the first stage of evaporation would be completed in about one day under similar conditions and the majority of the second stage in approximately two days. Thus, selection of two days test periods appeared to be reasonable based on preliminary tests. At the end of experiment, the

samples were taken out of the wind tunnel and weighed. The soil sample was divided into three layers, each of 3 cm for the measurement of gravimetric moisture content at each layer. The 3 cm layer thickness was selected based on the previous studies in the literature; Chanzy and Bruckler (1993) and Toya and Yasuda (1988) recommended that soil thickness of between 3 cm to 10 cm would be adequate for such a study. Furthermore, because the height of the soil sample was 9 cm, thus selection of 3 cm layer thickness for each layer is assumed to be reasonable. Moisture content was determined from two samples from the centre of each layer.

Table 3.8 The details of evaporation tests on block samples

	Soil moulds		
	1	2	3
Soil type	Medium grained SAND	Clayey sandy SILT	Clayey very silty SAND
Water content (%)	13.0, 19.0 and 27.0	13.0, 19.0 and 27.0	13.0, 19.0 and 27.0
Wind velocity (m/s)	0.0, 1.0, 3.0 and 6.0	0.0, 1.0, 3.0 and 6.0	0.0, 1.0, 3.0 and 6.0
Wind movement	Laminar and Turbulent	Laminar and Turbulent	Laminar and Turbulent
Test duration (days)	2	2	2

4 RESULTS AND DISCUSSION

4.1 *General*

As discussed in Table 3.1 in Section 3.2, two sets of laboratory experiments were undertaken. They were designed to assess capillary rise of water in soils and assess the effect of removal of water by evaporation (by the action of wind) from the soils surface on the extent of capillary rise.

The first set of experiments was carried out in three parts. The first part involved carrying out soil column tests in order to evaluate the capillary rise of water in soils where the free surface of water was at the bottom of the column. The aim of the first part was to evaluate capillary rise of water in soils and more importantly how to improve capillary rise and the volume of water that could be drawn up within the duration of test. The second part involved carrying out soil column tests where water for the column was supplied by saturated soil at the bottom of the column. The aim of the second part was to assess the capability of capillary action to suck water vertically from a moist soil at a range of moisture contents. The third part involved carrying out soil column tests where the top of the column was subjected to wind action and the free water surface was at the bottom of the column. The aim of the third part was to assess the feasibility of using a capillary column to draw up water from a free water surface to a higher level where water was removed by wind action with a view to continuously remove water.

The second set of experiments involved carrying out tests on compacted soil specimen where the soil moulds were placed inside a wind tunnel. The aim of the second set was to evaluate the effect of wind, soil types, and moisture contents on loss of water from soils.

A background theory to this research area is presented in Chapter 1 and a detailed methodology of laboratory work is described in Chapter 3. All laboratory test results are both presented and discussed in this chapter.

4.2 *Capillary rise tests*

4.2.1 Capillary rise test in a free surface of water

Six types of soils column were tested. These comprised loosely compacted SAND, densely compacted SAND, layered SAND system, clayey sandy SILT, clayey very silty SAND and layered SAND/SILT system as discussed in Section 3.5.2. The soil columns were stood in the container of water for 0.0625, 0.125, 0.25, 1, and 2 days for the loosely compacted SAND; 0.125, 0.25, 1, and 2 days for the densely compacted SAND; 2 days for the layered SAND system; 1, 2, and 4 days for the clayey sandy SILT; 1 and 2 days for the clayey very silty SAND; and 1 and 2 days for the layered SAND/SILT system. The results of capillary rise experiments for the six tests are presented in Figure 4.1, 4.2, 4.3, 4.4, 4.5, and 4.6. The results are presented in terms of moisture content as a function of height above the water table. The datum point is located at the water level so, zero height represents the free surface of the water that is 2.5 cm above the base of the column. Because the bottom end of the soil column was immersed 2.5 cm in water and the moisture content measurements represent the mid-point of each 5-cm section of the soil column, therefore the start point (first reading) on Y-axis is 2.5 cm above the base of the column as shown in Figure 1 in Appendix D.1. In majority of the cases, the moisture content decreases as the height above the water table increases, in particular, for the sandy soils, where the decrease is more significant. The results show gradually decreasing values of moisture content up to a certain height from the water table above which they decrease more steadily. This is in agreement with the results of previous capillary rise tests (Lu and Likos, (2004); Jitrapinate et al., (2006); Sriboonlue et al., (2006) and Jitrapinate et al. (2011)).

The results of capillary rise for the layered SAND/SILT system (2 days test) and the clayey sandy SILT (4 days test) however, show that at first, the moisture content gradually

decreases with height above the water surface up to a certain height above which, it then gradually increases with height above the water table particularly, in the top sections of the soil column as illustrated in Figure 4.4 and 4.6. This can be due to the inadequate height of tubes to accommodate further capillary rise. Because the height of the soil column was 75 cm and the maximum theoretical height of capillary rise for both soil samples is more than 75 cm. For instance, the maximum height of capillary rise observed after (within) 2 days for the clayey sandy SILT and the layered SAND/SILT system were 65 cm and <72.5 cm respectively, so that the soil column was not high enough to accommodate further capillary rise and more amount of water was accumulated in the upper parts of the soil column. This mostly explains the higher volumetric moisture contents, which were measured in the uppermost sections of the soil columns in the above-mentioned cases. Additionally, because a fine-textured layer of silty soil with lower hydraulic conductivity overlies a coarse-textured layer of sandy soil with higher hydraulic conductivity in the layered SAND/SILT system, the water moves at a higher rate in the SAND layer and when it gets into the SILT layer, this rate decreases significantly and the results show higher water contents in the upper layers.

The total volume of water drawn up and accumulated in each soil column after 1 and 2 days is presented in Figures 4.12 and 4.14 respectively.

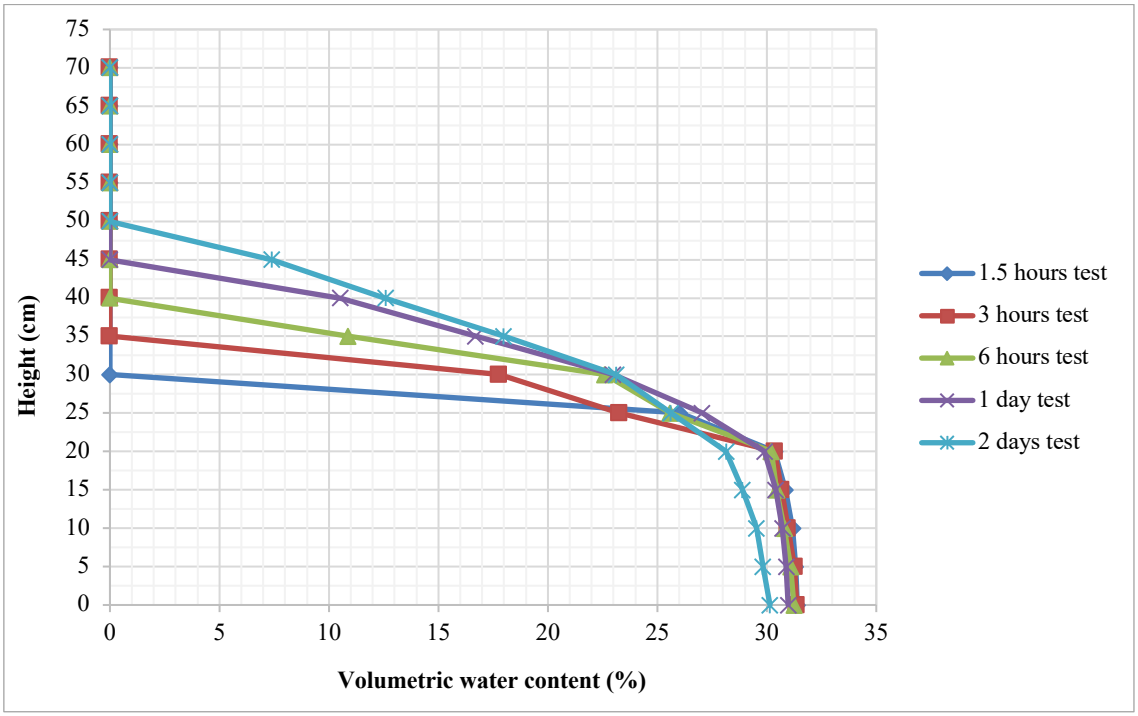

Figure 4.1 Capillary rise and volumetric water content distribution relationship for loosely compacted SAND in free water surface.

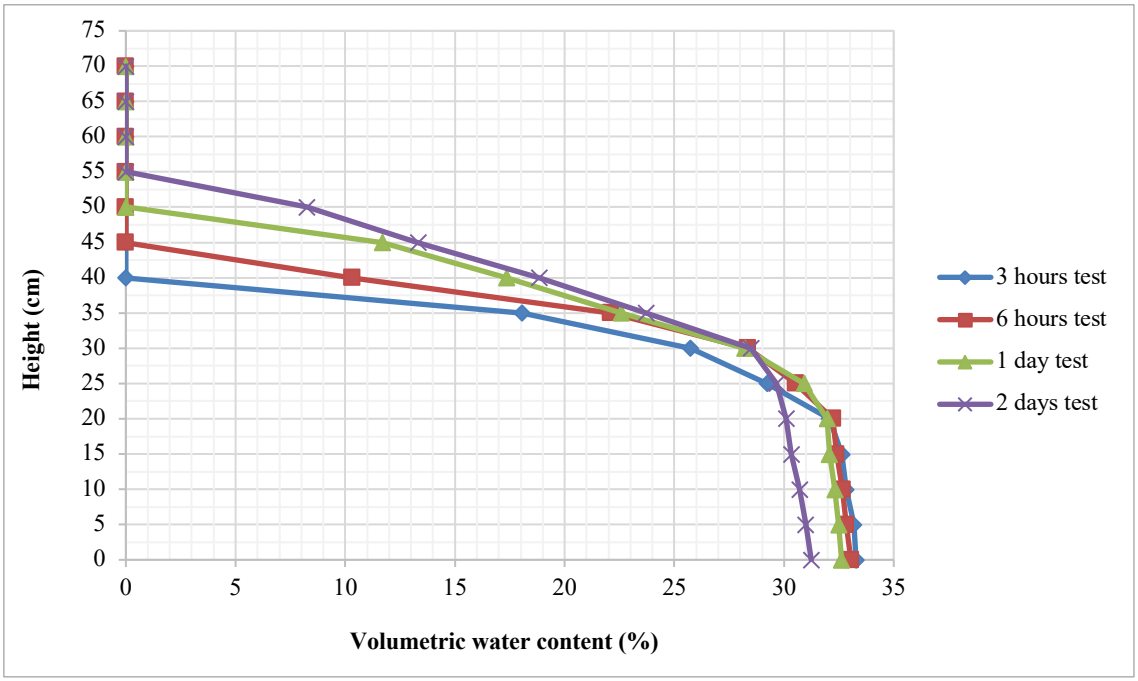

Figure 4.2 Capillary rise and volumetric water content distribution relationship for densely compacted SAND in free water surface.

The result shown in Figure 4.3 is related to the layered SAND system (1), which was described in Section 3.5.1. This layered system comprised medium grained sand only.

The schematic illustration of layered SAND system (1) along with the position, thickness and particle size ranges of each layer was shown in Figure 3.2 in Section 3.5.1. This layered system was made up of several layers having particle size ranges of 0.300 - 2.00 mm, 0.212 - 0.300 mm, 0.150 - 0.212 mm, and 0.063 - 0.150 mm. The first layer, at the base of the column was stood in a container of free water. This layer comprised medium grained SAND with particle size of 0.300 - 2.00 mm. the fourth layer, at the top of the column comprised medium grained SAND with particle size of 0.063 - 0.150 mm.

The dogleg at about 20 cm in Figure 4.3 can be due to the change in the layers, which was repeated in the tests.

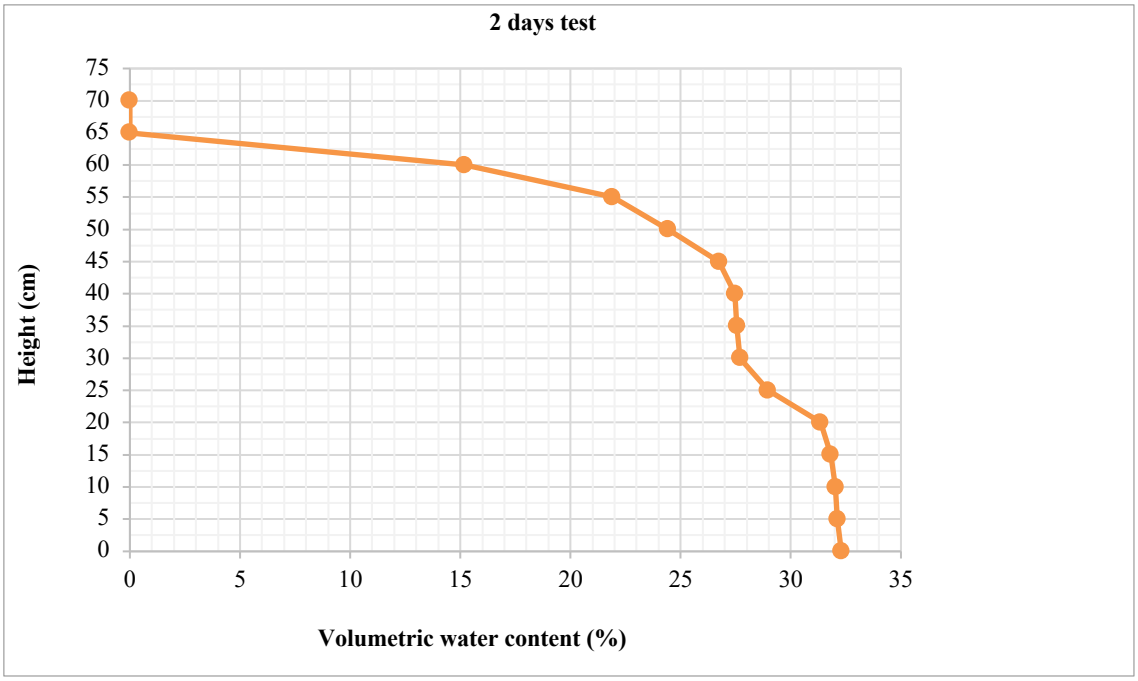

Figure 4.3 Capillary rise and volumetric water content distribution relationship for layered SAND system in free water surface.

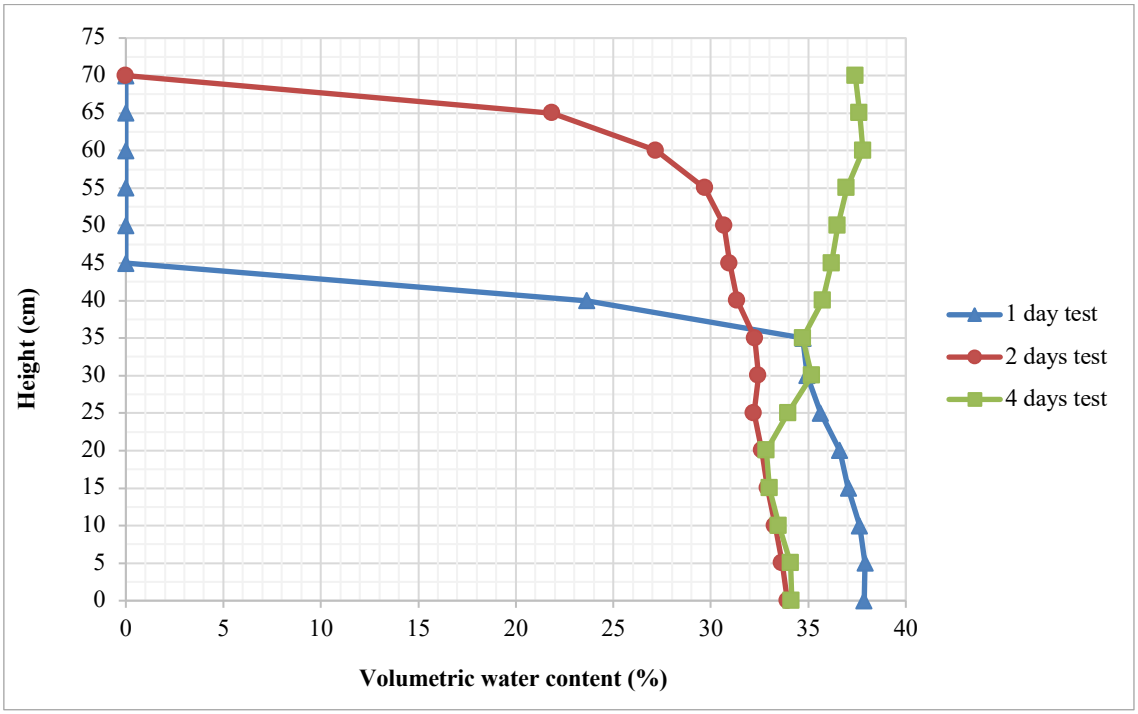

Figure 4.4 Capillary rise and volumetric water content distribution relationship for clayey sandy SILT in free water surface.

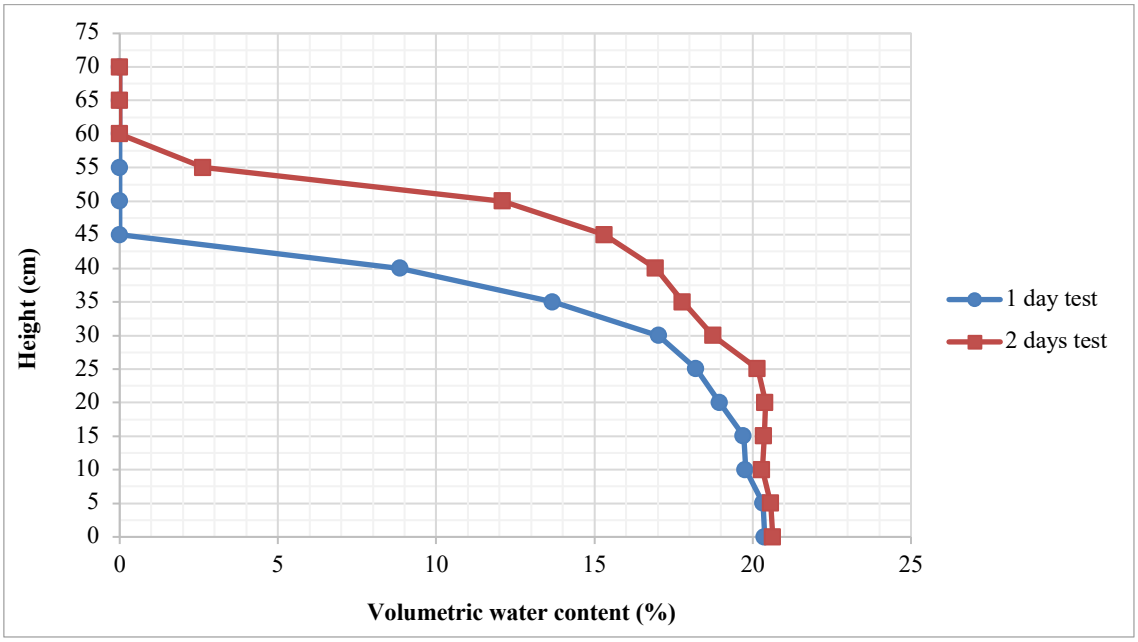

Figure 4.5 Capillary rise and volumetric water content distribution relationship for clayey very silty SAND in free water surface.

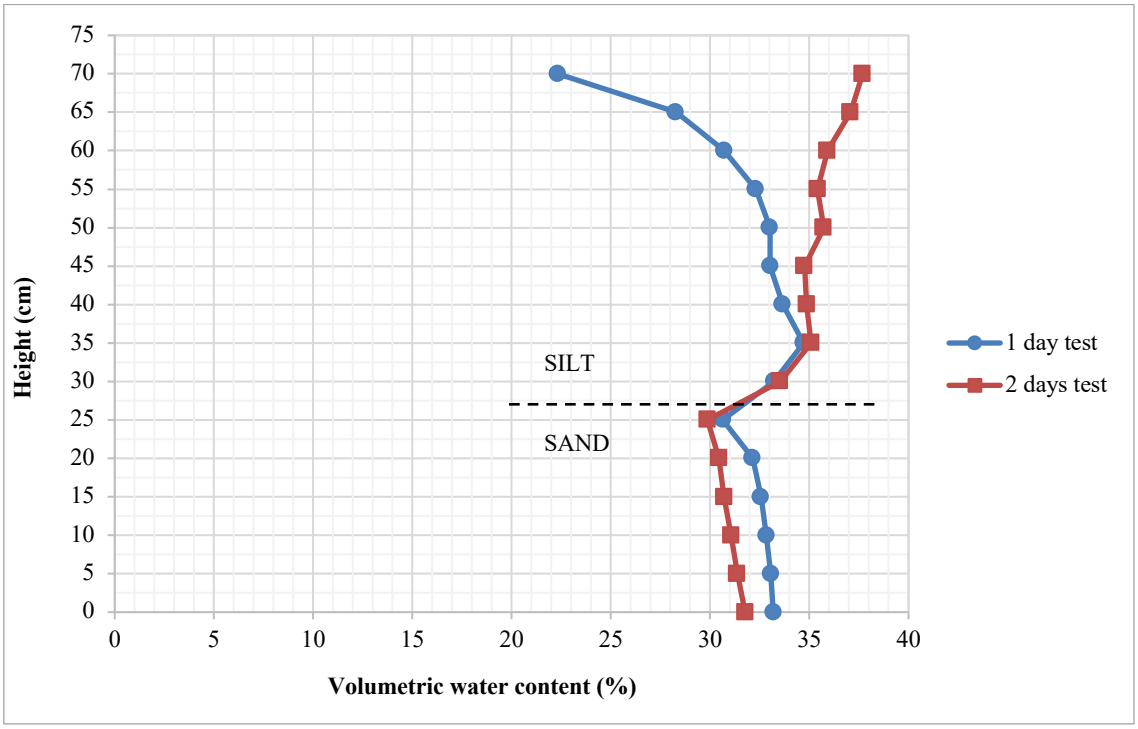

Figure 4.6 Capillary rise and volumetric water content distribution relationship for layered SAND/SILT system in free water surface.

For repeatability of experimental data, each test in this part was repeated for five times and the repeatability achieved was quite satisfactory as shown in Fig. 4.7. Figure 4.7 shows an example of capillary rise test for layered SAND/SILT system in free water surface, which was repeated for five times. The error band of the measurements was 0.7 for gravimetric water content and 1.2 for volumetric water content.

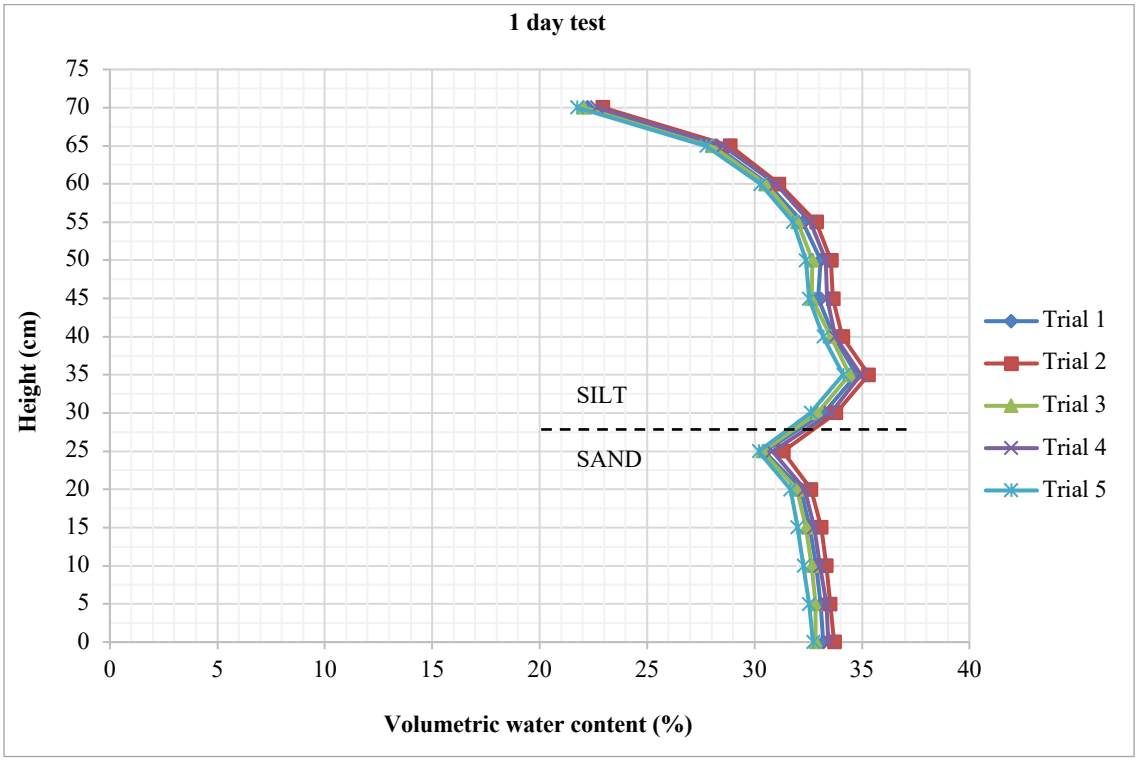

Figure 4.7 Repeatability of data for capillary rise and volumetric water content distribution relationship for layered SAND/SILT system in free water surface.

4.2.1.1 Effect of compaction on capillary rise

To study the effect of compaction on capillary rise, the medium grained SAND sample was compacted loosely and densely to two dry densities of 1.50 Mg/m^3 (85% MDD) and 1.65 Mg/m^3 (94% MDD) respectively. The results of capillary rise, in terms of the volumetric moisture content, for loosely compacted SAND and densely compacted SAND are presented in Figure 4.8 and Figure 4.9. The results show that, as the level of compaction increases, the height of capillary rise and the volume of water that can be drawn up also increases. This can be attributed to the formation of smaller capillaries i.e. narrower/finer pore sizes, which can enhance capillary performance of the soil. Thus, in general, the capillary rise of water within soil increases as the level of compaction increases. However it should be noted that too much compaction might result in breakdown in particles, which may lead to blockage of capillary tubes already formed and decreases the volume of water that can be drawn up. The average pore size diameter was estimated for loose SAND and dense SAND based on void ratio and average particle size (D_{50}). Accordingly, the average pore size diameter for loosely compacted SAND and densely compacted SAND was approximately 0.2 mm and 0.16 mm respectively.

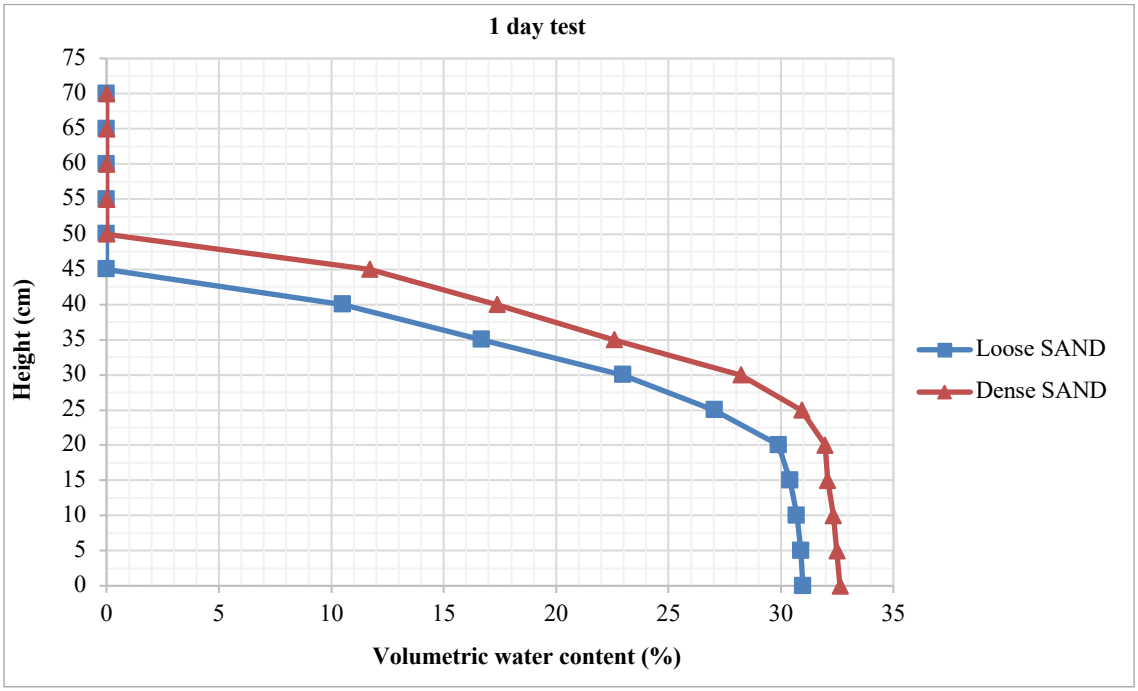

Figure 4.8 Capillary rise and volumetric water content distribution relationship for loosely compacted SAND and densely compacted SAND in free water surface.

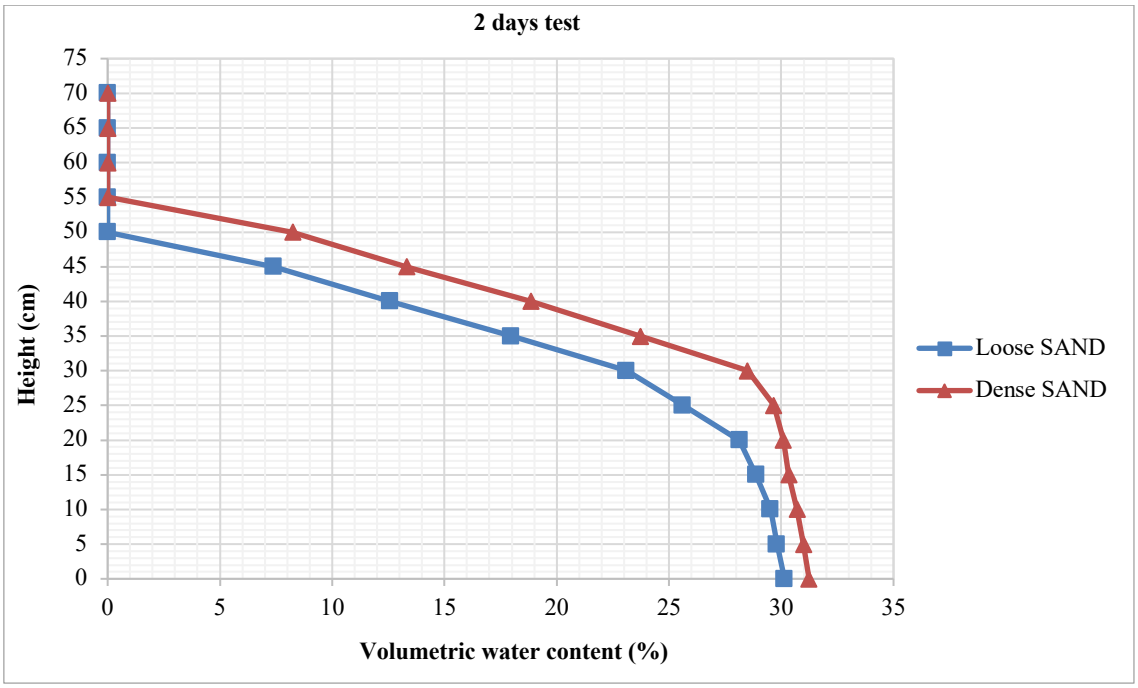

Figure 4.9 Capillary rise and volumetric water content distribution relationship for loosely compacted SAND and densely compacted SAND in free water surface.

4.2.1.2 The effect of soil type on capillary rise

The results of the capillary rise for all tested soil samples are plotted and presented in Figures 4.11 and 4.13. Additionally, The total volume of water drawn up and accumulated in each soil column after 1 and 2 days is presented in Figures 4.12 and 4.14.

In general, as particle size decreases from coarse-grained to fine-grained, the height of capillary rise increases. Smaller particle size generally creates narrower (smaller) pore/void space that means finer capillaries leading to higher capillary rise. Accordingly, the smaller the soil pore size, the higher the capillary rise of groundwater above the water table will be. The maximum height of capillary rise observed within the duration of experiment (i.e. two days) for medium grained SAND samples shows lower values than that of clayey sandy SILT as seen in Figure 4.13. The average pore size diameter was estimated for each soil type based on void ratio/porosity and average particle size (D_{50}). Accordingly, the average pore size for medium grained SAND, clayey sandy SILT and clayey very silty SAND was approximately 0.16 mm, 0.005 mm and 0.07 mm respectively. It should be noted that, the aim of this study was not to measure the ultimate height of capillary rise for infinite duration of time until the capillary rise stops. Thinking of engineering application of this method, shorter duration of time, i.e. a few hours up to a few days was preferred. Thus, the shorter duration of two days was selected and the maximum height of capillary rise for each soil column for this duration was measured. This work may be extended for longer period as deemed suitable for the target application. The maximum height of capillary rise for loosely compacted SAND, densely compacted SAND, layered SAND, clayey sandy SILT, and clayey very silty SAND was approximately 45 cm, 50 cm, 60 cm, 65 cm, and 55 cm after two days.

The maximum theoretical height of capillary rise was estimated for each soil type based on Equation 2.17 (Section 2.5.1), Equation 2.27 (Section 2.5.5) and Equation 2.29 (Section

2.5.5) and presented in Table 4.1. Equations 2.27 and 2.29 suggest that D_{10} may be sufficient to represent as the effective diameter of the smallest continuous capillary fingers in soil. Equation 2.17 assumes soil pores as ideal capillary tubes and therefore has limitations in soils. Accordingly, average pore size diameter was estimated based on D_{10} and D_{50}, to give more reasonable prediction of height of capillary rise.

Table 4.1 Maximum theoretical height of capillary rise for tested soils in this study

Soil type	Theoretical height of capillary rise (mm)			
	Peck et al. (1974) (Eq. 2.27)	Lu and Likos (2004a) (Eq. 2.29)	Jurin's law (Eq. 2.17)	
			D_{10}	D_{50}
Medium grained SAND	98 – 491	214	292	184
Clayey sandy SILT	12540 – 62698	4773	37223	6328
Clayey very silty SAND	8434 – 42169	4353	25035	434

In general, as particle size increases from fine-grained to coarse-grained, the rate of capillary rise also increases. This may also be due to the size of pore space between soil particles leading to generally lower unsaturated hydraulic conductivity in fine-grained soils and higher unsaturated hydraulic conductivity in coarse-grained soils. Accordingly, the greater the soil pore size, the higher the rate of capillary rise of groundwater above the water table may be. The rate of capillary rise for the medium grained SAND for the first, 6 hours of the experiment was recorded and shown in Figure 4.10. The rate was higher in the beginning of the experiment, particularly for the first few hours, as the water level in the medium grained SAND column raised to approximately 28 cm, 35 cm, and 40 cm in 1 hour, 3 hours, and 6 hours respectively. However, after that the rate of capillary rise for the medium grained

SAND significantly reduced. On the other hand, the water levels in the clayey sandy SILT and the clayey very silty SAND columns raised to approximately 40 cm in a day.

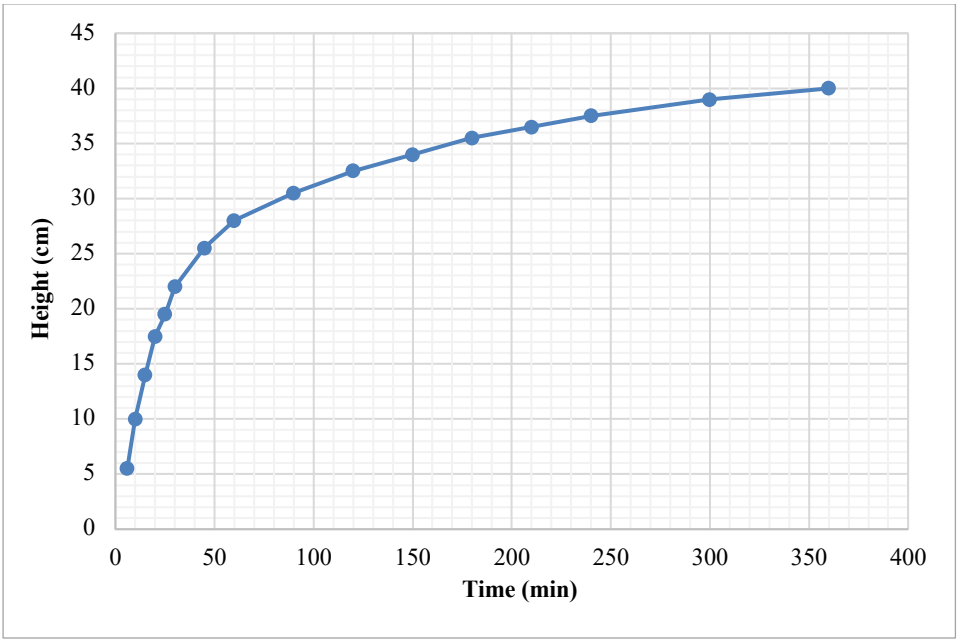

Figure 4.10 The rate of capillary rise for medium grained SAND (dense) in free water surface.

From the results shown in Figure 4.11 to 4.14, the clayey very silty SAND which was obtained from a mixture of medium grained SAND and clayey sandy SILT showed poor capillary rise (in terms of height and rate and volume of water raised) in comparison with the individual soil samples, i.e. the medium grained SAND and the clayey sandy SILT. The reduced height of capillary rise could be due to the presence (or addition) of medium grained SAND with larger particle/pore size in the mixture (or to the clayey sandy SILT) that lowered the height of capillary rise of the total sample. The reduced rate of capillary rise is due to the presence (or addition) of clayey sandy SILT with lower unsaturated hydraulic conductivity in the mixture (or to the medium grained SAND) that lowered the rate of capillary rise of the total sample. Finally, the reduced volume of water raised or the reduced water holding capacity of the sample could be due to the reduced porosity/void ratio of the whole sample

i.e. the reduced pore space between the soil particles as the space between SAND particles could be filled with SILT particles which are smaller in size and although SILT may generally have higher water holding capacity than SAND and is thought to improve the water holding capacity of the sample in total, due to the reduced pore space, the volume of water raised was decreased. Thus, the clayey very silty SAND shows poor capillary rise results due to the reduced pore/void space between soil particles with porosity and void ratio of approximately 0.31 and 0.45 respectively; compared to medium grained SAND with porosity and void ratio of 0.37 and 0.59; and clayey sandy SILT with porosity and void ratio of 0.32 and 0.47. The average pore size diameter was estimated for each soil type based on void ratio/porosity and average particle size (D_{50}). Accordingly, the average pore size for medium grained SAND, clayey sandy SILT and clayey very silty SAND was approximately 0.16 mm, 0.005 mm and 0.07 mm respectively.

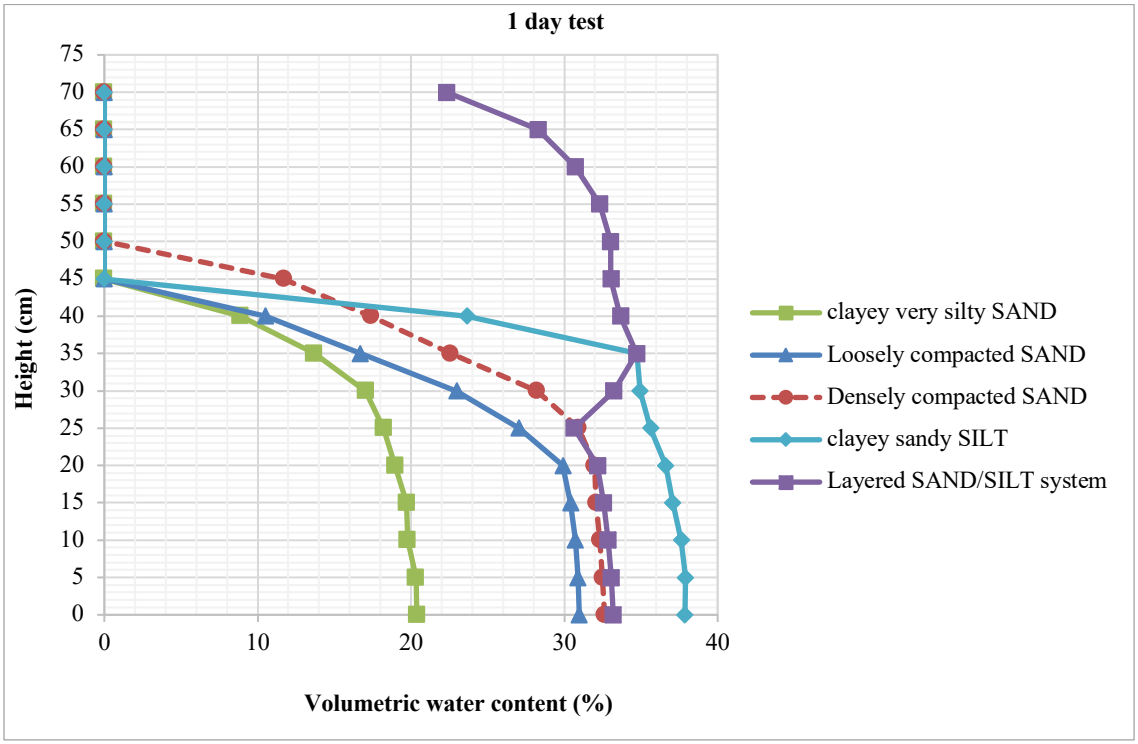

Figure 4.11 Capillary rise and volumetric water content distribution relationship for tested soil columns in free water surface.

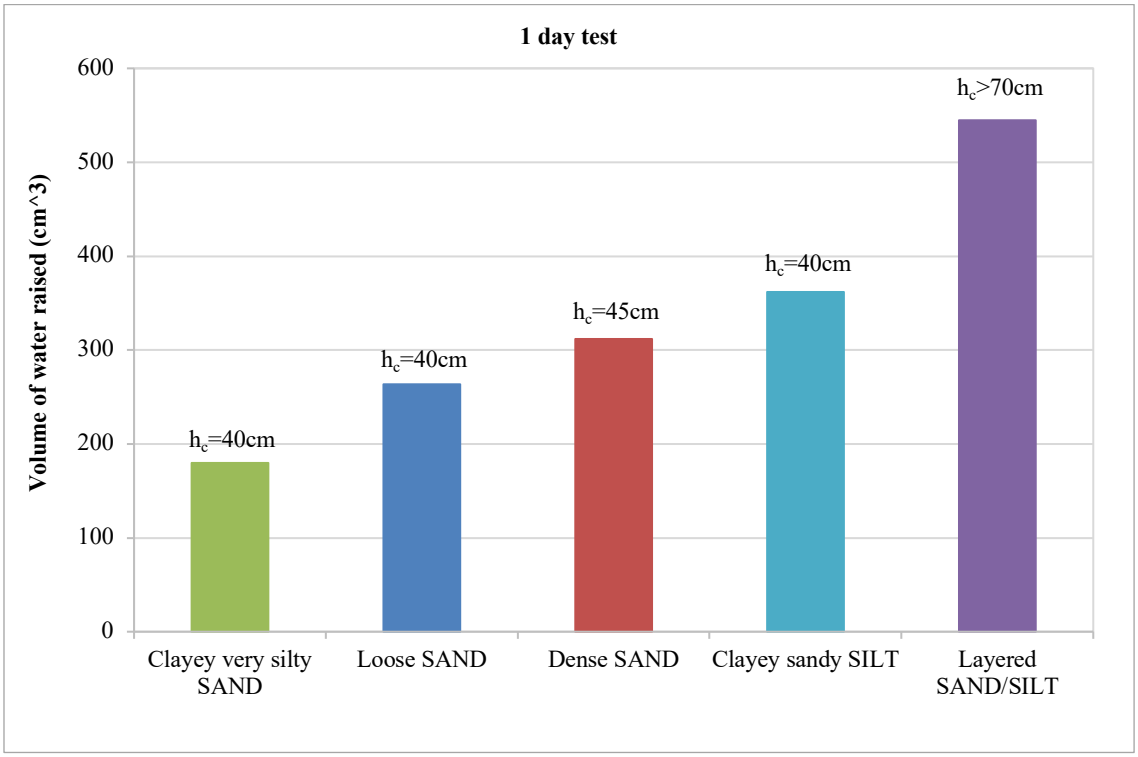

Figure 4.12 The volume of water drawn up in tested soil columns in free water surface; h_c represents as the height of capillary rise.

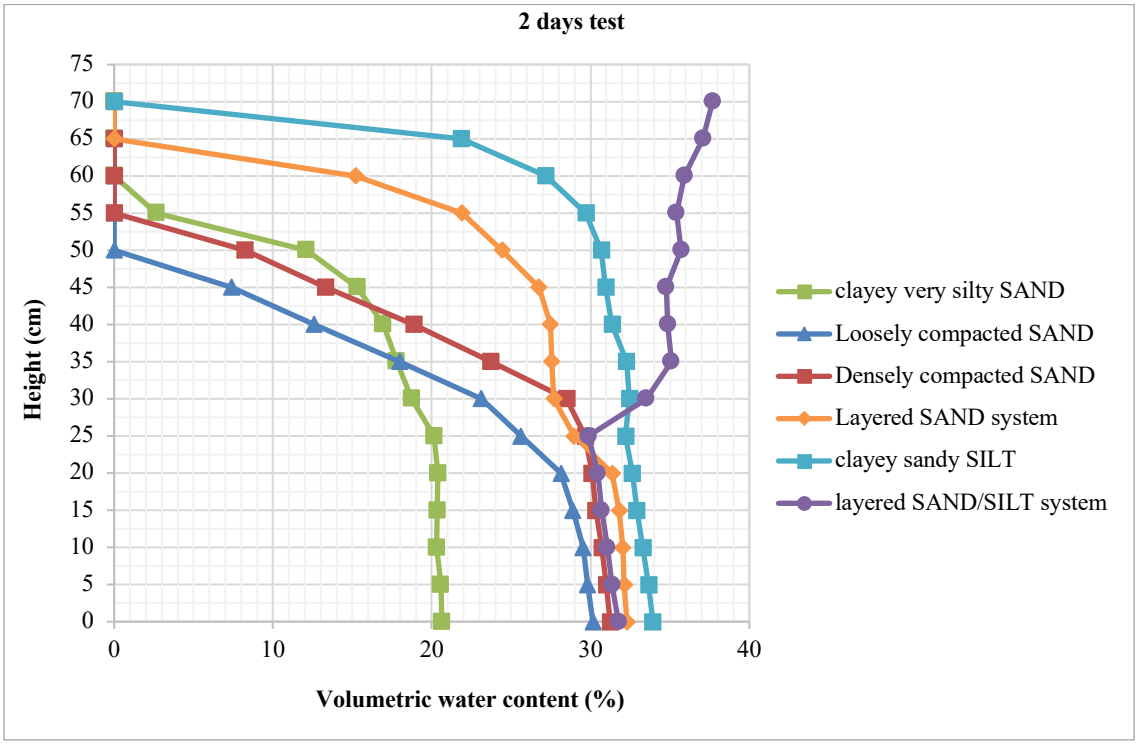

Figure 4.13 Capillary rise and volumetric water content distribution relationship for all tested soils column in free water surface.

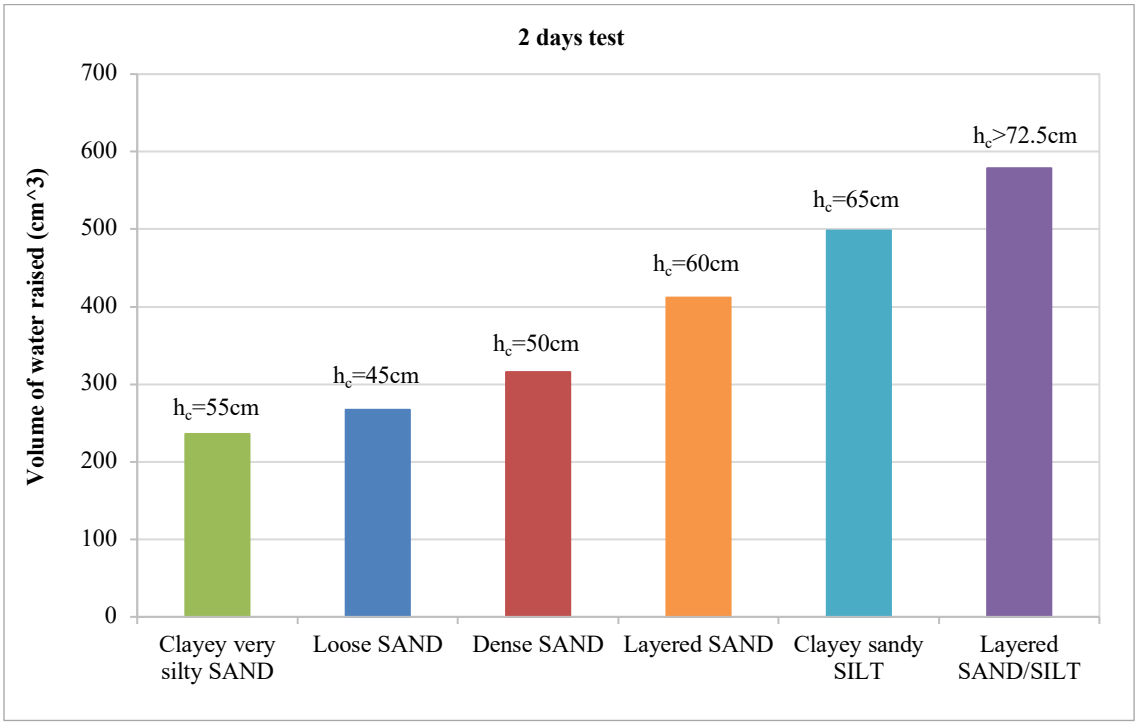

Figure 4.14 The volume of water drawn up in tested soil columns in free water surface; h_c represents as the height of capillary rise.

4.2.1.3 The effect of layering of soils on capillary rise

(1) The effect of layering of soils with different particle sizes on capillary rise

As described in Section 3.5.1 two soils with different particle size were placed in layers (coarse material at the base underlying a layer of fine material at the top) in a column in order to improve the height, rate of capillary rise and the volume of water that could be drawn up. The layered SAND/SILT system comprised of a coarse-grained soil layer (i.e. medium grained SAND) with larger particle/pore sizes underlying a fine-grained soil layer (i.e. clayey sandy SILT) with smaller particle/pore sizes. The thickness of coarse-grained layer (i.e. the medium grained SAND) and fine-grained layer (i.e. the clayey sandy SILT) was determined based on the capillary rise results of each individual soil sample. The layer configuration and thickness of each layer was shown in Figure 3.3 in Section 3.5.1.

Based on the experimental data shown in Figure 4.11 to 4.14, the layered SAND/SILT system improves capillary rise significantly, thus the water could be lifted to a higher level at a higher rate compared to each individual soil sample. This can be due to the following reasons:

(1) The layered SAND/SILT system is comprised of a coarse-grained soil layer (i.e. medium grained SAND) with larger particle/pore sizes underlying a fine-grained soil layer (i.e. clayey sandy SILT) with smaller particle/pore sizes. In general, as the soil type varies from coarse-grained to fine-grained, the height of capillary rise increases. This is due to the size of pore space between soil particles that is smaller in silty soils and greater in sandy soils. Smaller particle size generally creates narrower pore/void space that means finer capillaries leading to higher capillary rise because, the resisting force exerted by the weight of the elevated liquid against the rise of the liquid is smaller due to the small diameter of the capillary. Thus, in the layered SAND/SILT system, at first the water will rise due to larger

capillaries of the underlying SAND layer up to a certain height and then it will be pulled up (from the top of the sand layer) by finer capillaries of the overlying SILT layer. Additionally, the thickness of the coarse-grained (medium grained SAND) layer was a significant factor that could affect upward water flow in a way that if the coarse-grained layer was too thick and the capillary rise in this layer was less than the thickness of the layer, water would not even reach the interface between the coarse-grained layer and the overlying fine-grained (clayey sandy SILT) layer. In that case, the coarse-grained layer could either reduce or even impede the upward water flow.

(2) The hydraulic conductivity of coarse-grained material is, in general, greater than the fine-grained material. Thus, the water moved at a higher rate through the SAND layer and when it entered the SILT layer, this rate decreased but, it was still enough and it could still manage to reach the maximum height of the soil column as the thickness of the layers was selected based on the capillary rise data of individual soil sample.

The water level in the layered SAND/SILT system reached the maximum height of the column within 2 days. None of the soils columns experienced this height of capillary rise. In the layered SAND/SILT system, the gravimetric and volumetric moisture contents and the actual volume of water that was lifted to a height of 70 cm are equal to 21.07%, 37.68% and 43.15 cm^3 within 2 days, respectively compared to zero values at the same conditions in other soil samples as illustrated in Figure 4.13. The total amount of water that was drawn up in the layered SAND/SILT soil column was also significantly higher than that of other soil column samples as shown in Figure 4.12 and Figure 4.14. The total volume of water that was drawn up in the loose SAND, dense SAND, clayey sandy SILT, clayey very silty SAND, and layered SAND/SILT soil columns within 1 day was approximately 264 cm^3, 312 cm^3, 362 cm^3, 180 cm^3, and 545 cm^3 respectively. The total volume of water that was drawn up in the

loose SAND, dense SAND, layered SAND, clayey sandy SILT, clayey very silty SAND, and layered SAND/SILT soil columns within 2 days was approximately 267 cm^3, 316 cm^3, 412 cm^3, 498 cm^3, 236 cm^3, and 579 cm^3 respectively.

(2) The effect of particle size layering of single soil on capillary rise

As described in Section 3.5.1 different particle sizes of a single soil type (medium grained SAND) were placed in layers (coarse material at the base and layers of reduced particle size with height) in a column in order to improve the height of capillary rise and the volume of water that could be drawn up. This multi-layered system was introduced to improve the capillary rise of the medium grained SAND samples. This layered system was made up of several layers having particle size ranges of 0.300 - 2.00 mm, 0.212 - 0.300 mm, 0.150 - 0.212 mm, and 0.063 - 0.150 mm. The thickness of the layers was selected to be 10 cm, 10 cm, 10 cm, and 45 cm. The layered SAND system comprised a soil column of medium grained SAND in which larger (coarser) particle size layers underlying smaller (finer) particle size layers. Thus, as the height of layers in soil column increases, the particle size of layers decreases to achieve higher capillary rise. Therefore, in the layered SAND system, at first the water will rise due to larger capillaries of the underlying layer up to a certain height and then it will be pulled up by finer capillaries of the overlying layers. It should be noted that the thickness of underlying layer was a significant factor that could affect upward water flow in a way that if the underlying layer was too thick and the capillary rise in this layer was less than the thickness of the layer, water would not even reach the interface between the underlying larger particle size layer and the overlying finer particle size layer. In that case, the underlying larger particle size layer could either reduce or even impede the upward water flow.

The maximum height of capillary rise observed within 2 days for loosely compacted SAND, densely compacted SAND, and layered SAND was approximately 45 cm, 50 cm, and 60 cm respectively, as seen in Figure 4.13. Thus, the height of capillary rise of layered SAND was higher than that of loosely compacted SAND and densely compacted SAND by 15 cm and 10 cm respectively. The total volume of water that was drawn up in the layered SAND column was also higher than that of loose SAND and dense SAND as shown in Figure 4.14. The total volume of water that was drawn up in the loosely compacted SAND, densely compacted SAND, and layered SAND, soil columns within 2 days was approximately 267 cm^3, 316 cm^3, 412 cm^3 respectively.

One of the objectives of this study was to experimentally design an apparatus to improve the height of capillary rise and the volume of water that could be drawn up within the duration of the test. Both layered systems significantly increased the height of capillary rise and the volume of water that could be drawn up within the duration of the test compared to the other soil samples. Consequently, the layered system shows higher capillary performance than the other soil samples and a replicated model based on this approach has the potential to be further developed for field applications.

4.2.2 Capillary rise tests in a moist soil

The main aim of these tests was to assess the capability of capillary action to suck water away from a moist soil with a range of moisture contents.

Soil used as the base soil (i.e. soil in the container that was in contact with the base of the columns) for all tests was medium grained SAND. The base soil samples were prepared to three different moisture contents of 35 % (sample 1), 28 % (sample 2) and 20 % (sample 3).

In this part, two different types of soil column samples were tested. They comprised the medium grained SAND and the layered SAND/SILT system. The medium grained SAND soil column was stood in the container of moist soil i.e. sample 1, sample 2 and sample 3 and capillary rise was measured for 2, 4, 5, and 10 days; 4, 10, and 14 days; and 4, and 5 days respectively. The layered SAND/SILT soil column was stood in the container of moist soil with moisture content of 35 % (sample 1), and capillary rise was measured for 4 days.

The results of capillary rise for the medium grained SAND soil column in moist soil sample 1, sample 2, and sample 3 along with that of the layered SAND/SILT soil column in sample 1 after duration of 4 days are presented in Figure 4.15, Figure 4.16, Figure 4.17 and Figure 4.18, respectively. The results show that as the moisture content of the base soil increases, the capillary rise within the soil column also increases. This is because as the water content increases, the thickness of the layer of water decreases. Since there is reduction in strength of bond with distance from the surface of the materials, then water farthest away can be removed more easily. Thus when water content increases, it can be removed more readily.

The results show gradually decreasing values of moisture content with increase in height above the soil surface. Unlike the capillary rise above the free water, in the case of all moist soil, the moisture content decreases with increase in height above the soil surface. From the result for the layered SAND/SILT system (4 days test in moist soil) shown in Figure 4.18, it

can be seen that the water content decreases as the height increases, which is very different from Figure 4.13. This is conjectured to be due to strength of bond between soil particles and water; when the capillary rise pressure is less than or equal to the strength of water/soil bond, there will be no rise in water. Thus water will only rise in the capillary tubes if the capillary pressure is greater than the soil/water bond strength.

The maximum height of capillary rise that was observed within 4 days for the medium grained SAND column in moist soil sample 1, sample 2, and sample 3 along with that of the layered SAND/SILT soil column in sample 1 was approximately 35 cm, 25 cm, 15 cm, and 60 cm respectively.

Each test in this part was repeated for three times. The error band of the measurements was approximately 0.8 for gravimetric water content and 1.3 for volumetric water content.

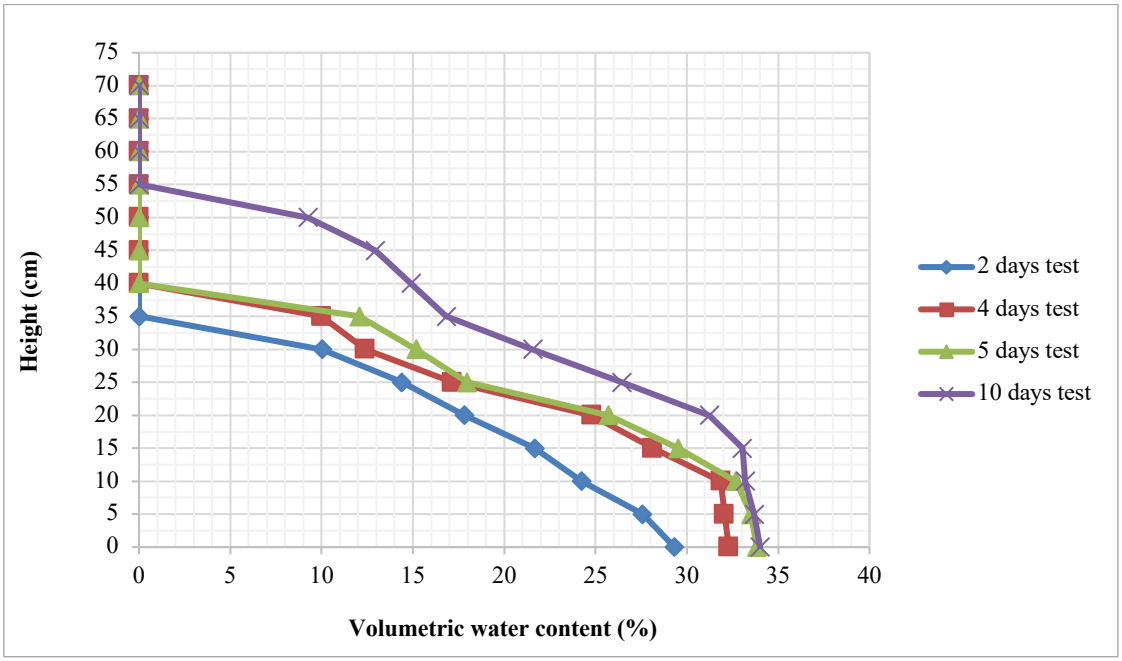

Figure 4.15 Capillary rise and volumetric water content distribution relationship for the medium grained SAND column with the base of the column in moist soil Sample 1.

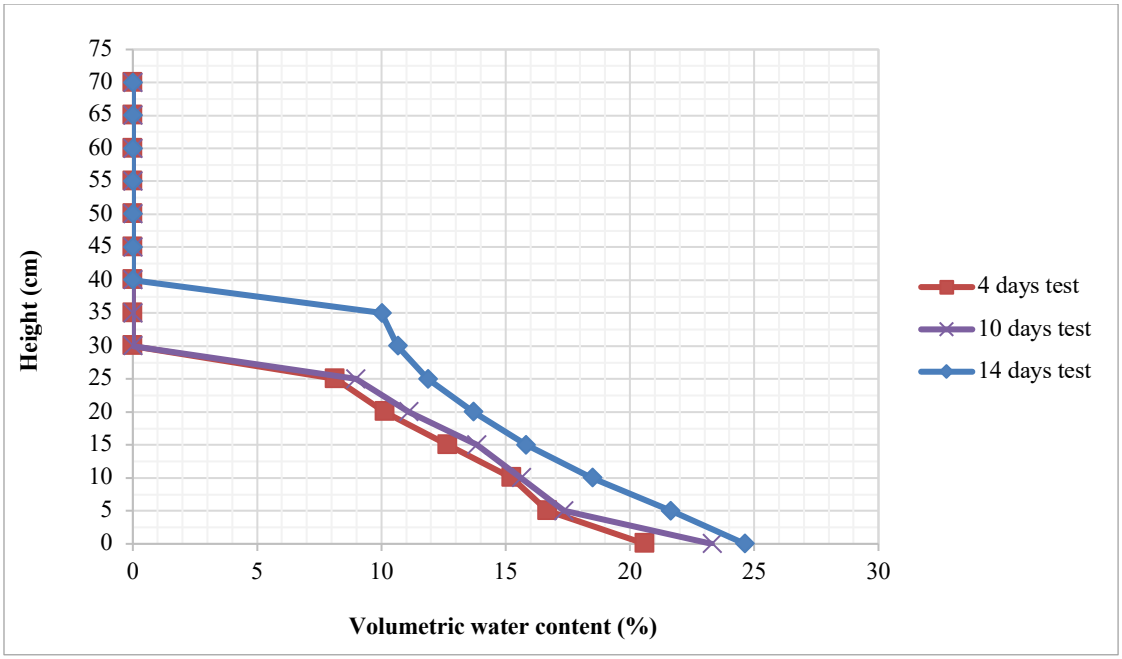

Figure 4.16 Capillary rise and volumetric water content distribution relationship for the medium grained SAND column with the base of the column in moist soil Sample 2.

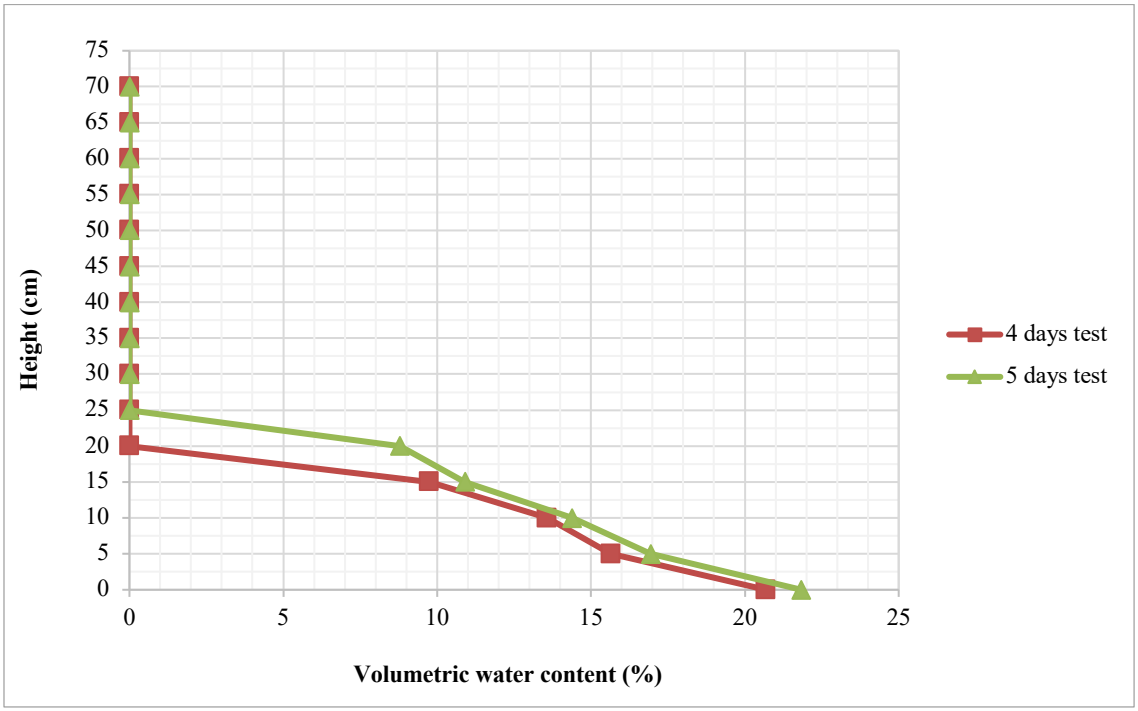

Figure 4.17 Capillary rise and volumetric water content distribution relationship for the medium grained SAND column with the base of the column in moist soil Sample 3.

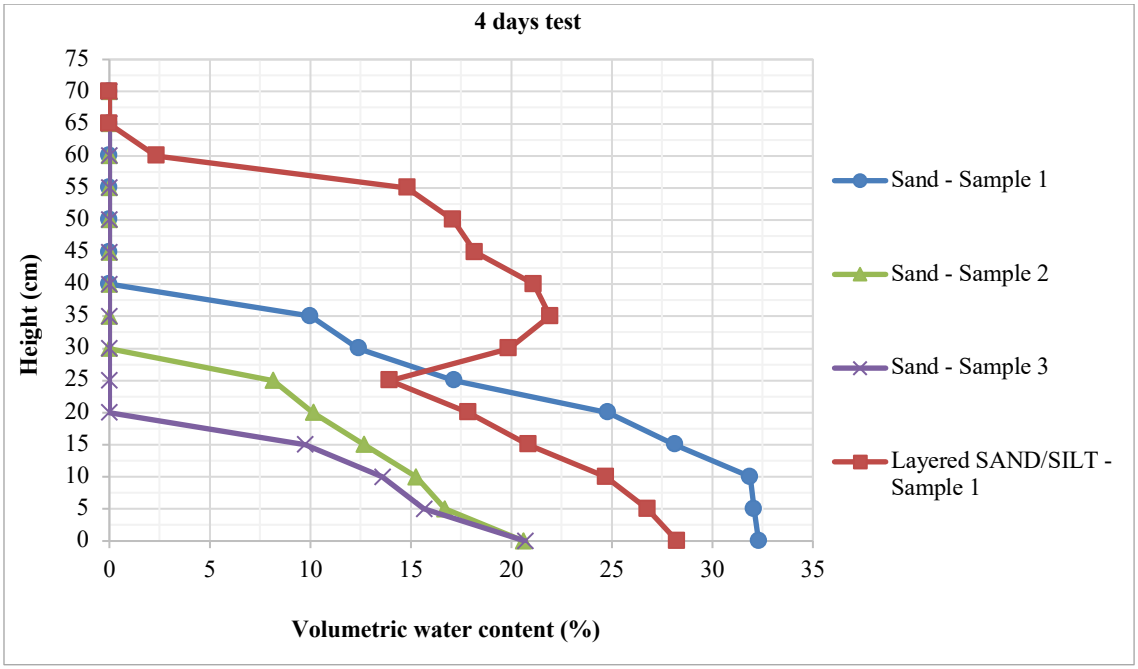

Figure 4.18 Capillary rise and volumetric water content distribution relationship for all tested soils column with the base of the column in moist soil.

4.2.3 Capillary rise tests for soil column in a free surface of water with top of column subjected to wind action

This part involved carrying out soil column tests with the base of the columns in water and the top surface of the column exposed to wind in a wind tunnel. The aim of these experiments was to assess the effect of removal of water from the surface of the column on capillary action.

4.2.3.1 The effect of wind velocity on capillary rise

In this part, the soil column sample of the medium grained SAND was tested at wind velocities of 1.3 m/s, 3.0 m/s and 4.9 m/s. The soil sample was additionally tested in the same setup under windless (i.e. zero wind) conditions. Each test was run for 4 days and the change in the mass of water in test container, water check, and soil column were recorded after every 24 hours.

The results of capillary rise for soil columns at different wind velocities at the end of 4 days are shown in Figure 4.19. The results show that as the wind speed increases, the capillary rise of water also increases. This is due to reduction in pressure at the soil surface caused by the action of wind, which acts on the water and drive it upward further. When a difference in atmospheric pressure exists, air moves from the higher to the lower pressure area. In fact, every system moves from the state of higher energy to the state of lower energy and works toward equilibrium.

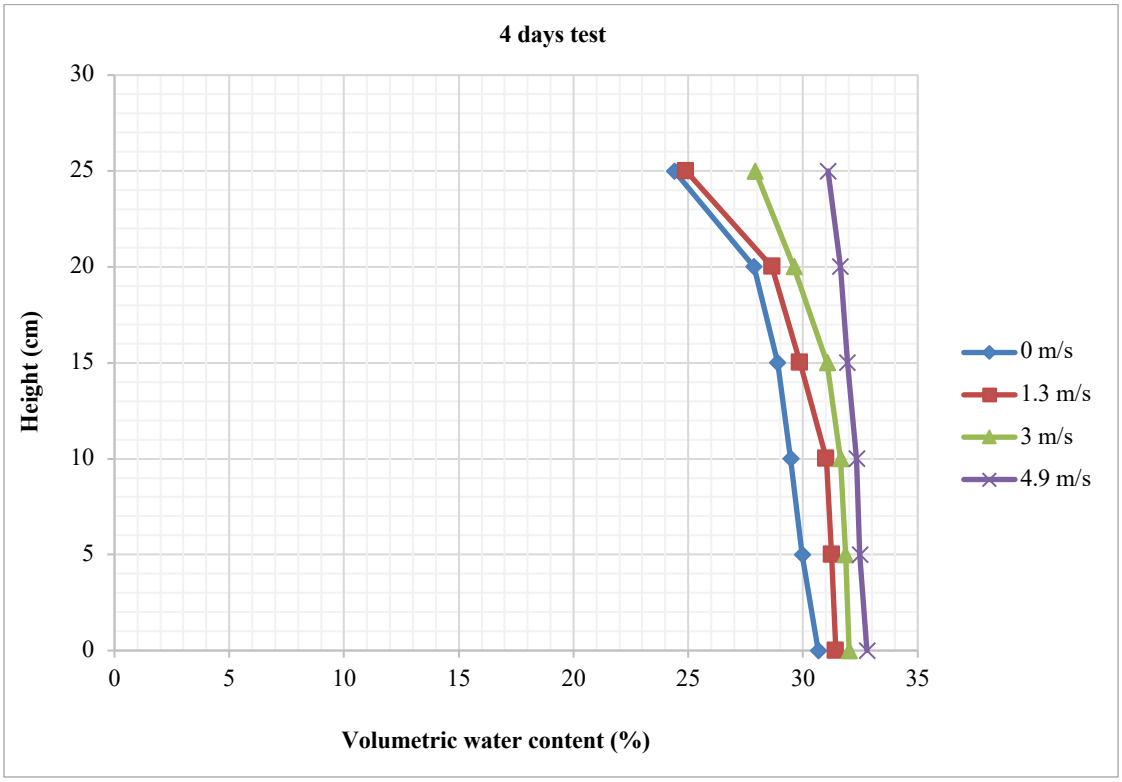

Figure 4.19 Capillary rise and volumetric water content distribution relationship for medium grained SAND column in free water surface with top of column subjected to wind action.

4.2.3.2 Capillary removal of water through soil column

If a column of dry soil, in a tube covered at the bottom with fine wire gauze, is placed with its lower end in a container of water, the water begins to rise in the soil, the dry soil sucking water away from the moister soil below. If the tube be not too long, and if its upper end be exposed to evaporation into the air, a steady state of flow is eventually established in which the percentage of moisture at any level in the soil does not change with the time. When this state of affairs has been set up the amount of water that reaches any level from below must be the same as the amount that leaves that level to the soil above, and the same as evaporates from the surface at the top of the column. Before this steady state is set up, the capillary flow is not constant and the water content at any given point in the tube changes with the time. It is a fact that when capillary tube or soil column is cut below the level of water in it that it can

raise, the water will not move out but remain bonded with material or soil walls so it was planned to use wind action (wind powered suction system) for successful lifting and removal of water, which creates a negative pressure at the top of the capillary tube.

The average water loss per unit surface area per day through the soil column of medium grained SAND at wind velocities of 0.0 m/s, 1.3 m/s, 3.0 m/s, and 4.9 m/s was 4.3 g/cm^2, 4.6 g/cm^2, 5.1 g/cm^2, and 5.3 g/cm^2 respectively, as shown in Figure 4.20. The results show a gradual increase in average water loss per unit surface area per day as the wind velocity increases. The trend of results is in agreement with the literature. The percentage increase in water loss from wind velocities of 0.0 m/s to 1.3 m/s, 1.3 m/s to 3.0 m/s, and 3.0 m/s to 4.9 m/s was approximately 7 %, 9 %, and 4 % respectively. The percentage increase in water loss from wind velocity of 1.3 m/s to 3.0 m/s is slightly greater than that at other wind velocities and the percentage increase from 3.0 m/s to 4.9 m/s was found to be approximately 4 %, thus 1.3 m/s to 3.0 m/s could be the critical velocity range from which the evaporation is no longer dependent on the wind velocity. Davarzani et al. (2014) also stated that at the critical wind velocity, the temperature rises to the wind temperature and the vapor concentration falls to the wind vapor concentration above the soil surface. Therefore, a higher wind velocity cannot change the evaporation processes.

The percentage increase in average total water loss per unit surface area per day at different wind velocities for this study and a study by Davarzani (2014) is shown in Table 4.2. The percentage increase in water loss from wind velocity of 1.0 m/s to 3.0 m/s shows quite similar values. However, the percentage increase in water loss at other wind velocities are somewhat different particularly from wind velocity of 0.0 m/s to 1.3 m/s and the reason for this is not completely clear but it may be due to different test conditions, depth to water table, and area of evaporating surface etc.

Table 4.2 Percentage increase in water loss per unit surface area per day at different wind velocities

Davarzani (2014)		This study	
Wind velocity (m/s)	Percentage increase in water loss	Wind velocity (m/s)	Percentage increase in water loss
From 0.6 to 1.2	14 %	From 0.0 to 1.3	7 %
From 1.2 to 3.0	10 %	From 1.3 to 3.0	9 %
From 3.0 to 3.6	2 %	From 3.0 to 4.9	4 %

The total mass of water removed from the system through the soil column at different wind velocities over four days duration of tests is shown in Figure 4.21. The results show that as the wind velocity increases, the total mass of water lost from the system also increases. This is due to higher upward lifting of water i.e. higher capillary rise and higher evaporation of water from the soil surface, which creates a negative pressure acting on the water and drive it upward even further. Increasing wind velocity can remove the water available for evaporation quite rapidly due to the energy supplied by wind. However it should be noted that, as the wind velocity increases, the capillary rise and the mass of water that is drawn up and accumulated within the soil column also increases and this amount is deducted from the total mass of water lost from the test container. As all the experiments were carried out in quite similar atmospheric conditions (i.e. laboratory conditions) having quite similar potential evaporation, then with increasing wind velocity, a greater value is deducted from the total mass of water lost from the test container. This decreases the mass of water removed from the system through the soil column for higher wind velocities. Because the water that exists in the soil column is still in the system and not removed from it completely. This can be a reason for higher wind velocities not experiencing considerably higher water removal results

than lower wind velocities. Another reason could be the quite small area of influence of wind, i.e. the surface area of the soil column. The area of evaporating surface was approximately 22.9 cm^2. Thus, greater wind action such as designing a windmill might be required to remove the water from the system through the soil column more effectively which, can be considered in future studies.

Praneesh et al. (2017) proposed the design of a pump working principally by capillary action, which has 3 major components comprised of (1) Pressure maintaining tank, (2) Capillary pipe, and (3) Wind powered suction system. Each component's task is briefly explained as follows. Pressure maintaining tank maintains constant pressure (at the desired head) in the capillary pipe. It is mainly designed to take in the running water from municipal connection and keep feeding the capillary pipe through a constant cross-section connection. Capillary pipe is the main component of the capillary pump. It carries the capillary tubes along its area and absorbing material to withhold the water to fight the accidental negative pressures. The capillary pipe is comprised of a number of sets of capillary tubes of same diameters and absorbing material up to a specific height and the same set is repeated and placed one above the other until it fills the remaining length of capillary pipe. Absorption material is similar to the water filter candle clay or ceramic. It holds the water for next capillary set when there is backward suction. Wind powered suction system that is basically a compacted windmill, is designed to increase the discharge rate and velocity of water in to the main delivery tank. The water is delivered into over-hear water holding tank through the delivery pipe.

Thus, from this experimental study and theoretical study by Praneesh, et al., (2017), it can be assumed that employing both capillarity and suction created by the wind has a potential to be developed for successful lifting of water and making system of pumping possible.

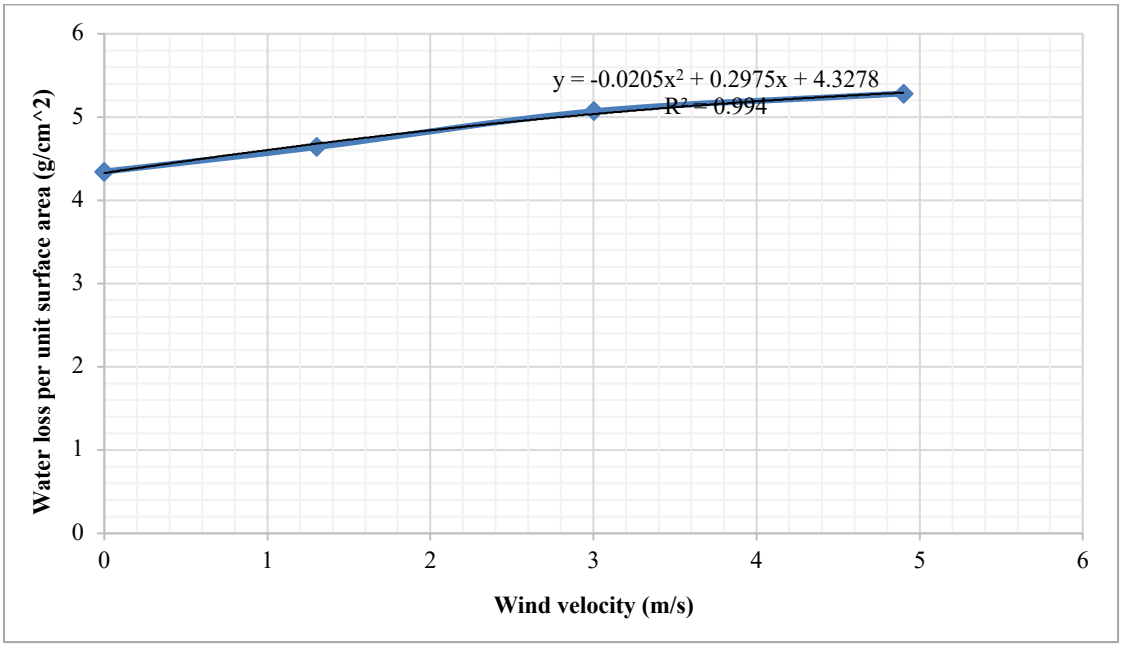

Figure 4.20 The average water loss per unit surface area per day through the medium grained SAND column in free water surface with top of column subjected to wind action.

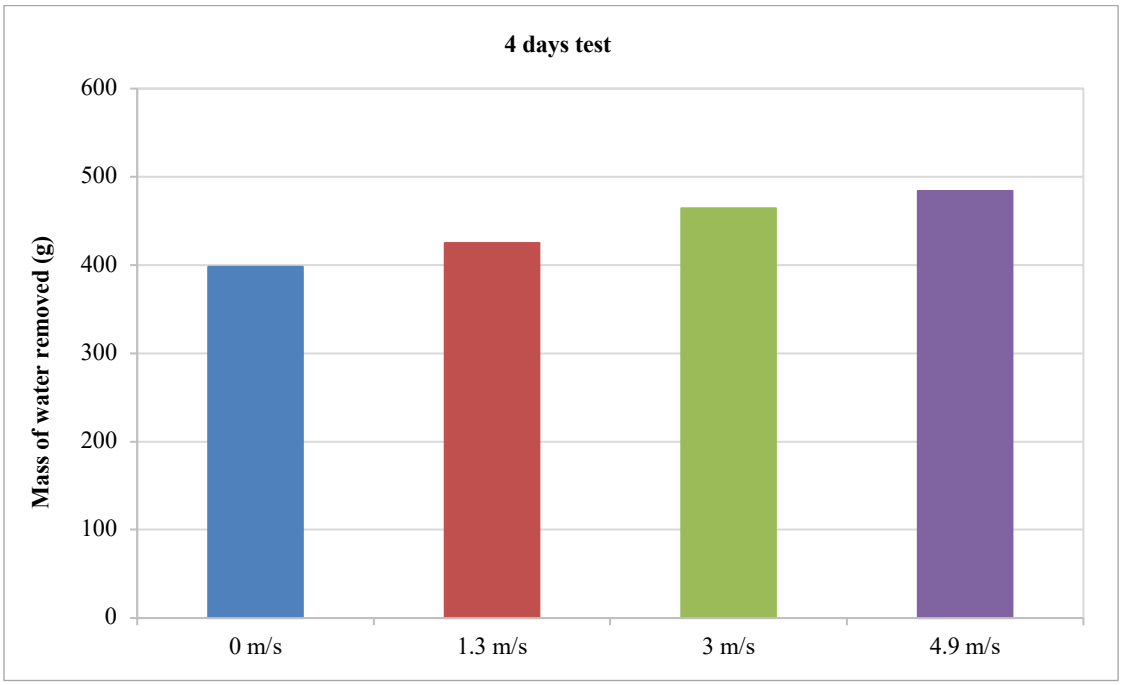

Figure 4.21 The mass of water removed by the medium grained SAND column in free water surface with top of column subjected to wind action.

4.3 *Evaporation tests on block samples*

4.3.1 Effect of wind velocity and wind movements on evaporation

The changes in evaporation that were recorded over two days duration of tests are illustrated in Figure 4.22 and Figure 4.23. The results shown in Figure 4.22 are related to the soil samples with initial moisture content of 27 %, while the results shown in Figure 4.23 are related to the samples with initial moisture content of 13 %. For all tested soil samples shown in Figures 4.22 and 4.23, an increase in wind velocity results in an increase in the evaporation of water from soil samples. This rise is generally greater in setup number 2, which mimics turbulent wind conditions than in setup number 1 that mimics laminar wind conditions. Both of these setups were described in Section 3.6.3. For example, for the medium grained SAND sample with moisture content of 27 %, an increase in wind velocity from 0 m/s to 6 m/s resulted in an increase in the cumulative evaporation by approximately 6 times and 8 times for laminar and turbulent wind movements respectively, as illustrated in Figure 4.22a. As another example, for the clayey very silty SAND sample with moisture content of 27 %, an increase in wind velocity from 0 m/s to 6 m/s resulted in an increase in the cumulative evaporation by approximately 6.5 times and 8 times for laminar and turbulent wind movements respectively, as illustrated in Figure 4.22b.

Davarzani, et al., (2014) observed a similar trend of results for silica sand, as shown in Figure 4.22a. Whilst the trend of results of this study and Davarzani's results are similar there are significant differences in cumulative evaporation for similar wind velocities. The reason for this is not completely clear but it may be due to different test conditions, depth to water table, and area of evaporating surface etc. The effect of wind velocity on cumulative evaporation is more considerable at the first stage of evaporation process. At the second stage of evaporation however, that effect becomes less significant. Increasing wind velocity at the

soil surface during the first stage of evaporation, can remove the water available for evaporation quite rapidly due to the energy supplied by wind. Subsequently, as the amount of water available for evaporation becomes limited and evaporation enters the second stage, i.e. the falling or intermediate rate stage, the evaporation is controlled by the soil profile properties and by the hydraulic properties of soil, rather than atmospheric conditions, as this is a soil-controlled stage. Thus, from the experimental results of this study and literature review, it can be understood that the wind velocity has a significant effect on the evaporation of water from soil.

The transition from first stage to second stage of evaporation and falling of evaporation rate is more evident in Figure 4.23 as the initial water content is limiting to 13 % in that case. As shown in Figure 4.23, almost all experiments with wind velocity $<$ 3 m/s, the Stage-1 evaporation did last for approximately 2 days, while, experiments with wind velocity $>$ 3 m/s, Stage-1 evaporation did last for approximately 1 day. This can be noticed from the trend of curves shifting from linear to non-linear indicative of a decrease in evaporation due to a decrease in moisture content as it becomes limited.

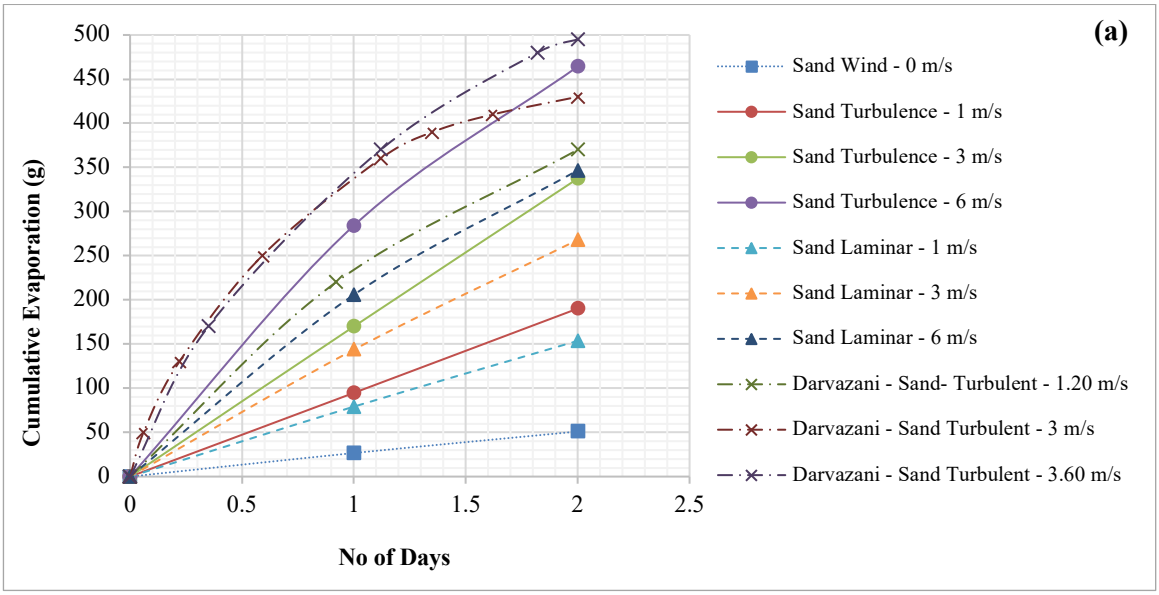

a) Medium grained SAND – 27 % moisture content

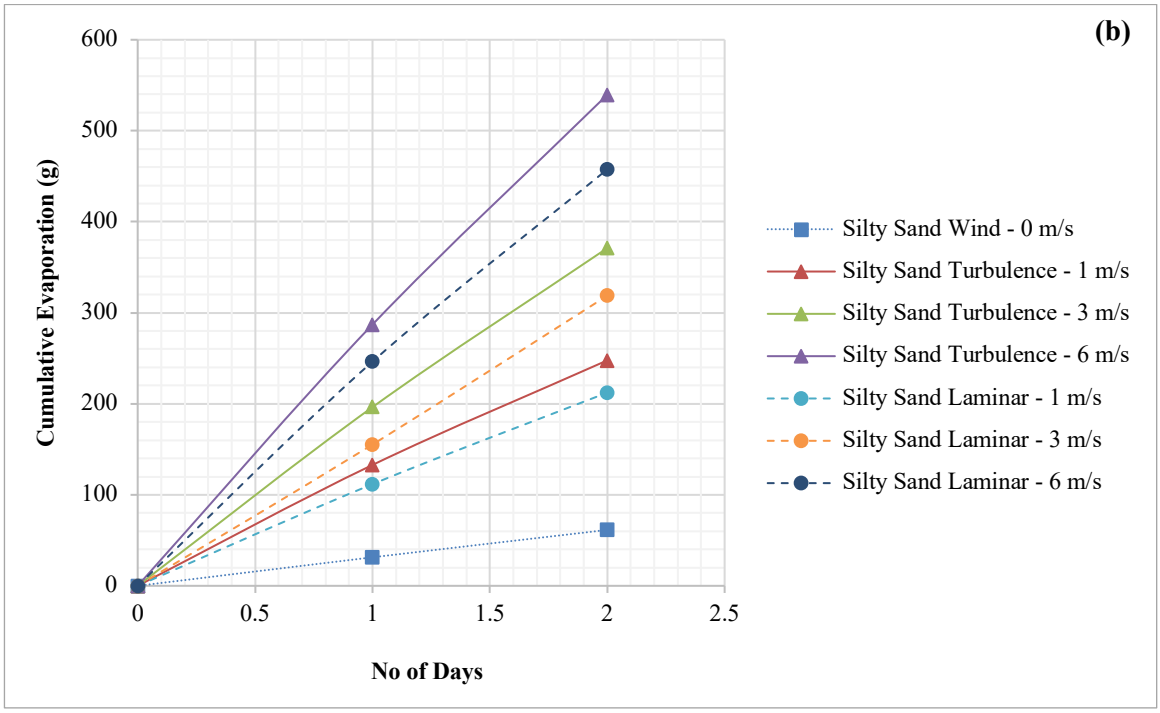

b) Clayey very silty SAND – 27 % moisture content

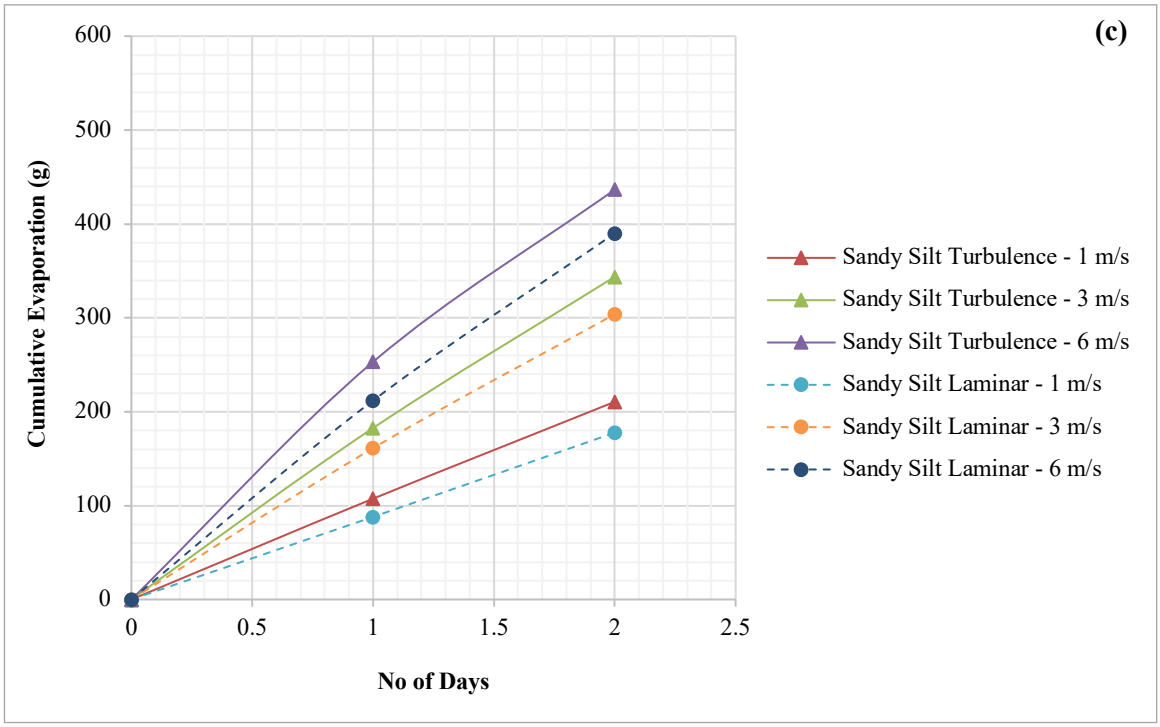

c) Clayey sandy SILT – 27 % moisture content

Figure 4.22 Impact of wind velocities/wind flows on evaporation processes: a) medium grained SAND – 27 % b) clayey very silty SAND – 27 % and c) clayey sandy SILT – 27 %.

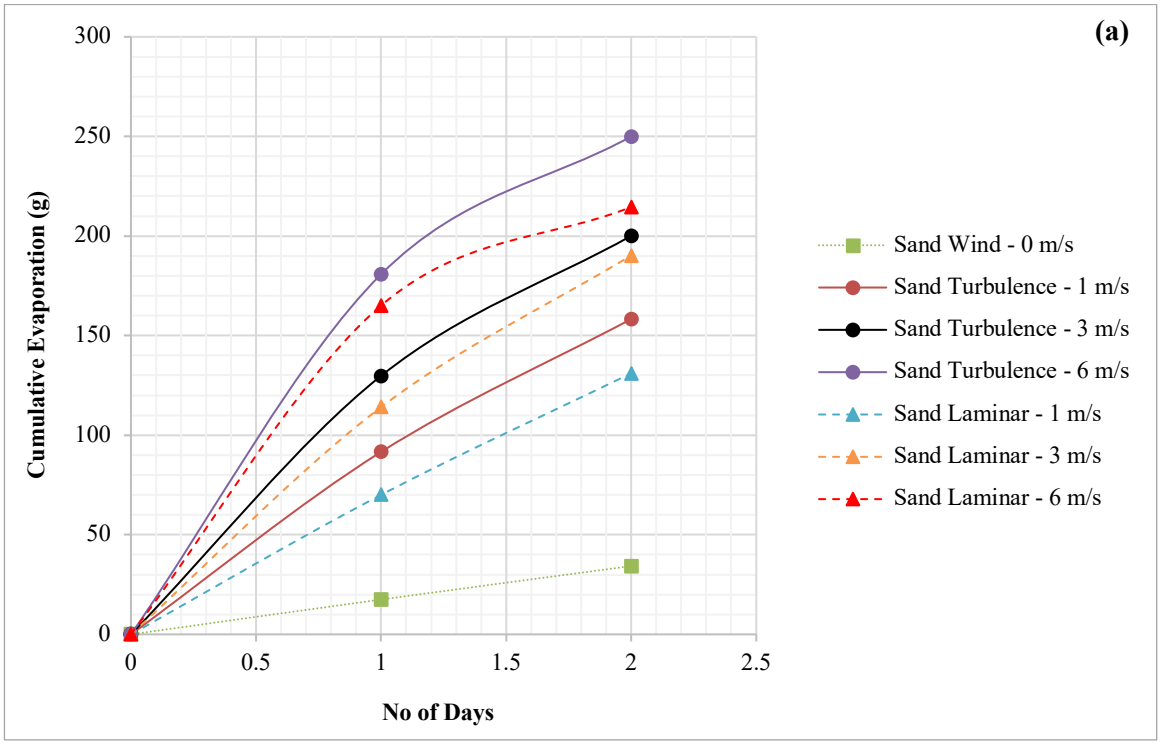

a) Medium grained SAND – 13 % moisture content

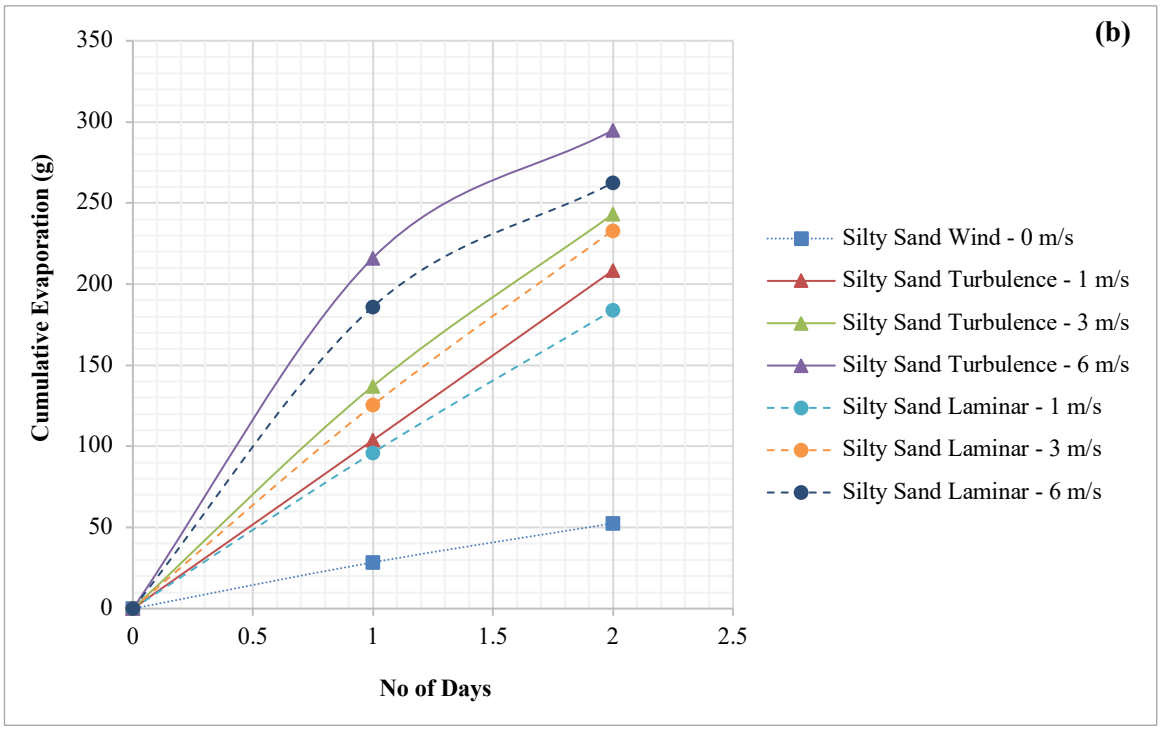

b) Clayey very silty SAND – 13 % moisture content

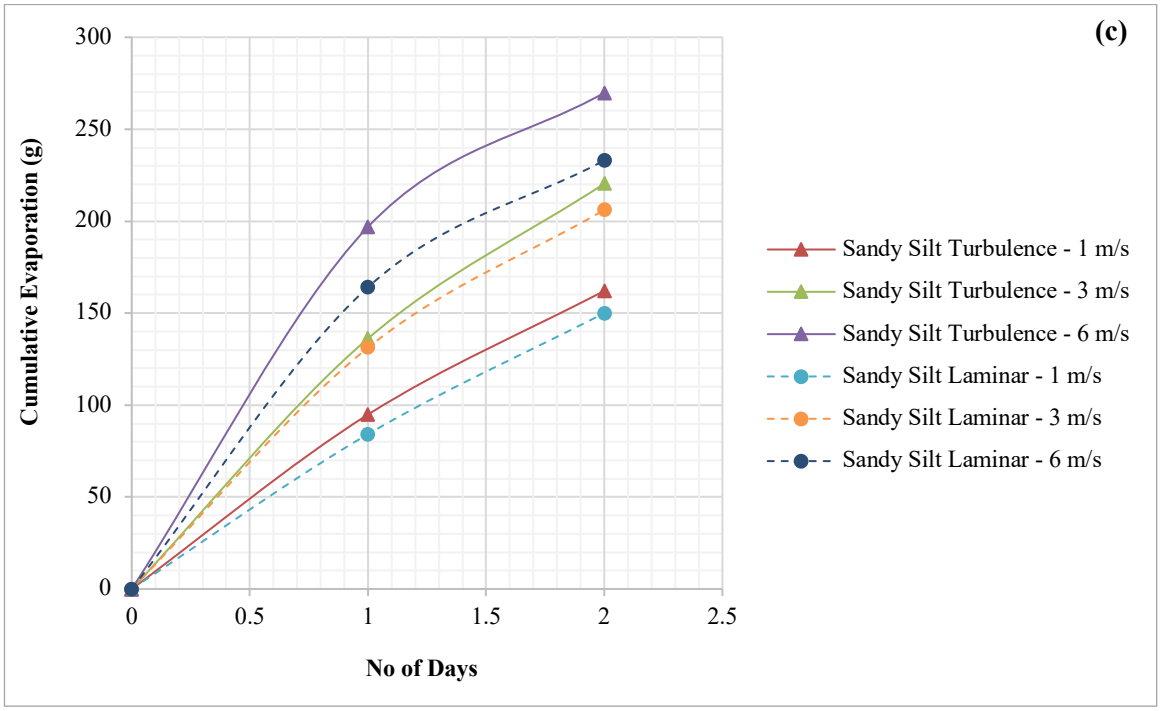

c) Clayey sandy SILT – 13 % moisture content

Figure 4.23 Impact of wind velocities/wind flows on evaporation processes: a) medium grained SAND – 13 % b) clayey very silty SAND – 13 % and c) clayey sandy SILT – 13 %.

For repeatability of experimental data, each test in this part was repeated three times and the repeatability achieved was quite satisfactory as shown in Fig. 4.24. Figure 4.24 shows an example of evaporation tests for medium grained SAND, which was repeated for three times. The error band of the measurements for cumulative evaporation was approximately 8%.

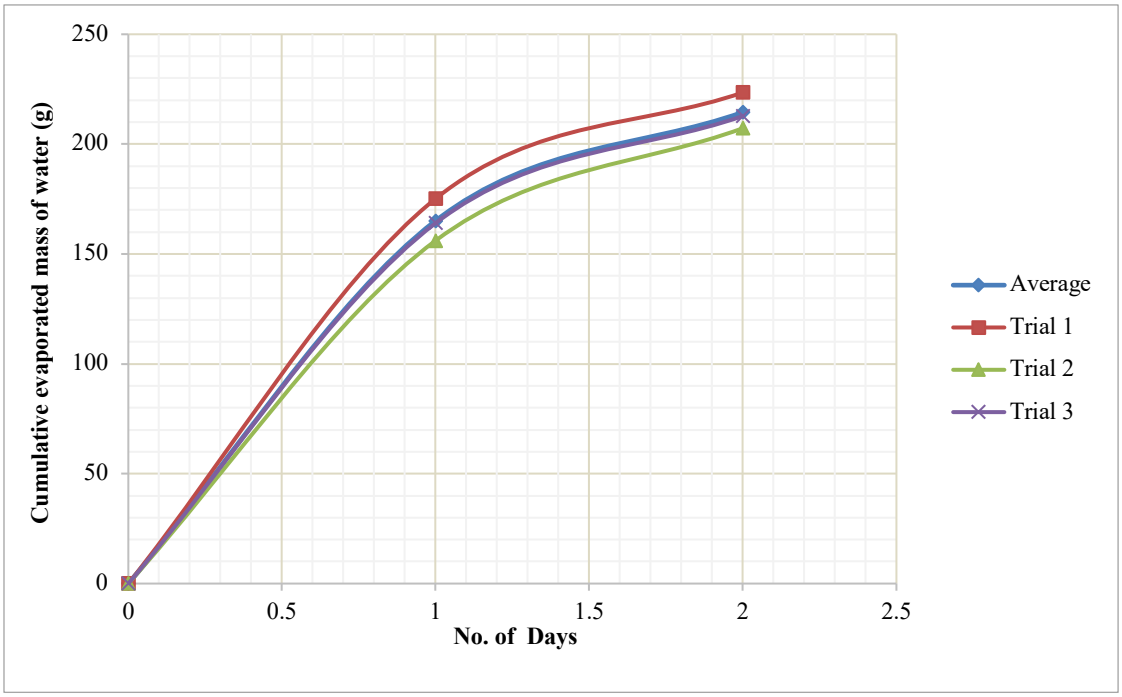

Figure 4.24 Repeatability of experimental data for evaporation from medium grained SAND at 6 m/s laminar wind and initial water content of 13 %.

4.3.2 Effect of soil type on evaporation

Figure 4.25 shows the cumulative evaporation plotted against drying time for each soil types of medium grained SAND, clayey very silty SAND and clayey sandy SILT. Figure 4.25a and Figure 4.25b correspond to initial moisture contents of 27 % and 13 % for all three samples respectively.

Results in Figure 4.25 show that the cumulative evaporation for different soil types starts to differ as the evaporation progresses in Stage-1 after one day. However, the significant difference in evaporation between different soil types can be seen after two days of evaporation in Stage-2, which is a soil-controlled stage. Soil type can have a significant effect on cumulative evaporation, particularly at the second stage of evaporation, which is a soil-controlled stage. According to Jalaota and Prihar (1986), as the percentage of fine particles in soil increases, the cumulative evaporation of water from soil also increases. Thus, a fine-grained soil is expected to experience higher total evaporation than a coarse-grained material. The clayey very silty SAND experienced the highest total cumulative evaporation followed by the clayey sandy SILT. The medium grained SAND experienced the least total cumulative evaporation out of the three soil samples due to its larger particle size range, as it contains larger particles than the other two soil samples. According to the findings of Hillel and Van Bavel (1976), as the percentage of coarse materials in soil increases, the cumulative evaporation of water from soil decreases. Thus in general, a coarse-grained soil is expected to experience lower total evaporation than a fine-grained material. Larger particles create larger pore space within the soil. When the surface of this soil is exposed to air or wind, the surface and upper layers dry out quite rapidly leading to the formation of a dry surface layer breaking the capillary connectivity within the soil pores and at the soil particle contacts.

It was seen that the evaporation for the clayey sandy SILT started to drop after one day of experiment and that is why this soil did not experience the highest total cumulative evaporation. This can be due to the formation of a dry surface layer or a crack breaking the capillary connectivity within the soil pores and at the soil particle contacts consequently, evaporation loss could be curtailed (Bonsu, 1997). Convey (1963) and Bonsu (1997) approved this theory that the formation of a dry surface layer can have a considerable effect on the evaporation rate and can significantly decrease or even terminate the evaporation of water from soil. Therefore, the findings of Convey (1963) and Bonsu (1997) regarding this concept that the formation of a dry surface layer decreases the cumulative evaporation has further approved by the experimental results of the present study.

The clayey very silty SAND, as a mixture of the other two soils i.e. the medium grained SAND and the clayey sandy SILT, showed promising results to improve the cumulative evaporation as it experienced the highest total cumulative evaporation of water from soil. The mixture of medium grained sand and silt was a well graded soil and may have formed an improved balance between the capillary connectivity, water retention capacity, unsaturated hydraulic conductivity and appropriate pore size to prevent the formation of a dry surface layer leading to an increased total cumulative evaporation of water from soil. For the clayey sandy SILT and clayey very silty SAND which contain a greater percentage of silt and fine-grained materials than medium grained SAND, the evaporation rate is generally higher than the latter and it continues to increase due to the higher moisture-retention of silt leading to a greater overall cumulative evaporation as compared to sand. Keen (1914), Tuffour, et al., (2014) and Shukla (2014) have also acknowledged the profound influence of soil type on evaporation.

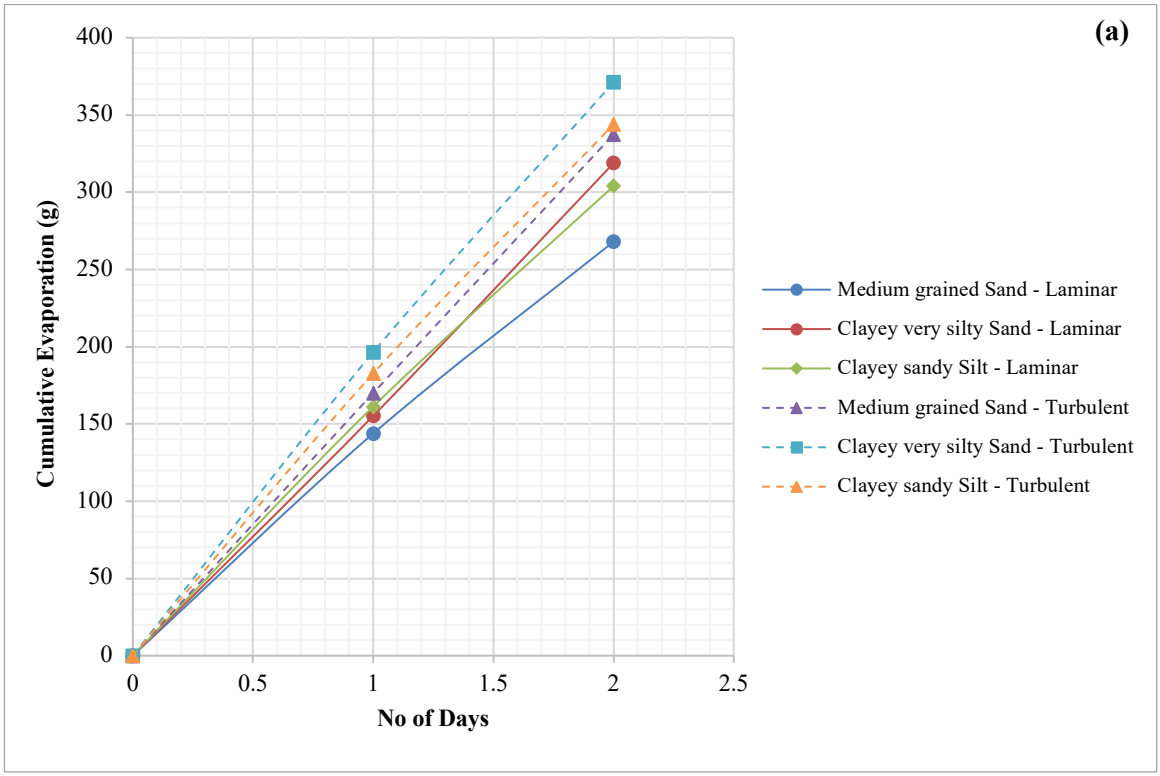

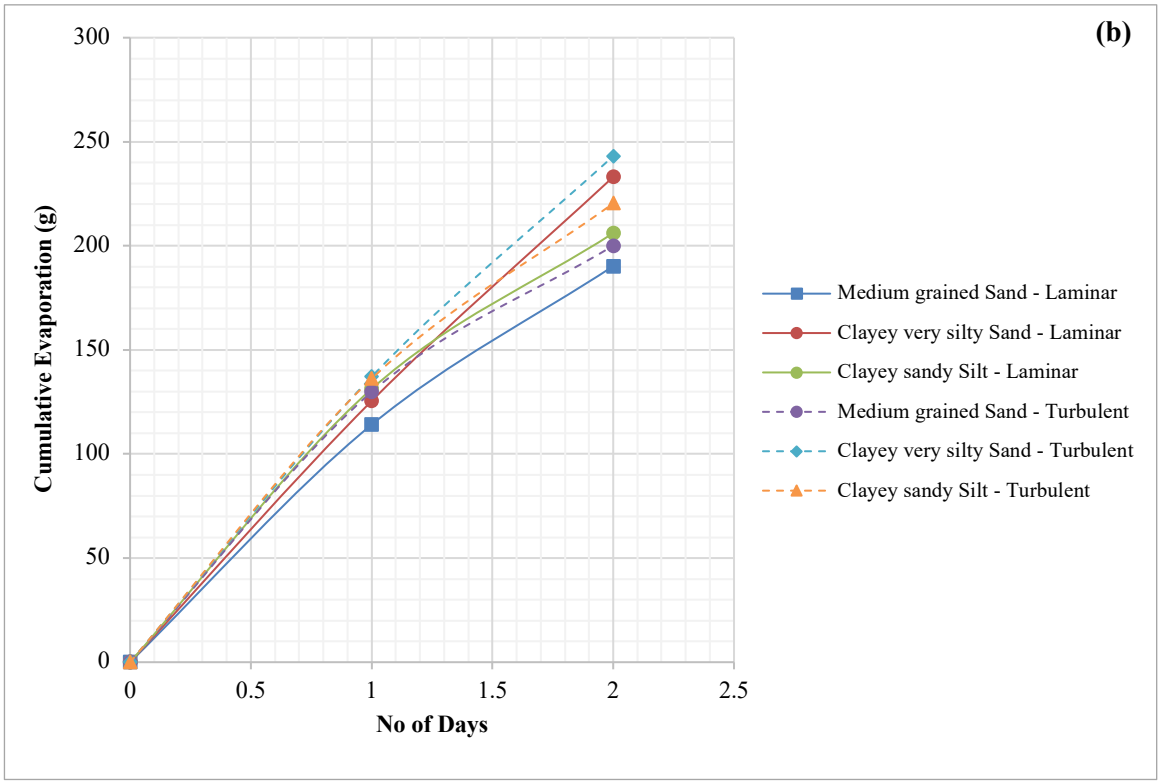

Figure 4.25 Cumulative evaporation for the three soil types at 3 m/s laminar and turbulent wind conditions a) with initial moisture content of 27 % b) with initial moisture content of 13 %.

4.3.3 Influence of moisture content on evaporation

The percentage loss in moisture content at each layer below the soil surface for different soil samples is shown in Figure 4.26. The majority of results show that the percentage loss in moisture content at each layer decreases as the depth below soil surface increases. Only at zero wind condition however, the percentage loss in moisture content at each layer increases as the depth below soil surface increases. This may be attributed to the insufficient wind action to remove the water that was stagnated at the surface or drawn up by capillary action within two days.

On the other hand, when the surface of soil is subjected to wind, the wind action is sufficient to remove the water that was drawn up by capillary action leading to a rapid increase in evaporation of water from soil and drying of the soil surface. Lehmann et al., (2008), Shokri et al., (2009) and Shokri et al., (2010) also highlighted the role of capillary action in evaporation and water movement to upper layers of soil and soil surface. It should be noted that Figure 4.26 shows the percentage loss in moisture at each layer below the soil surface and NOT the actual moisture content of soil at each layer below the soil surface.

At the surface layer (depth 0 to 30 mm) (layer 1), the medium grained SAND experiences a greater percentage loss in moisture content than the clayey sandy SILT and clayey very silty SAND. This may be attributed to the larger pore space of the medium grained SAND compared to the other two soils. The medium grained SAND has larger particle size as compared to the other two soils that have finer particles. This may resulted in an increase in evaporation at the surface and drying of the surface layer as there are larger gaps between soil particles and water can be removed more freely.

On the other hand, the percentage loss in moisture content at the middle layer (depth 30 to 60 mm) (layer 2) and bottom layer (depth 60 to 90 mm) (layer 3) of the clayey sandy SILT

and clayey very silty SAND is greater than that of the medium grained SAND. Consequently, the higher percentage loss in moisture content at the second and third layers of the clayey very silty SAND and the clayey sandy SILT samples leading to a greater total water loss of these soils as compared to the medium grained SAND. This also confirms that the formation of a dry surface layer and breakage of the capillary connectivity within the soil pores can considerably decrease the total cumulative evaporation; especially when the soil moisture content decreases (Keen, 1914).

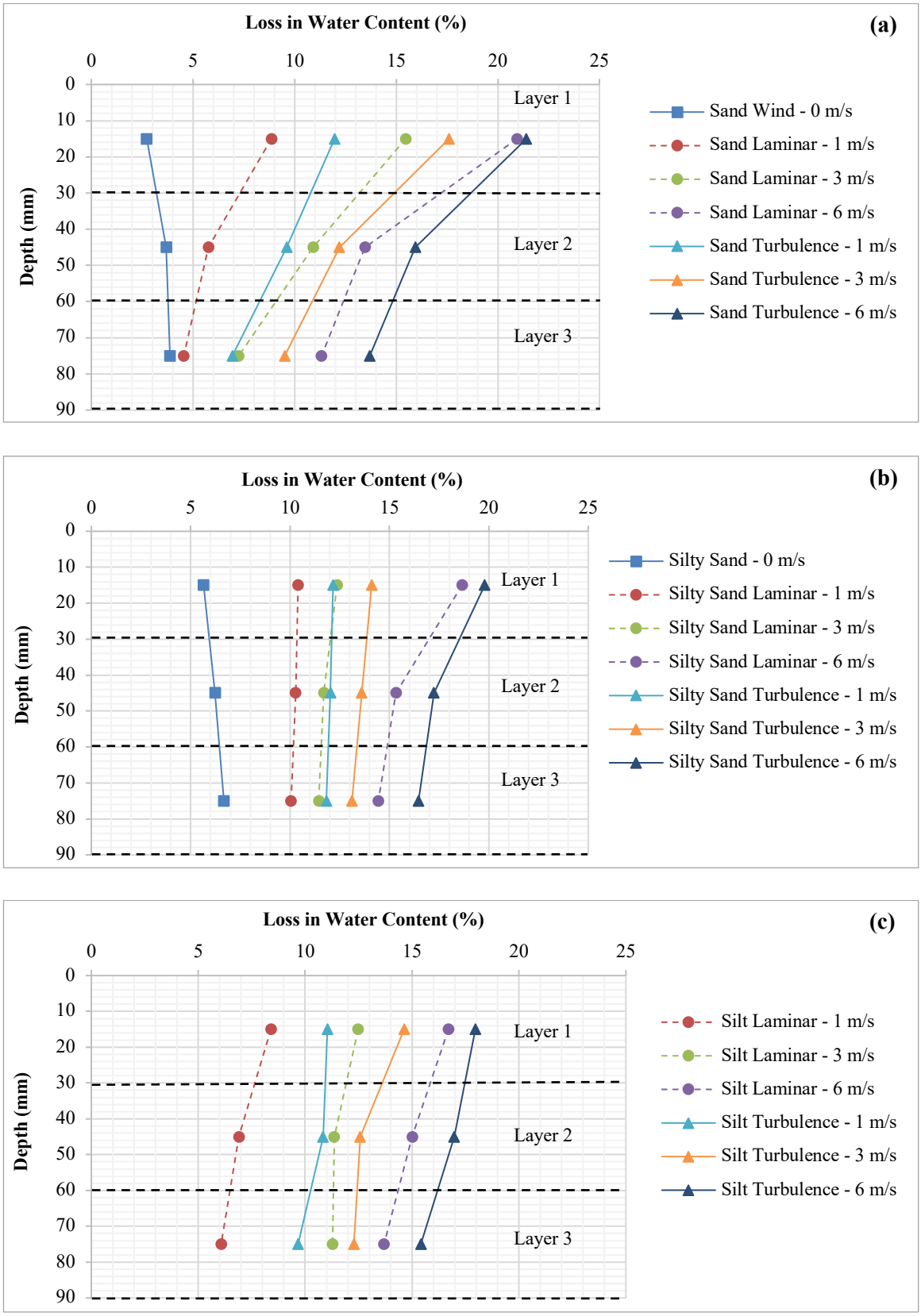

Figure 4.26 Percentage loss in water content at centre of each layer of soil samples with initial moisture content of 27 % a) medium grained SAND b) Clayey very silty SAND and c) Clayey sandy SILT.

The variation of cumulative evaporation with different initial moisture contents for all tested soil samples is shown in Figure 4.27. The majority of the results show that as the initial moisture content of soil increases, the total cumulative evaporation of water from soil at different wind conditions also increases. Since there is an increased amount of water available for evaporation. This is because as the water content increases, the thickness of the layer of water decreases. Since there is reduction in strength of bond with distance from the surface of the materials, then water farthest away can be removed more easily. Thus when water content increases, it can be removed more readily. The reason for the medium grained SAND – 27 % and the clayey sandy SILT – 19 % not following the expected trend is not clear and needs further investigation.

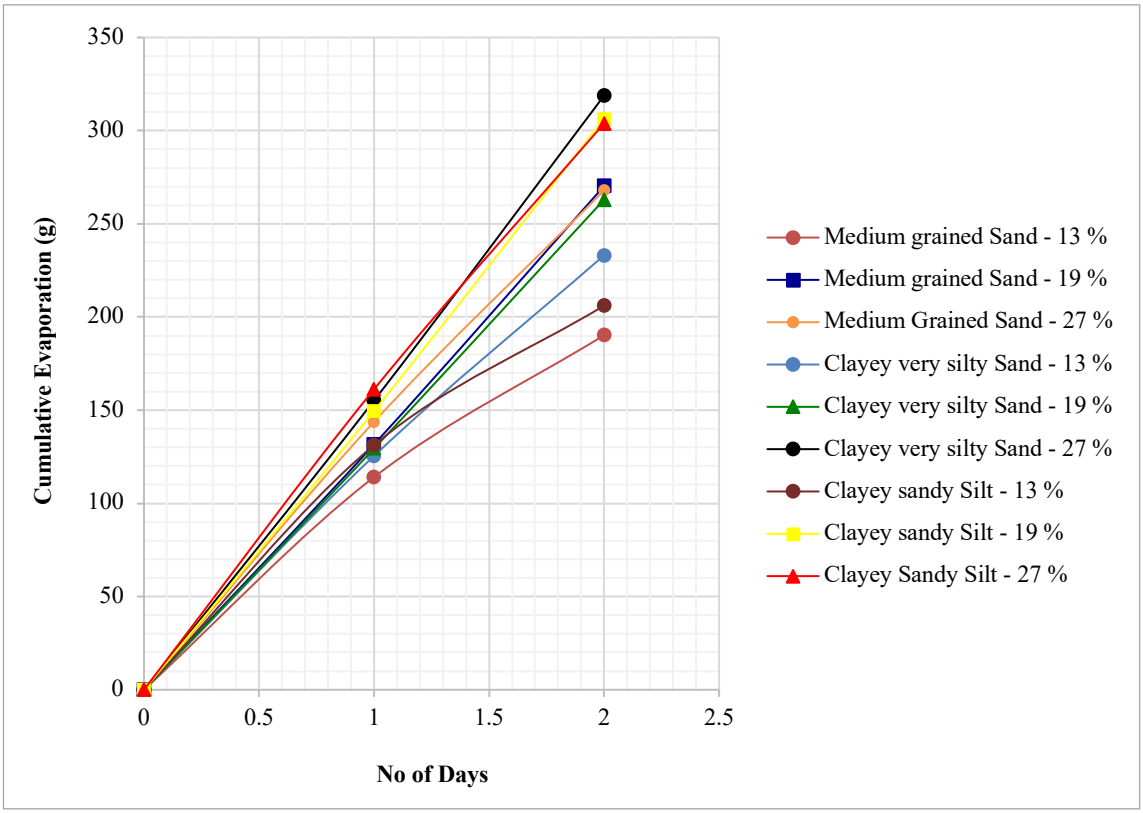

Figure 4.27 Variation of cumulative evaporation with different initial moisture contents for the tested soil samples.

4.3.4 Soil water evaporation vs. free water evaporation

Generally during first stage of evaporation, when the moisture content of soil is not limited and there is a plenty of water available for evaporation, soil water evaporation and free water evaporation occur at approximately the same rates. As can be seen in Figure 4.28, from the experimental results obtained for medium grained SAND at the moisture content of 27 % and different wind conditions, when the moisture content is not limited, the increase in soil water evaporation and free water evaporation is approximately the same. On the other hand, when the moisture content becomes limited and evaporation process enters the second stage, the evaporation of water from soil starts to decrease more rapidly than the free water evaporation. Consequently, as the evaporation process starts to transit from the climate-controlled stage to the soil-controlled stage, the difference between the soil water evaporation and the free water evaporation starts to increase considerably. Wilson (1993), Gray (1970), Morton (1975), and Brutseart (1982) stated that the relationship between the soil water evaporation and the free water evaporation highly depends on the saturation of the soil. Thus, when the moisture content of the soil becomes limited and evaporation process enters the second stage, the soil water evaporation starts to decrease more rapidly than the free water evaporation.

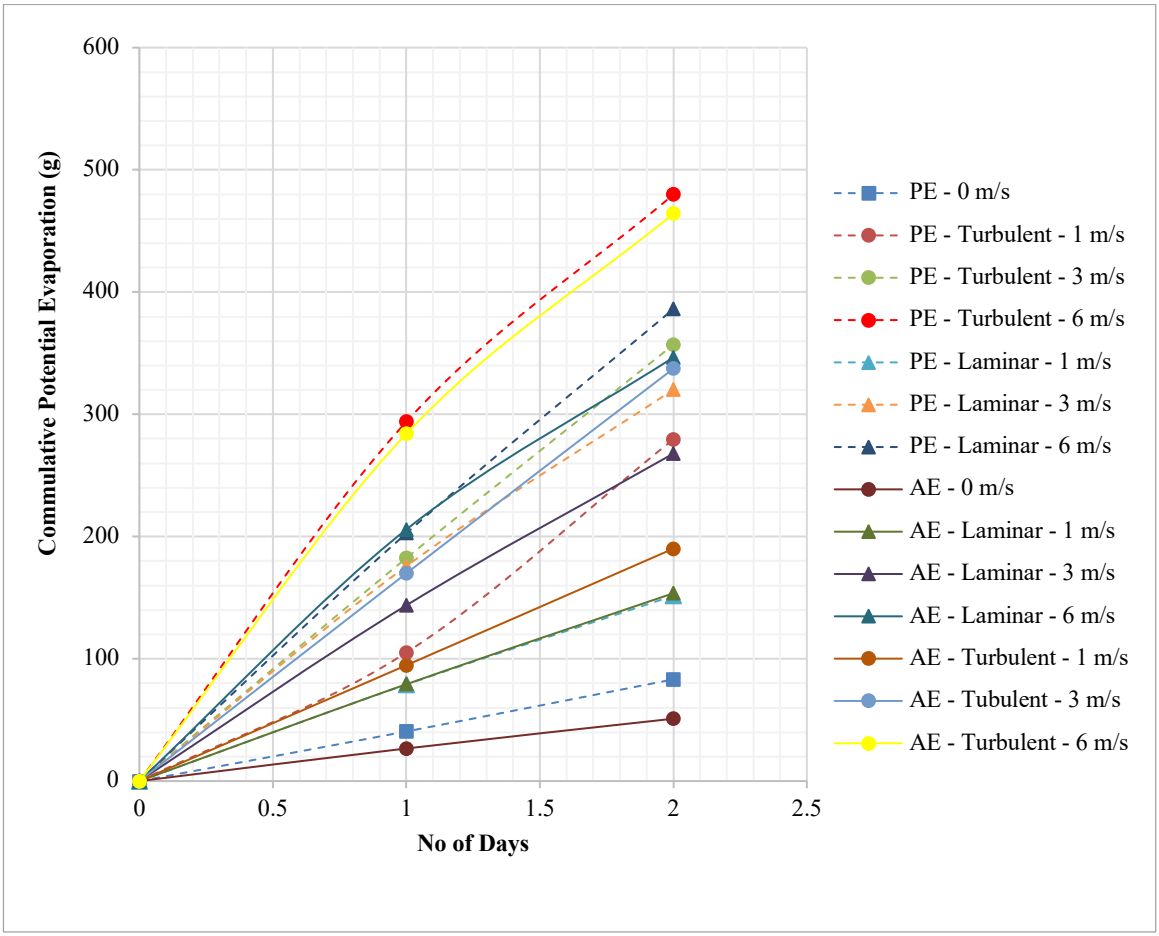

Figure 4.28 variation of cumulative evaporation from free water surface and from medium grained SAND with initial moisture content of 27 %.

5 CONCLUSIONS AND RECOMMENDATIONS FOR FURTHER WORK

5.1 *Introduction*

The main focus of this study was to accelerate raising water by capillary action and to remove water from the soil surface by the action of wind using experimental techniques. Two sets of laboratory experiments were designed to assess capillary rise and effect of evaporation on capillary rise in soils. The main laboratory tests conducted in this study are shown in Table 3.1.

The first set of experiments was carried out in three parts. The first part involved carrying out soil column tests where the free surface of water was at the bottom of the column. The aim of the first part was to evaluate capillary rise of water in soils and more importantly how to improve capillary rise and the volume of water that could be drawn up within the duration of test. The second part involved carrying out soil column tests where water for the column was supplied by saturated soil at the bottom of the column. The aim of the second part was to assess the capability of capillary action to suck water vertically from a moist soil at a range of moisture contents. The third part involved carrying out soil column tests where the top of the column was subjected to wind action and the free water surface was at the bottom of the column. The aim of the third part was to assess the feasibility of using a capillary column to draw up water from a free water surface to a higher level where water was removed by wind action with a view to continuously remove water.

The second set of experiments involved carrying out tests on compacted soil specimen where the soil moulds were placed inside a wind tunnel. The aim of the second set was to evaluate the effect of wind, soil types, and moisture contents on loss of water from soils.
Three soil types of medium grained SAND, clayey sandy SILT, and the mixture of the two, clayey very silty SAND, were selected for the experiments.

Conclusions drawn from this study are presented in the following section.

5.2 *Conclusions*

5.2.1 Capillary rise tests in free surface of water

- The maximum height of capillary rise for loosely compacted SAND, densely compacted SAND, layered SAND, clayey sandy SILT, clayey very silty SAND and layered SAND/SILT was approximately 45 cm, 50 cm, 60 cm, 65 cm, 55 cm and 72.5 cm after two days.
- The total volume of water that was drawn up in the loose SAND, dense SAND, clayey sandy SILT, clayey very silty SAND, and layered SAND/SILT soil columns within 1 day was approximately 264 cm^3, 312 cm^3, 362 cm^3, 180 cm^3, and 545 cm^3 respectively. The total volume of water that was drawn up in the loose SAND, dense SAND, layered SAND, clayey sandy SILT, clayey very silty SAND, and layered SAND/SILT soil columns within 2 days was approximately 267 cm^3, 316 cm^3, 412 cm^3, 498 cm^3, 236 cm^3, and 579 cm^3 respectively.
- The multi-layered SAND system was developed to improve the capillary rise of the medium grained SAND samples. Accordingly, the height of capillary rise of layered SAND was higher than that of loosely compacted SAND and densely compacted SAND by 15 cm and 10 cm respectively.
- One of the objectives of this study was to improve the height of capillary rise and the volume of water that could be drawn up using capillary action. Both layered systems significantly increased the height of capillary rise and the volume of water that could be drawn up within the duration of the test compared to the other soil samples.

- The capillary rise of water within soil column increases as the level of compaction increases, as discussed earlier in Section 4.2.1.1. However it should be noted that too much compaction might result in breakdown in particles, which may lead to blockage of capillary tubes already formed and decreases the volume of water that can be drawn up.
- The rate of capillary rise for the medium grained SAND was higher in the beginning of the experiment, particularly for the first few hours, as the water level in the medium grained SAND column raised to approximately 28 cm, 35 cm, and 40 cm in 1 hour, 3 hours, and 6 hours respectively. However, after that the rate of capillary rise for the medium grained SAND significantly reduced. On the other hand, the water levels in the clayey sandy SILT and the clayey very silty SAND columns raised to approximately 40 cm in a day.

5.2.2 Capillary rise tests in a moist soil

- The maximum height of capillary rise that was observed within 4 days for the medium grained SAND column in moist soil sample 1, sample 2, and sample 3 along with that of the layered SAND/SILT soil column in sample 1 was approximately 35 cm, 25 cm, 15 cm, and 60 cm respectively.

5.2.3 Capillary rise tests for soil column in a free surface of water with top of column subjected to wind action

- The average water loss per unit surface area per day through the soil column of medium grained SAND at wind velocities of 0.0 m/s, 1.3 m/s, 3.0 m/s, and 4.9 m/s was 4.3 g/cm^2, 4.6 g/cm^2, 5.1 g/cm^2, and 5.3 g/cm^2 respectively.

- The percentage increase in water loss from wind velocities of 0.0 m/s to 1.3 m/s, 1.3 m/s to 3.0 m/s, and 3.0 m/s to 4.9 m/s was approximately 7 %, 9 %, and 4 % respectively.

5.2.4 Evaporation experiments on block samples

- For the medium grained SAND sample with moisture content of 27 %, an increase in wind velocity from 0 m/s to 6 m/s resulted in an increase in the cumulative evaporation by approximately 6 times and 8 times for laminar and turbulent wind movements respectively.
- For the clayey very silty SAND sample with moisture content of 27 %, an increase in wind velocity from 0 m/s to 6 m/s resulted in an increase in the cumulative evaporation by approximately 6.5 times and 8 times for laminar and turbulent wind movements respectively.
- The clayey very silty SAND experienced the highest total cumulative evaporation followed by the clayey sandy SILT. The medium grained SAND experienced the least total cumulative evaporation out of the three soil samples.
- The formation of a dry surface layer or a crack breaking the capillary connectivity within the soil pores can decrease or even terminate the evaporation of water from soil; especially when the soil moisture content decreases.
- The majority of results show that the percentage loss in moisture content at each layer decreases as the depth below soil surface increases.
- At the surface layer (depth 0 to 30 mm) (layer 1), the medium grained SAND experienced a greater percentage loss in moisture content than the clayey sandy SILT and clayey very silty SAND. On the other hand, the percentage loss in moisture content at the middle layer (depth 30 to 60 mm) (layer 2) and bottom

layer (depth 60 to 90 mm) (layer 3) of the clayey sandy SILT and clayey very silty SAND was greater than that of the medium grained SAND. Consequently, the higher percentage loss in moisture content at the second and third layers of the clayey very silty SAND and the clayey sandy SILT samples lead to a greater total water loss of these soils as compared to the medium grained SAND. This also confirms that the formation of a dry surface layer can decrease the total cumulative evaporation.

Overall this study shows that both capillarity and suction created by the wind has the potential to be developed for successful lifting of water. Such a system would not require much energy input, however, it may take longer to lift water at a lesser rate compared to conventional pumping systems.

Recommendations for future works are presented in the following section.

5.3 Recommendations for further work

The primary objective of this thesis was to evaluate capillary rise of water in soils and the effect of removal of water by the action of wind from the soil surface on the extent of capillary rise. Although this principal objective has been achieved, further study is required before the contribution made by this thesis may be extended into engineering practice. Some areas where additional research is required are listed as follows:

5.3.1 Capillary rise tests in free surface of water

- The medium grained SAND used for the layered SAND system was a uniformly graded soil and therefore, it was difficult to obtain the entire range of sand particle size (i.e. between 0.063 mm and 2.0 mm) by sieving. Further research on capillary

rise in layered systems based on particle size distribution with a wider available range of particle size in sandy soils or soil alternative beads is recommended.

- One of the objectives of this study was to experimentally design an apparatus to improve the height of capillary rise and the volume of water that could be drawn up within the duration of the test. Both layered systems significantly increased the height of capillary rise and the volume of water that could be drawn up within the duration of the test compared to the other soil samples. Consequently, the layered system shows higher capillary performance than the other soil samples and a replicated model based on this approach has the potential to be further developed for field applications.

5.3.2 Capillary rise tests in a moist soil

- Samples could be taken from the soil at the base of the column laterally to find the area of influence of capillary rise in soil column on variation in moisture content distribution within (or the loss of water in) soil at the base of the column in lateral direction. Alternatively samples can be taken from the soil at the base of the column vertically to assess the effect of capillary rise in soil column on variation in moisture content distribution within (or the loss of water in) the soil at the base of the column in vertical direction. The latter was intended and the soil at the base of the column was divided into three, 2 cm layers for the measurement of gravimetric moisture content at each layer. However, the layers were not thick enough to notice a significant change in moisture content with depth. Accordingly, the result is not included in this thesis. It is recommended to take the above-mentioned measurements of water content in a bigger container. It will also help to optimise columns spacing.

5.3.3 Capillary rise tests for soil column in a free surface of water with top of column subjected to wind action

- It is recommended to carry out the test for a longer duration to assess the applicability of the system to lift and remove water continuously for an increased period of time in future works.
- Future work could be design of a suction device such as a windmill at the soil surface to assist capillary action to remove water from the soil more effectively.

6 REFERENCES

Abbas, N. (2015), Evaporation of Water from Soil. M.Sc. Thesis, School of Civil Engineering, University of Birmingham, UK.

Aghajani, H.F., Soroush, A., and Shourijeh, P.T. (2011) An improved solution to capillary rise of water in soils. International Journal of Civil Engineering, Vol. 9, No. 4, Tehran, Iran.

Alfnes, E., Kinzelbach, W., and Aagaard, P. (2004). Investigation of hydrogeologic processes in a dipping layer structure: 1. The flow barrier effect. J. Contam. Hydrol. 69(3–4): 157–172. doi:10.1016/j.jconhyd.2003.08.005.

Aung, H.H. (2012). Estimation of the rate of capillary rise in sand and sandy loam based on one dimensional soil column. M.Sc. Thesis, School of Civil Engineering, Suranaree University of Technology, Nakhronrachasima, Thailand.

Bache D.H. and Macaskill I.A. (1984). Vegetation in civil and landscape engineering. Granada publishing, London.

Bear, J. (1972). Dynamics of Fluids in Porous Media, American Elsevier, New York, p. 764.

Bikerman JJ (1970) Physical surfaces. Academic, New York.

British Standards Institute (BSI) (1990). Methods of Test for Soils for Civil Engineering Purposes, BS 1377, London.

Brown RC (1941) Note on the energy associated with capillary rise. Proc Phys Soc 53:233–234.

Brown RC (1947) The fundamental concepts concerning surface tension and capillarity. Proc Phys Soc 59:429–446.

Bruch, P.G. (1993). Laboratory study of evaporative fluxes in homogeneous and layered soils. M.Sc. thesis, Department of Civil Engineering, University of Saskatchewan, Saskatoon, SK.

Buckingham, E. (1907). Studies on the movement of soil moisture. Bull. No. 38. Bureau of Soils, USDA, Washington, DC.

Campbell, G.S. (1985). Soil physics with Basic. Transport models for soil–plant systems: Developments in soil sciences 14. Elsevier, Amsterdam, the Netherlands.

Capiphon Drainage. URL: http://www.capiphon.com.au [Online], Accessed in March 2016.

Cardon, G.E., and Letey, J., (1992). Soil based irrigation and salinity management model: II Water and solute movement calculations. Soil Sci. Soc. Am. J., 56: Biochem; Biophys. Acta, 1724: 367–374.

Chapin EK (1959) Two contrasting theories of capillary action. Am J Phys 27(9): 617–619.

Coppin N.J. and Richards I.G. (1990). Use of vegetation in civil engineering. CIRIA Report, Butterworths, London.

Ehlers W. and Goss M. (2003). Water dynamics in plant production. CABI, Cambridge, UK.

Escarameia M.E. and Todd A.J. (2006) Grassed surface water channels for road drainage. Report SR 662. HR Wallingford Limited.

Fenn, G. R. (2012), Drainage Characteristics of Capiphon Belt and Capiphon Pipe - Some Comparisons with Slotted Pipe with Sock, ICID Working Group on Drainage, GreenAbility Pty Limited, Tasmania, Australia.

Fetter C.W. (1994). Applied Hydrogeology. 3rd Edition, Macmillan, New York.

Fetter, C.W. (2001). Applied Hydrogeology. 4th Edition, Prentice Hall, Inc., Upper Saddle River, NJ.

Finlayson D.M., Greenwood J.R., Cooper C.G. and Simons N.E. (1984). Lessons to be learnt from an embankment failure. Proc. Institution of Civil Engineers, Part 1, Vol. 76, pp207-220.

Fredlund, D.G. and Rahardjo, H. (1993) Soil Mechanics for Unsaturated Soils. John Wiley and Sons Inc., New York, NY.

Fredlund D.G., Rahardjo H. and Fredlund, M.D. (2012) Unsaturated soil mechanics in engineering practice. Wiley, Hoboken.

Gardner, H.R., (1974). Prediction of water loss from a fallow field soil based on soil water flow theory. Soil Science Society of America Proceedings, Vol. 38, p.379-382.

Gardner, W.R. (1958). Some steady state solutions of the unsaturated moisture flow equation with application to evaporation from a water table. Soil Sci. 85:228–232.

Gardner, W.R., and Fireman, M. (1958). Laboratory studies of evaporation from soil columns in the presence of a water table. Soil Sci. 85(5): 244–249. doi:10. 1097/00010694-195805000-00002.

Gardner, W. and Widtsoe, J.A. (1921). The movement of soil moisture. Soil Sci. 11:215–232.

Gilboa A., Bachmann J., Woche S.K. and Chen Y. (2006). Applicability of interfacial theories of surface tension to water-repellent soils. Soil Sci Soc Am 70:1417–1429.

Glendinning S., Hall J. and Manning L. (2009). Asset-management strategies for infrastructure embankments. Proceedings of the Institution of Civil Engineers, Engineering Sustainability, 2009, 162, No. 2, 111–120.

Glendinning S., Hughes P.N. and Davies O. (2007). Impacts of Climate Change on UK Infrastructure Slopes. Proceedings of the 1st Expert Symposium on Climate Change, Modelling, Impacts and Adaptations, Singapore, 2007, 1, CD-rom.

Glendinning S., Loveridge F., Starr-Keddle R.E., Bransby M.F. and Hughes P.N. (2009). Role of vegetation in sustainability of infrastructure slopes. Proceedings of the Institution of Civil Engineers, Engineering Sustainability, 2009, 162, No. 2, 101–110.

Guo, G., Araya, K., Jia, H., Zhang, Z., Ohomiya, K. and Matsuda, J. (2006). Improvement of salt-affected soils: 1. Interception of capillarity. Biosystems Eng. 94(1): 139–150. doi:10.1016/j.biosystemseng.2006.01.012.

Haines, W.B. (1930). Studies in the physical properties of soil. V. The hysteresis effect in capillary properties, and the modes of moisture distribution associated therewith. J. Agr. Sci.

20:97–116.

Halcrow Group Ltd (2007). Review of the use of horizontal drainage systems. Highways Agency Framework Agreement, Contract HA2/367.

Halcrow Group Ltd and TRL Limited (2008). Drainage of earthwork slopes. Highways Agency Technical Consultancy Framework Contract HA153 (666).

Hanks, R.J. (1983). Yield and water use relationships: an overview, Ch.9. In Taylor, H.M., et al., Limitations of Efficient Water Use in Crop Production. Madison, WI: ASA, CSSA, and SSSA.

Hanks, R.J. (1991). Soil evaporation and transpiration, Ch.11. In Modeling Plant and Soil Systems. Agronomy Monograph 31. Madison, WI: American Society of Agronomy.

Hanks, R.J. (1992). Applied Soil Physics – Soil Water and Temperature Applications. New York: Springer.

Heath, D.L., Shenton, M.J., Sparrow, R.W., and Waters, J.M. (1972). Design of Conventional Rail Track Foundations. ICE Proceedings 51(2): 251-267.

Hellwig, D.H.R. (1973). Evaporation of water from sand: 4. The influence of the depth of the water-table and the particle size distribution of the sand. J. Hydrol. 18(3–4): 317–327. doi:10.1016/0022-1694(73)90055-3.

Henriksson U. and Eriksson J.C. (2004). Thermodynamics of capillary rise: Why is the meniscus curved? J Chem Educ 81(1):150–154.

Hillel, D. (1971). Soil and water: physical principles and processes. Academic press: New York; London.

Hillel, D. (1980). Applications of soil physics. Academic Press, New York.

Hillel, D. and Talpaz, H. (1977). Simulation of soil water dynamics in layered soils. Soil Sci. 123(1): 54–62. doi:10.1097/00010694-197701000-00007.

Hillel, D. (1998). Environmental soil physics. Academic Press, San Diego, California. USA.

Hillel, D. (2004). Introduction to environmental soil physics. Elsevier Science, Academic Press, San Diego, California, USA.

Hillel, D. et al. (Ed.), (2004). Encyclopedia of soils in the environment, four-volume set. Elsevier Science, Academic Press; 1st edition, New York, USA.

Hird, R., and Bolton, M.D. (2017). Clarification of capillary rise in dry sand. Engineering Geology, 230, 77-83.

Huang, M., Barbour, S.L., Elshorbagy, A., Zettl, J.D. and Si, B.C. (2011). Infiltration and drainage processes in multi-layered coarse soils. Can. J. Soil Sci. 91(2): 169–183. doi:10.4141/cjss09118.

Huang, P.M. et al. (Ed.), (2012). Handbook of Soil Sciences: Properties and Processes, 2nd Edition. CRC press, Taylor & Francis Group, Boca Raton, Florida, USA.

Hughes, P., Glendinning, S. and Mendes, J. (2007). Construction Testing and Instrumentation of an Infrastructure Testing Embankment. In: Liong, S.Y., Phoon, K.K. and Toll, D.G. (eds) Proceedings Expert Symposium on Climate Change: Modelling, Impacts and Adaptations. Singapore, Research Pub- lishing Services, 159–166.

Hughes, P.N., Glendinning, S., Mendes, J., Parkin, G., Toll, D.G., Gallipoli, D. and Miller, P. (2009). Full-Scale Testing to Assess Climate Effects on Embankments. Special Issue of Engineering Sustainability, Proceedings of the Institution of Civil Engineers, 162, No. ES2, 67–79.

Hulme, M., Jenkins, G.J., Lu, X., Turnpenny, J.R., Mitchell, T.D., Jones, R.G., Lowe, J., Murphy, J.M., Hassell, D., Boorman, P., McDonald, R. and Hill, S. (2002). Climate Change Scenarios for the United Kingdom: The UKCIP02 Scientific Report. Tyndall Centre for Climate Change Research, School of Environmental Sciences, University of East Anglia,

Norwich, UK.

Hunter, R.J. (2001). Foundations of colloid science. 2nd Edition. Oxford University Press, Oxford.

Idso, S.B., (1974). The three stages of drying a field soil. Soil Science Society of America Proceedings, Vol. 38, p. 831-837.

IPCC (2007) Summary for Policymakers. In: Climate Change 2007: The Physical Science Basis. Contribution of Working Group I to the Fourth Assessment Report of the Intergovernmental Panel on Climate Change. Cambridge University Press, Cambridge, United Kingdom and New York, NY, USA.

IPCC (2011) Summary for Policymakers. In: Intergovernmental Panel on Climate Change Special Report on Managing the Risks of Extreme Events and Disasters to Advance Climate Change Adaptation [Field, C.B., Barros, V., Stocker, T.F., Qin, D., Dokken, D., Ebi, K.L., Mastrandrea, M.D., Mach, K.J., Plattner, G.-K., Allen, S.K., Tignor, M. and P.M. Midgley (eds.)]. Cambridge University Press, Cambridge, United Kingdom and New York, NY, USA.

IPCC (2012) Managing the Risks of Extreme Events and Disasters to Advance Climate Change Adaptation. A Special Report of Working Groups I and II of the Intergovernmental Panel on Climate Change [Field, C.B., V. Barros, T.F. Stocker, D. Qin, D.J. Dokken, K.L. Ebi, M.D. Mastrandrea, K.J. Mach, G.-K. Plattner, S.K. Allen, M. Tignor, and P.M. Midgley (eds.)]. Cambridge University Press, Cambridge, UK, and New York, NY, USA.

Jackson, R.D., Kimball, B.A., Reginato, R.J., and Nakayama, F.S., (1973). Diurnal soil water evaporation: time–depth–flux patterns. Soil Sci. Soc. Am. Proc., 37: 509–513.

Jenkins, G.J., Perry, M.C. and Prior, M.J. (2008). The Climate of the United Kingdom and recent trends. Met Office Hadley Centre, Exeter, UK.

Jenkins, G.J., Murphy, J.M., Sexton, D.M.H., Lowe, J.A., Jones, P. and Kilsby, C.G. (2009). UK

Climate Projections: Briefing report. Met Office Hadley Centre, Exeter, UK.

Jitrapinate, N., Sriboonlue, V., Srisuk, K. and Hormdee, D. (2011). Simplified Procedure for Unsaturated Flow Parameters. American Journal of Applied Science 8 (6): pp. 635-643.

Jitrapinate, N., Sriboonlue, V., Srisuk, K. and Muangson, N. (2006). A method for capillary rise modelling. Unsaturated soils 2006, ASCE: pp. 2535-2545.

Jones C.J.F.P. and Pugh R.C. (2001). A full-scale field trial of electro-kinetically enhanced cohesive reinforced soil using electrically conductive geosynthetics. Proceedings of International Symposium Kyushu 2001. Landmarks in Earth Reinforcement Vol. 1, pp 219-223 – Editors Ochia H., Otani J., Yasafuku N. and Omine K. Balkema, The Netherlands.

Jury, W.A. and Horton, R. (2004) Soil physics, 6th Edition, Wiley, Hoboken, NJ.

Kirkham, M.B. (2005). Principles of soil and plant water relations. Elsevier, Amsterdam.

Kilsby, C.G., Glendinning, S., Hughes, P.N., Parkin, G. and Bransby, M.F. (2009). Climate-Change Impacts on Long-Term Performance of Slopes. Special Issue of Engineering Sustainability, Proceedings of the Institution of Civil Engineers, 162, No. ES2, 59–66.

Kirkham, D., and W.L. Powers. (1972). Advanced soil physics. R.E. Krieger Publishing Company, Malabar, FL.

Koorevaar, P., Menelik, G. and Dirksen, C. (1983). Elements of soil physics, Developments in Soil Science 13. Elsevier, Amsterdam.

Kumar, S. and Malik, R.S. (1990). Verification of quick capillary rise approach for determining pore geometrical characteristics in soils of varying texture. Soil Science, Vol. 150, No. 6, pp. 883-888.

Lago, M, and Araujo, M. (2001). Capillary rise in porous media, Physcia A, 289, 1-17.

Lal, R. and Shukla, M.K. (2005). Principles of soil physics. Taylor & Francis, New York, USA.

Laloui, L. (2010). Mechanics of unsaturated geomaterials. John Wiley & Sons, London, UK.

Lane, K.S. and Washburn, S.E. (1946). Capillary tests by capillarimeter and by soil filled tubes. Proc. Highway Research Board: 26, pp.460–473.

Lehmann, P., Assouline, S. and Or, D. (2008). Characteristic lengths affecting evaporative drying of porous media. Phys. Rev. E, 77: 056309. doi:10.1103/ PhysRevE.77.056309.

Li, D., Hyslip, J., Sussmann, T. and Chrismer, S. (2016). Railway Geotechnics. Pages 302-305. CRC Press.

Lockington, D.A. and Parlange, J.Y. (2004). A new equation for macroscopic description of capillary rise in porous media. Journal of Colloid and Interface Science, 278, 404-409.

Loveridge, F. and Anderson, D. (2007). What to do with a vegetated clay embankment? Slope Engineering Conference, Thomas Telford, London, UK.

Lu, N. and Godt, J. (2013). Hillslope Hydrology and Stability, Cambridge University Press, New York, USA.

Lu, N. and Likos, W.J. (2004a). Unsaturated soil mechanics. John Wiley & Sons: Canada.

Lu, N. and Likos, W.J. (2004b). Rate of Capillary rise in soil. Journal of Geotechnical and Geoenvironmental engineering, ASCE. 130(6): pp. 646-650.

Ma, Y., Feng, S., Zhan, H., Liu, X., Su, D., Kang, S. and Song, X. (2011). Water infiltration in layered soils with air entrapment: modified Green–Ampt model and experimental validation. J. Hydrol. Eng. 16(8): 628–638. doi:10. 1061/(ASCE)HE.1943-5584.0000360.

MacNeil D.J., Steele D.P., McMahon W. and Carder D.R. (2001). Vegetation for slope stability. TRL Report 515. Wokingham, TRL Limited.

Malik, R.S., Kumar, S. and Dahiya, I.S. (1984). An approach to quick determination of some water transmission characteristic of porous media. Soil Science, Vol. 137, No. 6, pp. 395-400.

Malik, R.S., Kumar, S. and Malik, R.K. (1989). Maximal capillary rise flux as a function of

height from the water table. Soil Science, Vol. 148, No. 5, pp. 322-326.

Markworth, A.J. (1971). Liquid rise in a capillary tube: a treatment on the basis of energy. J Chem Educ 49(8): 528.

Marshall, T.J. and Holmes, J.W. (1988). Soil physics, 2nd Edition. Cambridge University Press, New York.

Maskong, H. (2010). Capillary cut for salinity control in sandy loam, M. Thesis, School of Civil Engineering, Suranaree University of Technology, Nakhronrachasima, Thailand.

McCartney, J.S. and Zornberg, J.G. (2010). Effects of infiltration and evaporation on geosynthetic capillary barrier performance. Can. Geotech. J. 47(11): 1201– 1213. doi:10.1139/T10-024.

McCaughan, J.B.T. (1987). Capillarity: a lesson in the epistemology of physics. Physics Education 22: 100–106.

McCaughan, J.B.T. (1992). Comment on "The upward force on liquid in a capillary tube", by Scheie, P.O. Am J Phys 60(1): 87.

McGown A. and Hughes F.H. (1982). Practical aspects of the design and installation of deep vertical drains. Vertical drains, ICE, Thomas Telford, London, pp3-18.

Meiers, G.P., Barbour, S.L., Qualizza, C.V. and Dobchuk, B.S. (2011). Evolution of the hydraulic conductivity of reclamation covers over sodic/saline mining overburden. J. Geotech. Geoenviron. 137(10): 968–976. doi:10.1061/(ASCE)GT. 1943-5606.0000523.

Mendes J., Gallipoli D., Toll D.G., Augarde C.E., Glendinning S. and Hughes P.N. (2008). The Influence of Climate Change on Suction of the Fill Material of the Bionics Embankment. Proceedings of the 10th Congresso Nacional de Geotecnia and 4th Congresso Luso Brasileiro de Geotecnia, GEO (XI IV Geo 2008), Coimbra, 2008, 3, 221–228.

Mendes, J. (2011). Assessing the Impact of Climate Change on an Instrumented Embankment:

An unsaturated soil mechanics approach, PhD thesis, Durham University (http://etheses.dur.ac.uk/612/).

Mitchell, J.K. (1993). Fundamentals of soil behaviour. Wiley & Sons, New York.

Moore, R.E. (1939). Water conduction from shallow water tables. Hilgardia, 12: 383– 426.

Murphy, J.M., Sexton, D.M.H., Jenkins, G.J., Booth, B.B.B., Brown, C.C., Clark, R.T., Collins, M., Harris, G.R., Kendon, E.J., Betts, R.A., Brown, S.J., Humphrey, K.A., McCarthy, M.P., McDonald, R.E., Stephens, A., Wallace, C., Warren, R., Wilby, R. and Wood, R.A. (2009). UK climate projections science report: Climate change projections, Met Office Hadley Centre, Exeter, UK.

Murray, E.J. and Sivakumar, V. (2010) Unsaturated soils - A fundamental interpretation of soil behaviour, 1st Edition, London, Wiley-Blackwell.

Narasimhan, T.N. (2005). Buckingham, 1907: An appreciation. Vadose Zone Journal, 4, 434–441, doi:10.2136/vzj2004.0126.

Narasimhan, T.N. (2007). Central ideas of Buckingham (1907): A century later. Vadose Zone J. 6:687–693. doi:10.2136/vzj2007.0080.

Nettleton I.M., Jones C.J.F.P., Clarke B.G. and Hamir R.B. (1998). Electro-kinetic geosynthetics and their applications. Proceedings of 6th International Conference on Geosynthetics. Atlanta, USA. Vol. 2, pp871-876.

O'Brien, A.S. (2001 and 2007). Rehabilitation of urban railway embankments: research, analysis and stabilization. Proceedings of the 14th European Conference on Soil Mechanics and Geotechnical Engineering, Madrid, 2007, 1, 125–143.

O'Riordan N.J. and Seaman J.W. (1994). Highway embankments over soft compressible alluvial deposits: Guidelines for design and construction. TRL Contractor Report 341. Wokingham, TRL Limited.

Orowan, E. (1970). Surface energy and surface tension in solids and liquids. Proceedings of the Royal Society of London, Vol. 316 (1527): 473–491.

Or, D. and Tuller, M. (2005). Capillarity. In: Hillel, D. (ed) Encyclopedia of soils in the environment. Elsevier, Amsterdam, pp 155–164.

Or, D. and Wraith, J.M. (2002). Soil water content and water potential relationships. In: Warrick, A.W. (ed) Soil physics companion. CRC, Boca Raton, FL.

Pavelic, P. and Johnston, C.D. (1993). A laboratory study of the flow processes through layered profiles in relation to clogging in artificial recharge basins. CSIRO, Division of Water Resources. Technical Memorandum 93/2.

Peiris, M.G.C. and Tannakone, K. (1980). Rate of rise of a liquid in a capillary tube. American Journal of Physics 48, 415.

Pellicer, J., Manzanares, J.A. and Mafe, S. (1995). The physical description of elementary surface phenomena: thermodynamics versus mechanics. American Journal of Physics 63 (6): 542–547.

Perry, J., Pedley, M. and Reid, M. (2001). Infrastructure Embankments: Condition Appraisal and Remedial Treatment. CIRIA publication, Report C550, London, UK.

Petropoulos, G.P. (2014). Remote sensing of energy fluxes and soil moisture content. CRC Press, Taylor & Francis Group, Boca Raton, Florida, USA, pp. 8-10.

Philip, J.R. (1957). The theory of infiltration. 1. The infiltration equation and its solution. Soil Sci. 83:345–357.

Philip, J.R. (1974). Fifty years progress in soil physics. Geoderma 12: 265–280.

Phillips, J.D. (2001). Contingency and generalization in pedology, as exemplified by texture-contrast soils. Geoderma, 102(3–4): 347–370. doi:10.1016/S0016-7061(01)00041-6.

Polubarinova-Kochina, P.Ya. (1962). Theory of ground water movement. Princeton University

Press, Princeton, N.J.

Rasheed, H.R., Al-Anaz, H. and Abid, K.A. (1989). Evaporation from soil surface in presence of shallow water tables. In Proceedings of the Baltimore Symposium, Baltimore, Maryland. IAHS Publ. no. 181.

Richards, L.A. (1931). Capillary conduction of liquids through porous mediums. Journal of Physics, 1 (1), pp. 318-333.

Richards, L.A. (1961). Advances in soil physics. p. 67–79. In Seventh Int. Congr. Soil Sci. 1960, Madison, WI. Vol. 1.

Rose, D.A. (1968). Water movement in porous materials III: Evaporation of water from soil. Br. J. Appl. Phys., 1 (1), PP.1779-1791.

Rose, D.A., Konukcu, F. and Gowing, J.W. (2005) Effect of water table depth on evaporation and salt accumulation from saline groundwater. Aust. J. Soil Res. 43(5): 565. doi:10.1071/SR04051.

Roura, P. (2007). Contact angle in thick capillaries: a derivation based on energy balance. Eur J Phys 28: L27–L32.

Royster D.L. (1980). Horizontal drains and horizontal drilling: An overview. In Transportation Research Record 783, TRB, National Research Council, Washington, pp. 16 – 20.

Salim, R.L. (2016). Extent of capillary rise in sands and silts. M.Sc. Thesis, Paper 688, Western Michigan University, Michigan, USA.

Santi P.M., Elifrits C.D. and Liljegren J.A. (2001a). Design *and installation of horizontal* wick drains for landslide stabilization. Transportation Research Record 1757, TRB, pp 58 – 66.

Santi P.M., Elifrits C.D. and Liljegren J.A. (2001b). Draining in a new direction. Civil Engineering, Vol. 71, No 6, ppA10 – A16.

Schiechtl H.M. and Stern N.R. (1992). Ground bioengineering techniques for slope protection

and erosion control. Blackwell Science, Oxford.

Selig, E.T. and Cantrell, D.D. (2001). Track substructure maintenance—from theory to practice. Proc., American Railway Engineering and Maintenance-of-Way Association Annual Conference.

Selig, E.T. and Waters, J.M. (1994). Track Geotechnology and Substructure Management, London, Thomas Telford.

Shah, N., Nachabe, M. and Ross, M. (2007). Extinction depth and evapotranspiration from ground water under selected land covers. Ground Water, 45(3): 329–338. doi:10.1111/j.1745-6584.2007.00302.x. PMID:17470122.

Shokri, N., and Salvucci, G.D. (2011). Evaporation from porous media in the presence of a water table. Vadose Zone J. 10(4): 1309–1318. doi:10.2136/vzj2011. 0027.

Shokri, N., Lehmann, P., and Or, D. (2008). Effects of hydrophobic layers on evaporation from porous media. Geophys. Res. Lett. 35: L19407. doi:10.1029/ 2008GL035230.

Shokri, N., Lehmann, P., and Or, D. (2010). Evaporation from layered porous media. J. Geophys. Res. 115: B06204. doi:10.1029/2009JB006743.

Shukla, M.K. (2014). Soil physics: An Introduction. CRC Press, Taylor & Francis Group, Boca Raton, Florida, USA.

Si, B., Dyck, M., and Parkin, G.W. (2011). Flow and transport in layered soils: preface. Can. J. Soil Sci. 91(2): 127–132. doi:10.4141/cjss11501.

Smart Drain. URL: http://www.smartdrain.com [Online], Accessed in March 2016.

Smedema, L.K. and Rycroft, D.W. (1983). Land drainage: planning and design of Agricultural Drainage Systems. Batsford, London, pp. 376.

Smethurst, J.A., Clarke, D. and Powrie, W. (2006). Seasonal Changes in Pore Water Pressure in a Grass Covered Cut Slope in London Clay. Proceedings of the Institution of Civil Engineers,

Geotechnique, 2006, Vol. 56, No. 8, pp. 523–537.

Smith, R.M. and Browning, D.R. (1946). Some suggested laboratory standards of subsoil permeability. Soil Sci. Soc. Am. Proc. 11:21-26.

Sophocleous, M. (2010). Understanding and explaining surface tension and capillarity: an introduction to fundamental physics for water professionals, Hydrogeology Journal (2010), Springer-Verlag, Kansas, USA, 18: 811–821. DOI: 10.1007/s10040-009-0565-5.

Sriboonlue, V., Srisuk, K., Konyai, S., and Khetkratok, N. (2006). Unsaturated hydraulic conductivity for upward flow in soil. Unsaturated soils 2006, ASCE: pp. 1503-1511.

Staley, R.W. (1957). Effect of depth of water table on evaporation from fine sand. M.Sc. thesis, Colorado State University, Fort Collins, USA.

Steele D.P., MacNeil D.J. and McMahon W. (2004). The use of live willow poles for stabilising highway slopes. TRL Report TRL619. Wokingham, TRL Limited.

Steenhuis, T.S., Hunt, A.G., Parlange, J.Y., and Ewing, R.P. (2005). Assessment of the application of percolation theory to a water repellent soil. Aust. J. Soil Res. 43(3): 357. doi:10.1071/SR04093.

Swartzendruber, D. (1969). The flow of water in unsaturated soils. p. 215–291. In R.J.M. de Wiest (ed.) Flow through porous media. Academic Press, New York.

Temperley HNV, Travena DH (1978). Liquids and their properties. Ellis Horwood series, Wiley, Chichester, UK.

Terzaghi, K. (1943). Theoretical Soil Mechanics. John Wiley and Sons, Inc., New York.

Terzaghi, K., Peck, R.B., and Mesri, G. (1996). Soil mechanics in engineering practice. 3rd Edition, John Wiley and Sons: Canada.

Tietje, O., and Hennings, V. (1996). Accuracy of the saturated hydraulic conductivity prediction by pedo-transfer functions compared to the variability within FAO textural classes.

Geoderma, 69(1–2): 71–84. doi:10.1016/0016- 7061(95)00050-X.

Toll, D.G., Mendes, J., Karthikeyan, M., Gallipoli, D., Augarde, C.E., Phoon, K.K. and Lin, K.Q. (2008). Effects of Climate Change on Slopes for Transportation Infrastructure, 1st ISSMGE International Conference on Transportation Geotechnics, Nottingham, UK, September 2008.

Toll, D.G., Tsaparas, I. and Rahardjo, H. (2001). The Influence of Rainfall Sequences on Negative Pore-water Pressures within Slopes, Proc. 15th International Conference on Soil Mechanics and Geotechnical Engineering, Istanbul, Rotterdam: Balkema, Vol. 2, pp. 1269–1272.

Tuller, M., Or, D. and Dudley, L.M. (1999). Adsorption and capillary condensation in porous media: Liquid retention and interfacial configurations in angular pores. Water Resour. Res. 35:1949–1964.

Unger, P.W. (1971). Soil profile gravel layers: I. Effect on water storage, distribution, and evaporation. Soil Sci. Soc. Am. J. 35(4): 631–634. doi:10.2136/ sssaj1971.03615995003500040041x.

Van Genuchten, M.T. (1980). A closed-form equation for predicting the hydraulic conductivity of unsaturated soils. Soil Sci. Soc. Am. J., 44, pp. 892– 898.

Vaughan, P.R., Hight, D.W., Sodha, V.G. and Walbancke, H.J. (1978) Factors controlling the stability of clay fills in Britain. Proceedings of the Conference on Clay Fills. Thomas Telford, London, pp. 205–217.

Willis, W.O. (1960). Evaporation from layered soils in the presence of a water table. Soil Sci. Soc. Am. J. 24(4): 239. doi:10.2136/sssaj1960.03615995002400040009x.

Wilson, G.W. (1990). Soil evaporative fluxes for geotechnical engineering problems. Ph.D. thesis, Department of Civil Engineering, University of Saskatchewan, Saskatoon, SK.

Wilson, G.W., Fredlund, D.G. and Barbour, S.L. (1994). Coupled soil-atmosphere modeling for soil evaporation. Canadian Geotechnical Journal, Vol. 31, No. 2, pp. 151–161.

Wingler, F. (2011) (Revised 2016). Water the enemy of the rail track. Accessed: [Online] on 21/03/2017: pp. 1-39.

Wösten, J.H.M., Pachepsky, Y.A. and Rawls, W.J. (2001). Pedotransfer functions: bridging the gap between available basic soil data and missing soil hydraulic characteristics. J. Hydrol. 251(3–4): 123–150. doi:10.1016/S0022- 1694(01)00464-4.

Yang, H., Rahardjo, H. and Leong, E.C. (2006). Behaviour of unsaturated layered soil columns during infiltration. J. Hydrol. Eng. 11(4): 329–337. doi:10.1061/ (ASCE)1084-0699(2006)11:4(329).

Zardava, K. (2012). Moisture retention and near saturated flow in mechanically biologically treated (MBT) waste. PhD Thesis. School of Civil Engineering and the Environment, University of Southampton, Southampton, UK.

Zornberg, J.G., Bouazza, A. and McCartney, J.S. (2010). Geosynthetic capillary barriers: current state of knowledge. Geosynth. Int. 17(5): 273–300. doi:10. 1680/gein.2010.17.5.273.

APPENDICES

APPENDIX A. SUPPLEMENTARY MATERIALS FOR CHAPTER 1

A.1 The importance of rail track drainage

Efficient drainage of a rail track is in general, a more challenging task than a regular road because unlike a road for rubber-tyre vehicles, a ballasted track does not have watertight tar sealing, which protects the sub-structure against rainfall (Selig et al. 1994).

Water can get into the rail track by rainfall from above (precipitation), by seeping from the side-banks (subsurface seepage), by flowing as surface water with mud particles from adjacent ground on same or from higher level from cutting-slopes (surface flow), by creeping up from the ground by capillary forces and even by percolating between the sleepers as ground water like a spring coming from adjacent higher water leading formation layers or stratas, as shown in Figure 1.

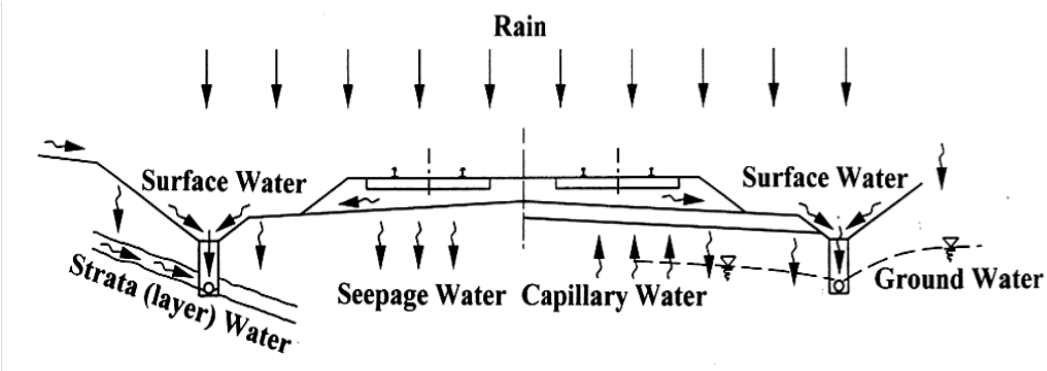

Figure 1 Water flow scheme at track bed (from Wingler, 2016).

Many of the problems arising in the track bed, are associated with track drainage occurring where drainage system is not operating effectively, or where variations in the position of the water table have generated the necessity for additional drains (Wingler, 2016).

Performance of a rail track in terms of stability and longevity is extensively dependent on efficiency of track drainage, i.e. if water can be taken out and kept away from the track-bed.

Poor drainage leads to a number of problems with track performance. High moisture content breaks down the bearing capacity of the sub-grade and decreases the shear-strength of the soil. Under the repeated train loading (pore) water pressure develops in the substructure layers and the water content in the soil increases. This reduces the strength and stiffness of the materials and increases the deformation. Water can transform soil into plastic slurry. A mixture of fine particles in the voids together with water can form slurry, which fouls the ballast and makes it difficult to maintain a smooth track surface. The slurry also erodes the ballast and concrete sleepers. The mud-pumping concrete sleeper crushes and mills the ballast stones to fines (Wingler, 2016).

The hydraulic pumping of the sub-ballast and subgrade layers represents another problem caused by poor drainage, which is a source of ballast fouling leading to geometry deterioration. Another problem occurs due to volume changes (swelling and shrinkage) of expansive soils as they swell when they absorb water during wet season and shrink when the water is removed from the soil by evaporation in periods of dry season. Because the volume changes on swelling and shrinkage are not equal, they usually cause substantial deterioration of track geometry leading to a “memory” for track-misalignment buried in the subgrade (Wingler, 2016).

Penetration of ballast into the soft subgrade subjected to repeated train loading will result in the formation of ballast pockets, which act as sump for water, leading to localised softening of the surrounding soil. Corrections of ballast pocket problems may vary in scope, cost, and effectiveness. The specific site location, extent of problem, and economics will drive the selection of a particular soil-improvement method (Li et al., 2016).

A.2 Buckingham's conceptual model of capillary flow

Buckingham (1907) developed a conceptual model to explain moisture flow in soils based on a dynamical approach. Accordingly, Buckingham (1907) stated that "in order to pull a definite mass of water away from a definite mass of moist soil of a given moisture content by purely mechanical means, a definite amount of mechanical work is required to be carried out; and if the water and the soil are allowed to come together again in respect to their mutual attraction, an appropriate mechanism is required to be constructed to be able to retrieve the same amount of work that had to be carried out to separate the water from the soil. This means that the attractive forces between the soil and the water are conservative or that they have a potential (i.e. mechanical potential to do mechanical work)." Accordingly, Buckingham made an assumption that the hydrophilic forces between the soil and water are reversible, and therefore that the mechanical potential is a conservative energy potential (Narasimhan, 2007). According to Buckingham (1907), the concept of mechanical potential can be considered as "free energy" or "potential" of water in the soil. Consequently from the above it can be concluded that the capillary potential is related to the work required to "pull a definite mass of water away from a definite mass of moist soil of a given moisture content."

Following the Buckingham's assumption that the mechanical work required to pull a given mass of water away from a moist soil is fully reversible, Haines (1930), in an important attempt, indicated that this assumption is not realistic for natural soils as a result of hysteresis in soil water retention curve.

According to Haines (1930), the modes of moisture distribution and water retention in soil result in two major values of capillary pull. The process of wetting or increasing moisture tends to be governed by the wider sections of the pores, while the process of drying or decreasing moisture tends to be governed by the narrower sections of the pores. In a soil

system, in general, a greater capillary pull against the extraction of water from the pores of a soil is generated than against absorption of water into them (Narasimhan, 2007).

According to Buckingham (1907), in a partially saturated soil, the water is in the form of menisci at the contacts between soil particles with the curvature concave to the air phase, indicating the water-phase pressure to be under normal atmospheric air pressure. The curvature of the meniscus depends on the pressure difference between the air and water phases. Away from the contacts, water is in the form of thin films on the surfaces of the soil particles (Narasimhan, 2007).

At relatively high water contents (i.e. near saturation), considerable amounts of water in the pores of the soil will form continuous pathways through water-filled capillaries. On the other hand, with decreasing moisture or at relatively low water contents, thin films of water on the surfaces of the soil particles begin to displace some of the water-filled capillary pathways, forming menisci at the contacts between neighboring particles. If the curvatures of menisci formed at the contacts between the neighboring soil particles was different, water would flow along the films from the meniscus with a larger radius representing higher potential to the one with a smaller radius representing lower potential, with the water being forced out of the films into the droplets by atmospheric pressure. Consequently, at relatively high water contents or nearly saturated soil conditions, the flow mechanisms will be dominated by the water-in-mass flow through connected capillaries. In moderately saturated soil conditions, the dominant mechanism of flow would be through films as well as some connected capillaries depending on the soil type. At relatively low water contents or low saturated soil conditions, the dominant flow mechanism would be through film flow. At extremely low water contents, films will be broken; consequently the connections of menisci

formed at the contacts between neighboring particles will be disrupted and finally the flow of liquid phase practically be ceased (Narasimhan, 2007).

A.3 Current commercialised capillary drainage technology

Two forms of Smart Drain/Capiphon are shown in Figure 2.

Figure 2 Two forms of Smart Drain/Capiphon: (a) a 10-cm wide belt showing the grooves on the underside (Fenn, 2012) (b) a PVC pipe around which the belt is wrapped (https://www.capiphon.com.au/; http://www.smartdrain.com/).

Close-up photos of Smart Drain/Capiphon belt are shown in Figure 3.

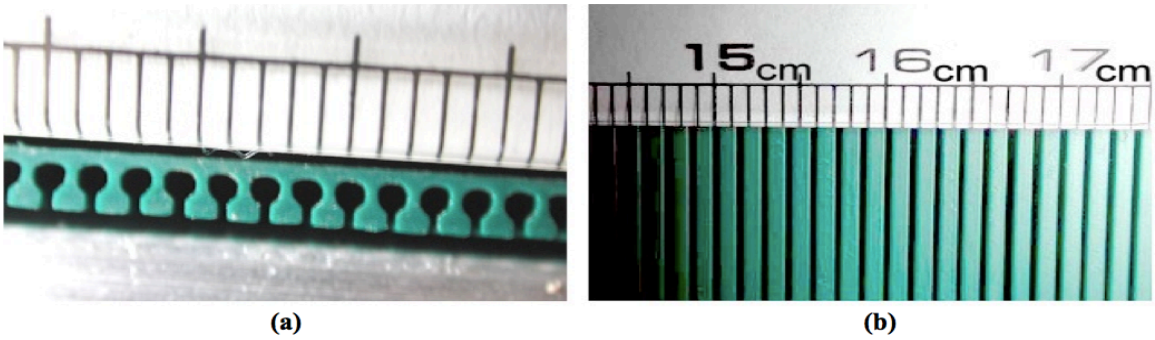

Figure 3 Close-up photos of Smart Drain/Capiphon belt (a) the cross section showing the omega-shaped grooves and (b) The underside of Smart Drain/Capiphon belt (Fenn, 2012).

The Smart Drain/Capiphon belt coupler is shown in Figure 4.

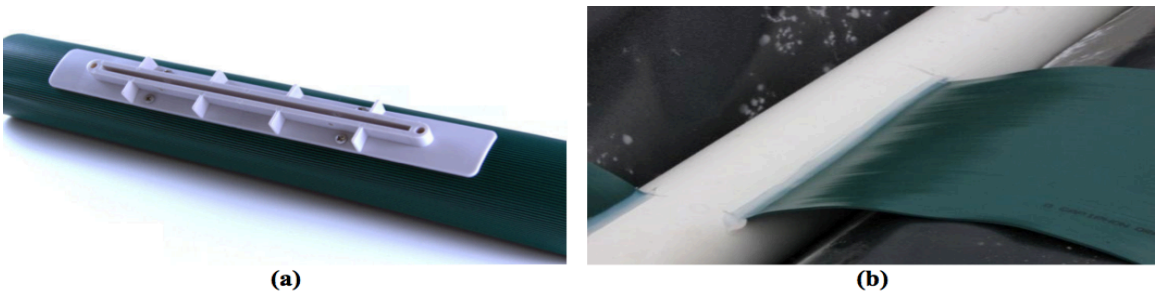

Figure 4 (a) Smart Drain/Capiphon belt coupler; (b) The belt is usually inserted into a collection pipe laid some 10 cm below the level of the belt to increase the capillary head (Fenn, 2012).

Figure 5 shows how the Smart Drain/Capiphon belt and pipe work.

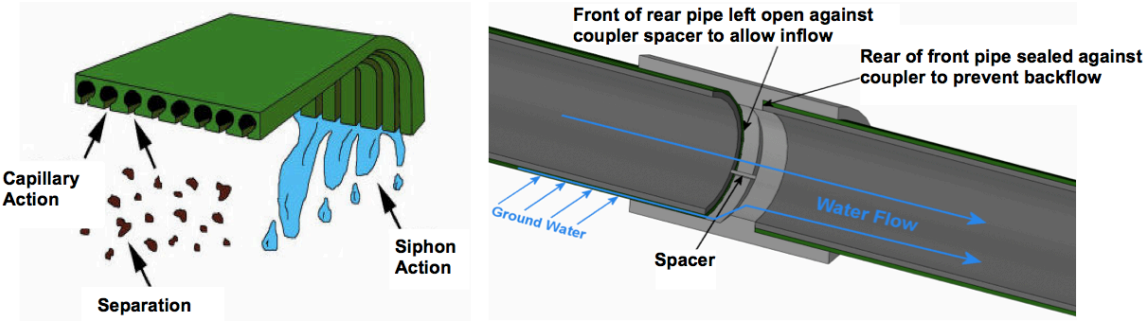

Figure 5 Illustration showing how the Smart Drain/Capiphon belt and pipe function (http://www.smartdrain.com/).

Figure 6 shows how the Smart Drain/Capiphon is installed in a field.

Figure 6 Smart Drain/Capiphon installed in a field (http://www.smartdrain.com/).

APPENDIX B. SUPPLEMENTARY MATERIALS FOR CHAPTER 2

B.1 Height of capillary rise in soils

Table 1 shows a summary of the experimental capillary rise results described in the literature (e.g., Lane and Washburn, 1946; Malik et al., 1989; Kumar and Malik, 1990) on different soils representing an extensive range of soil types.

Table 1 The experimental maximum height of capillary rise in different soil types (after Lu and Likos, 2004a)

Test No.	Soil	Gravel (%)	Sand (%)	Silt/Clay (%)	Clay (%)	Void ratio	h_a (cm)	h_c (cm)	$\frac{h_c}{h_a}$
1	Class 5	25.0	68.0	7.0	–	0.27	41.0	82.0 (220)·	2.0
2	Class 6	0.0	47.0	53.0	–	0.66	175.0	239.6 (440)·	1.4
3	Class 7	20.0	60.0	20.0	–	0.36	39.0	165.5 (245)·	4.1
4	Class 8	0.0	5.0	95.0	–	0.93	140.0	359.2 (400)·	2.6
5	Ludas sand	–	–	–	–	–	29.1	72.1	2.5
6	Rawalwas sand	–	–	–	–	–	29.6	77.5	2.6
7	Rewari sand	–	–	–	–	–	29.4	60.9	2.1
8	Bhiwani sand	–	–	–	–	–	27.6	65.6	2.4
9	Tohana loamy sand 1	–	–	–	–	–	37.4	117.0	3.1
10	Hisar loamy sand 1	–	–	–	–	–	37.5	149.4	4.0
11	Barwala sandy loam 1	–	–	–	–	–	41.2	158.4	3.8
12	Rohtak sandy loam 1	–	–	–	–	–	48.7	155.7	3.2
13	Hisar sandy loam 1	–	–	–	–	–	47.7	174.5	3.7
14	Pehwa sandy clay loam	–	–	–	–	–	44.5	154.6	3.5
15	Hansi clayey loam 1	–	–	–	–	–	29.6	127.5	4.3
16	Ambala silty clay loam 1	–	–	–	–	–	15.0	141.5	9.4
17	Tohana loamy sand 2	–	89.0	6.0	5.0	0.92	66.7	117.0 (97)·	1.8
18	Hissar loamy sand 2	–	82.5	11.5	6.0	0.90	72.9	149.4 (219)·	2.0
19	Barwala sandy loam 2	–	75.0	13.5	11.5	0.94	47.3	158.4 (260)·	3.3
20	Rohtak sandy loam 2	–	63.0	23.0	14.0	1.01	44.0	155.7 (259)·	3.5
21	Hissar sandy loam 2	–	63.0	24.0	13.0	0.99	66.0	174.5 (234)·	2.6
22	Pehowa sandy clay loam	–	55.0	27.0	18.0	1.06	59.6	154.6 (260)·	2.6
23	Hansi clayey loam 2	–	30.2	26.5	43.3	1.27	16.3	127.5 (247)·	7.8
24	Ambala silty clay loam 2	–	15.0	49.0	36.0	1.49	16.9	141.5 (315)·	8.4

Note the following from the above table:
Test No. 1-4: Lane and Washburn (1946): Apparatus consisted of 5- and 10-cm diameter soil-filled tubes of transparent plastic.
Test No. 5-16: Malik et al. (1989); Test No. 17-24: Kumar and Malik (1990): Test set-up used was 200-cm long glass columns of 2-cm inside diameter.
· Values in parenthesis indicate the number of days required to attain the apparent maximum height of capillary rise h_a.
Parameters used in this table are described in Section 2.5.5 and Figure 2.8 in Chapter 2 (Literature Review) of this thesis.

The results of capillary rise experiments for saline and non-saline sand and sandy loam samples are shown in Figure 1 and Figure 2, respectively (Maskong, 2010).

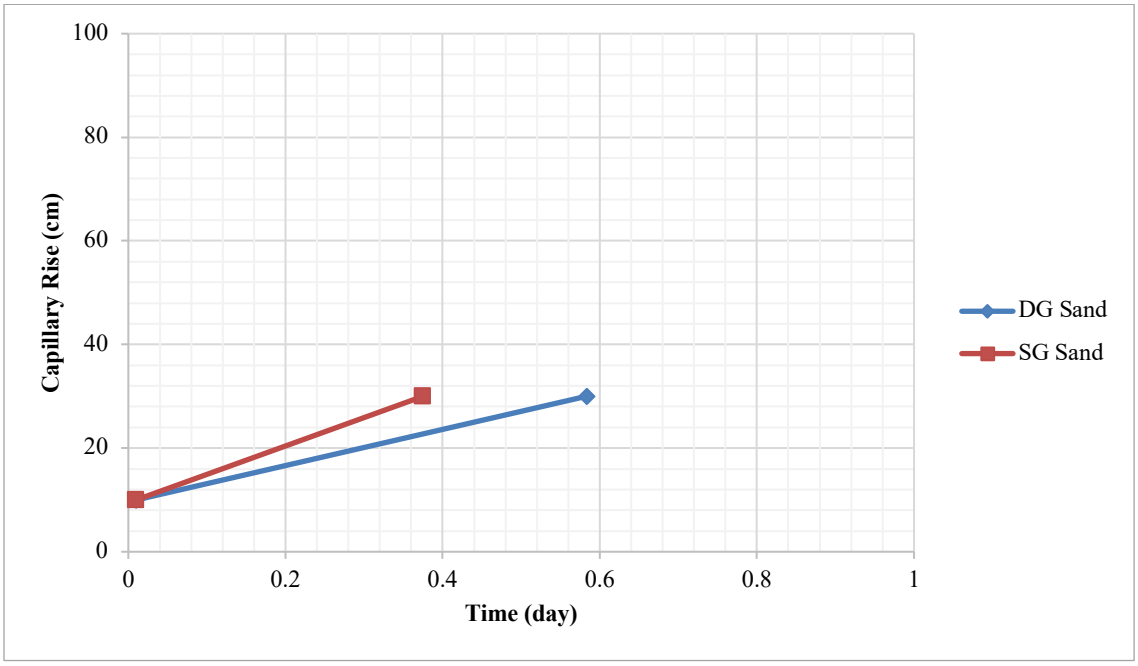

Figure 1 The capillary rise vs. time for saline and non-saline sand (after Maskong, 2010).

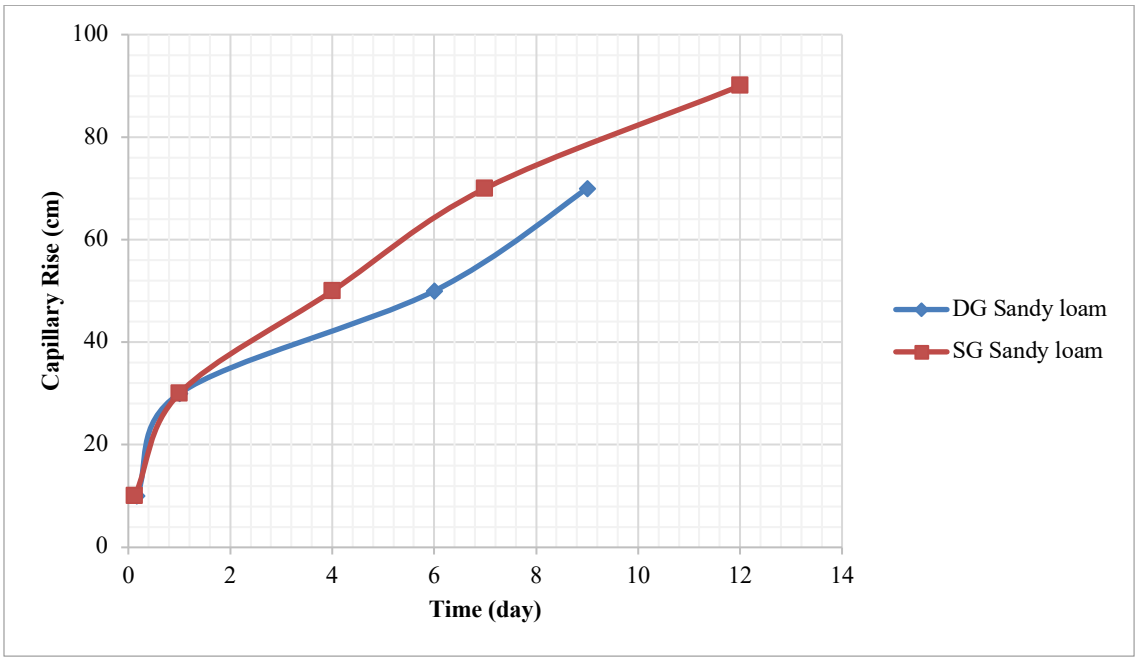

Figure 2 The capillary rise vs. time for saline and non-saline sandy loam (after Maskong, 2010).

B.2 Rate of capillary rise in soils

Two conditions are existed in which the rate of capillary rise is practically significant. (1) An initially dry soil profile subject to a precipitate water table, and (2) an initially moist soil profile subject to a constant humidity gradient at the ground surface. The first condition is controlled by the environment (i.e. gradient of relative humidity) near the ground surface and is frequently encountered in laboratory tests using soil columns or in newly constructed soil structures. The second condition is more common in many field settings. (Lu and Godt, 2013)

While there are a number of theories for capillary rise in ideal tubes, there are two theories representative of soil in laboratory or field conditions.

Terzaghi (1943) developed a theory predicting the rising wetting front z from the water table as a function of elapsed time, t, using the saturated hydraulic conductivity, K_s (m/s) (Lu and Godt, 2013). Accordingly, Terzaghi's (1943) model to predict the rate of capillary rise in a one-dimensional soil column can be written as:

Terzaghi (1943) developed a theory describing the location of the capillary wetting front z from the water table as an implicit function of elapsed time t. Accordingly, Terzaghi's (1943) model to predict the rate of capillary rise in a one-dimensional soil column can be written as (Lu and Likos, 2004a):

$$t = \frac{nh_c}{K_s}\left(\ln\frac{h_c}{h_c - z} - \frac{z}{h_c}\right) \qquad \text{(Eq. 1)}$$

In deriving the above equation (Eq. 1), Terzaghi assumed that (1) the driving head (upward hydraulic) gradient at the wetting front z above the water table can be approximated by $i = (h_c - z)/z$ (where z is a distance measured positive upward from the elevation of the water table) and (2) Darcy's law can be used to describe the upward seepage

(discharge) velocity v, i.e., $v = K_s i = n\, d_z/d_t$, where n represents as the porosity of the soil, K_s represents as the saturated hydraulic conductivity, and t is time.

The terzaghi's analytical solution is plotted against the capillary rise from tests for two soils conducted by Lane and Washburn (1946) shown in Figure 3.

Comparison of the rate of capillary rise for two soils based on Terzaghi's original analytical solution and experimental investigations carried out by Lane and Washburn (1946), illustrated in Figure 3, suggests that Terzaghi's solution significantly over-estimates the rate of capillary rise. This may be attributed to the assumption of a constant saturated hydraulic conductivity made by Terzaghi (1943). Because in reality, capillary rise above the air-entry head is no longer governed by the saturated hydraulic conductivity.

Subsequently Lu and Likos (2004a) developed an analytical solution for the rate of capillary rise and arrived at a theory by explicitly considering the unsaturated hydraulic conductivity function (i.e. Gardner's 1958 model), which can be expressed as:

$$t = \frac{n}{K_s}\sum_{j=0}^{\infty}\frac{\beta^j}{j!}\left(h_c^{j+1}\ln\frac{h_c}{h_c-z} - \sum_{s=0}^{j}\frac{h_c^s z^{j+1-s}}{j+1-s}\right) \quad \text{(Eq. 2)}$$

Where the material parameter, β (cm^{-1}), represents as the decay rate of the unsaturated hydraulic conductivity used in the Gardner's (1958) model which is defined as an exponential function in terms of the saturated hydraulic conductivity and suction head and can be expressed as follows:

$$K(h_m) = K_s \exp(\beta h_m) \quad \text{(Eq. 3)}$$

Where K_s is the saturated hydraulic conductivity, $K(h_m)$ represents as the unsaturated hydraulic conductivity at a given suction head h_m (cm). The pore size distribution parameter, β (cm^{-1}), represents as the rate of decrease in hydraulic conductivity with increasing suction head h_m. According to Lu and Likos (2004a), the practical magnitudes of

β range from $1.0\ cm^{-1}$ for coarse-grained materials to $0.001\ cm^{-1}$ or lower for relatively fine-grained soils. The air-entry head h_a, can also be interpreted as an inverse function of β, i.e. $h_a = 1/\beta$.

The Experimental capillary rise results conducted by Lane and Washburn (1946) and the theoretical predictions of capillary rise based on the analytical solutions developed by Terzaghi (1943) and Lu and Likos (2004) for two soils are illustrated in Figure 3. Because the highly non-linear reduction of hydraulic conductivity under increasing suction have been recognised, the theoretical solution by Lu and Likos (2004) Eq. 2 has significantly improved the predictability of the rate of capillary rise over the analytical solution by Terzaghi (1943) (Lu and Godt, 2013). In other words, because the non-linearity behaviour in hydraulic conductivity have been taken into account, the theoretical solution by Lu and Likos (2004) produces more accurate estimations of the rate of capillary rise over the analytical solution by Terzaghi (1943).

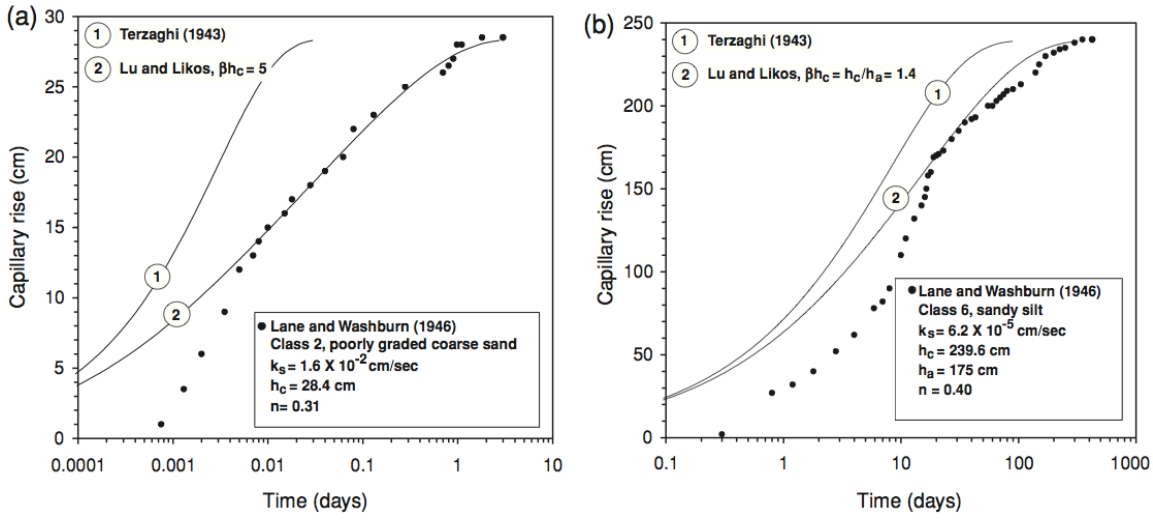

Figure 3 Comparison of two theoretical predictions of capillary rise by Terzaghi (1943) and Lu and Likos (2004) and experimental data in (a) coarse sand and (b) fine sand (from Lu and Likos, 2004a).

B.3 Theoretical considerations of water movement in layered soils

Whether in downward water flow during infiltration processes or in upward water flow during evaporation processes, there must be an effective hydraulic connection or water connectivity between soil layers for water to get into the interface of different soil layers. But if there is very low effective water conductivity, water is not able to break through the interface due to a break in the hydraulic connection. The effective hydraulic connection between the neighboring soil layers is of particular importance when the soil has low moisture content (Li et al. 2013).

The relationship between volumetric water content and water potential in a coarse-grained soil and a fine-grained soil is presented in Fig. 4. Soil 1 represents as coarse-grained soil, and soil 2 represents as fine-grained soil. When the two soils have the same matric potential, the coarse-grained soil (soil 1) has much lower water content than the fine-grained soil (soil 2); when the two soils have the same water content, the matric suction is lower in the coarse-grained soil (soil 1) than in the fine-grained soil (soil 2). The capillary break effect may happen: in downward water flow during infiltration when soil 2 overlies soil 1; or in upward water flow during evaporation when soil 1 overlies soil 2. The point on the soil water retention curve of coarse-grained soil at s_1 represents the turning point at which matric suction transits from residual to saturated conditions, assuming it is also the turning point at which coarse-grained soil establishes its effective water conductivity (Li et al. 2013).

If soil 2 overlies soil 1 during infiltration, whether water would cease to flow and become stagnant at the interface or not is dependent upon the soil water retention curve of the coarse-grained soil, and water can penetrate this layer just after soil 1 has built up effective hydraulic connection inside itself and with the neighbouring layer (McCartney and Zornberg 2010). Thus if fine-grained soil (soil 2) overlies coarse-grained soil (soil 1) during infiltration, water

can penetrate coarse-grained soil (soil 1) only if the matric suction is lower than s_1. From the statements above, it can be understood that the capillary break effect happens during infiltration only if the coarse-grained soil (soil 1) has water suction greater than s_1 that is associated with the low moisture/residual condition (high suction) part of the soil water retention curve of the underlying soil 1.

During the evaporation process on the other hand, the conditions for water flow get more complicated. Considering soil 1 overlying soil 2 in this case, the water flow is affected not only by the hydraulic properties of both soils but also the thickness of the lower soil 2, as the direction of the resultant force (mainly gravitational and matric potentials) changes with the variation of soil properties and the underlying layer. Assuming coarse-grained soil (soil 1) overlying fine-grained soil (soil 2) in Fig. 4 as an example, the following can be stated (Li et al. 2013):

- When the underlying fine-grained layer (soil 2) has a thickness greater than its maximum capillary rise, h_{max} (should be much greater than s_1), capillary water cannot get into overlying coarse-grained layer (soil 1) and only exists in the underlying fine-grained layer (soil 2).

- When the underlying fine-grained layer (soil 2) has a thickness of s_2, which is larger than s_1 but smaller than the maximum capillary rise (h_{max}) of soil 2, capillary water can reach the interface. However, when the system comes to equilibrium, the minimum water suction at the interface would be s_2, still greater than the maximum water suction in coarse-grained layer soil 1 (i.e. s_1) that is required to build up effective hydraulic connection and water conductivity. As a result, water still could not break through the interface in this case.

- When the underlying fine-grained layer (soil 2) has a thickness of s_3 that is less than s_1, capillary water can also reach the interface, but then again water flow will be hindered under the interface causing the capillary break effect. With more water moving to the interface, the suction at the interface would drop to s_1 and keep reducing to s_3. As a result of this, water could eventually break through the interface and penetrate the upper coarse-grained layer.

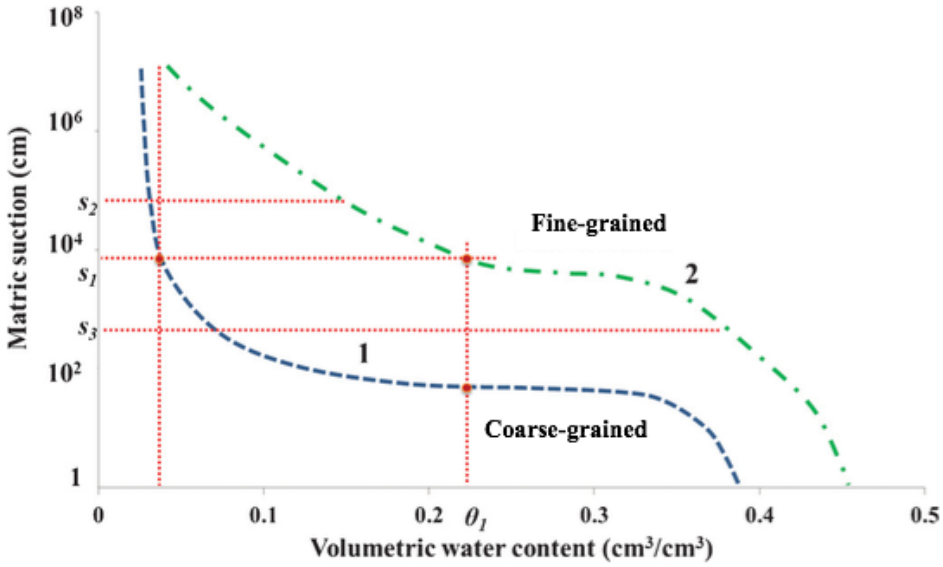

Figure 4 Soil water retention curves of a coarse-grained and a fine-grained soil (after Li et al. 2013).

Theoretical analysis above clearly shows that determining the turning point of matric suction transition from residual to saturated conditions or at which point effective water conductivity is built up on the soil water retention curve of the soil layer in the downstream direction, is of crucial importance (Hillel and Talpaz 1977; Yang et al. 2006).

APPENDIX C. SUPPLEMENTARY MATERIALS FOR CHAPTER 3

C.1 Layer thickness of the layered SAND system

The specimen calculation of layer thickness of the layered SAND system is shown in Table 1.

Table 1 Calculation of layer thickness of the layered SAND system

Estimated thickness of layers (cm)	**L**	**10.0000**					**10.0000**	**10.0000**	**45.0000**	
Estimated height of capillary rise (cm)	H	4.871441				14.1272	20.0043	28.2934	45.5209	74.2189
Estimated height of capillary rise (m)	H	0.048714				0.1413	0.2000	0.2829	0.4552	0.7422
Surface tension (N/m)	γ	0.0728	0.0728	0.0728	0.0728	0.0728	0.0728	0.0728	0.0728	0.0728
Contact angle (rad)	θ	0.0000	0.0000	0.0000	0.0000	0.0000	0.0000	0.0000	0.0000	0.0000
Density of liquid (kg/m^3)	ρ	1000.00	1000.00	1000.00	1000.00	1000.00	1000.00	1000.00	1000.00	1000.00
Acceleration due to gravity (m/s^2)	g	9.8100	9.8100	9.8100	9.8100	9.8100	9.8100	9.8100	9.8100	9.8100
Diameter of tube (m)	d	0.000609				0.000210	0.000148	0.000105	0.000065	0.000040
Bulk density (g/cm^3)	ρb	1.6700	1.6700	1.6700	1.6700	1.6700	1.6700	1.6700	1.6700	1.6700
Particle density (g/cm^3)	ρs	2.6380	2.6380	2.6380	2.6380	2.6380	2.6380	2.6380	2.6380	2.6380
Porosity	ϕ	36.6945	36.6945	36.6945	36.6945	36.6945	36.6945	36.6945	36.6945	36.6945
Particle size (m)		0.002000	0.001180	0.000600	0.000425	0.000300	0.000212	0.000150	0.000075	0.000063
Average particle size (m)		0.001051				0.000363	0.000256	0.000181	0.000113	0.000069
Pore size (m)		0.001159	0.000684	0.000348	0.000246	0.000174	0.000123	0.000087	0.000043	0.000037
Average pore size (m)		0.000609				0.000210	0.000148	0.000105	0.000065	0.000040

C.2 Capillary rise tests in a moist soil (Set 1/Part 2)

The Moisture contents and densities of base soils used in tests for the second part of the first set (Set 1/Part 2) are presented in Table 2.

Table 2 Moisture contents and densities of base soils used in tests for the second part of the first set (Set 1/Part 2)

Base soil	Moisture content (%)	Avg. density (Mg/m^3)	Percentage of saturation moisture content
Sample 1	34 - 35	1.707	105
Sample 2	28 - 29	1.743	86
Sample 3	20 - 21	1.749	62

C.3 Evaporation tests on block samples

The details of evaporation tests on block samples are presented in Table 3.

Table 3 The details of evaporation tests on block samples

	Soil moulds								
	1			2			3		
Soil type	Medium grained SAND			Clayey sandy SILT			Clayey very silty SAND		
Water content (%)	13.0	19.0	27.0	13.0	19.0	27.0	13.0	19.0	27.0
Avg. density (Mg/m^3)	1.79	1.88	1.84	1.80	1.92	1.94	1.94	1.95	1.98
Wind velocity (m/s)	0.0, 1.0, 3.0 and 6.0			0.0, 1.0, 3.0 and 6.0			0.0, 1.0, 3.0 and 6.0		
Wind movement	Laminar and Turbulent			Laminar and Turbulent			Laminar and Turbulent		
Test duration (days)	2			2			2		

APPENDIX D. SUPPLEMENTARY MATERIALS FOR CHAPTER 4

D.1 Positions where moisture content was measured within the soil column

The positions where moisture content was measured within the soil column are shown in Figure 1.

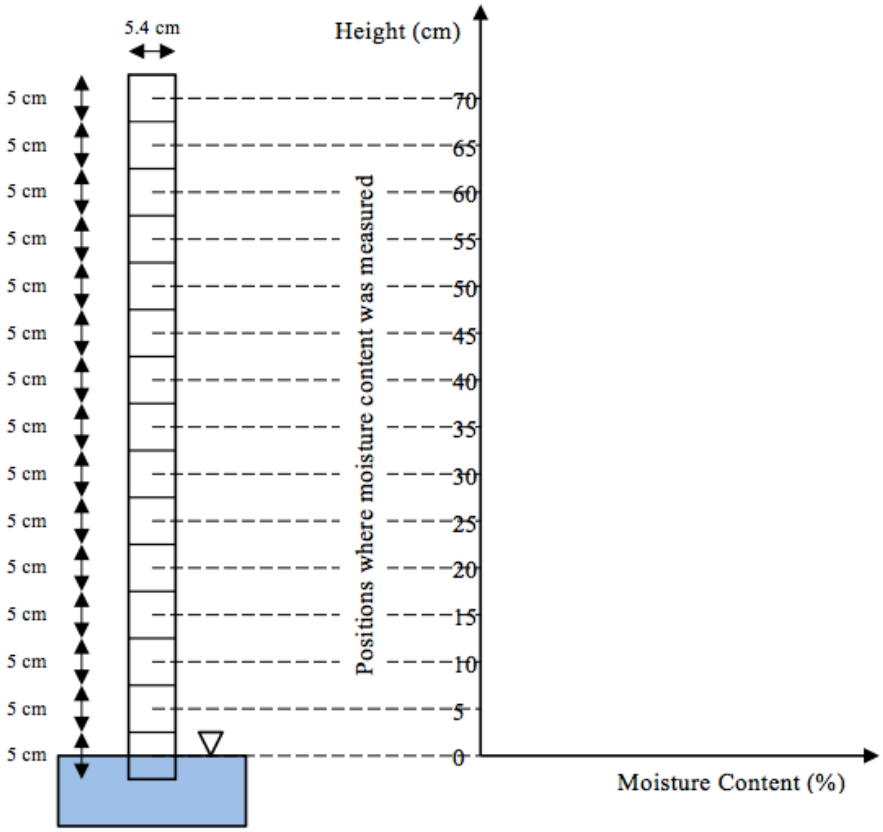

Figure 1 Positions where moisture content was measured within the soil column.